Arctic Coastal Dynamics

Report of the 3rd International Workshop

University of Oslo, Oslo (Norway) 2-5 December 2002

Edited by Volker Rachold, Jerry Brown, Steven Solomon and Johan Ludvig Sollid

Volker Rachold, Alfred Wegener Institute, Research Unit Potsdam, Telegrafenberg A43, 14473 Potsdam, Germany

Jerry Brown, International Permafrost Association, P.O. Box 7, Woods Hole, MA 02543, USA

Steven Solomon, Geological Survey of Canada (Atlantic), Bedford Institute of Oceanography, P.O. Box 1006, 1 Challenger Drive, Dartmouth, NS Canada B2Y 4A2, Canada

Johan Ludvig Sollid, Department of Physical Geography, University of Oslo, P.O. Box 1042, Blindern, N-0316 Oslo, Norway

Preface

Arctic Coastal Dynamics (ACD) is a joint project of the International Arctic Sciences Committee (IASC) and the International Permafrost Association. Its overall objective is to improve our understanding of circum-Arctic coastal dynamics as a function of environmental forcing, coastal geology and cryology and morphodynamic behavior.

The third IASC-sponsored ACD workshop was held in Oslo, Norway, on December 2-5, 2002. Participants from Canada (3), Germany (3), Great Britain (1), the Netherlands (1), Norway (6), Russia (11), Switzerland (1) and the United States (2) attended. The objective of the workshop was to review the status of ACD according to the Science and Implementation Plan, with the main focus on the quantitative assessment of the sediment and organic carbon input to the Arctic Ocean through coastal erosion.

During the first part of the workshop, 29 papers dealing with regional and/or circum-Arctic coastal dynamics were presented. Based on the material presented, three regional working groups and two circum-Arctic working groups were organized. The main task of the regional working groups was to continue previous efforts to segment and classify the coast for their sectors. The coastal segmentation and classification is the basis for the assessment of the sediment and organic carbon input through coastal erosion. The circum-Arctic working groups focused on GIS development and extraction and presentation of environmental data, respectively. Finally, the results of the workshop and the next steps were discussed in the ACD Steering Committee meeting. The present report summarizes the program of the workshop and the main results.

Financial support from the International Arctic Sciences Committee (IASC) is highly appreciated and was essential for conducting the workshop. Additional support of ACD activities is provided by the International Permafrost Association (IPA), INTAS (International Association for the promotion of co-operation with scientists from the New Independent States of the former Soviet Union), the International Arctic Research Center (IARC), and the Canadian Department of Foreign Affairs and International Trade (DFAIT).

IASC

International Permafrost Association

Participants of the 3rd International Workshop on Arctic Coastal Dynamics (ACD), Oslo (Norway), 2-5 December 2002
(photo by Feliks Rivkin).

Table of Contents

1 History and Development of ACD

Complex land-ocean interactions in the Arctic coastal environment play an important role in the balance of sediments, organic carbon and nutrients of the Arctic Basin. In the past, contribution of coastal erosion to the material budget of the Arctic seas has been underestimated, but recent investigations have underlined its importance. Reimnitz et al. (1988) presented calculations for 344 km of Alaskan coast in the Colville River area and found that coastal erosion here supplied seven times more sediments to the Alaskan Beaufort Sea than rivers. Are (1999) suggested that the amount of sediment supplied to the Laptev Sea by rivers and shores is at least of the same order and that the coastal erosion input is probably even larger than the input of the rivers. This finding was supported by Rachold et al. (2000), who concluded that the sediment input to the Laptev Sea through coastal erosion is twice as large as the river input. In the Canadian Beaufort Sea on the other hand, the Mackenzie River input is the dominant source of sediments and coastal erosion is much less important (MacDonald et al. 1998). These pronounced regional differences in the riverine and coastal erosion sediment input have to be considered in any research related to the fluxes and budgets of the Arctic seas.

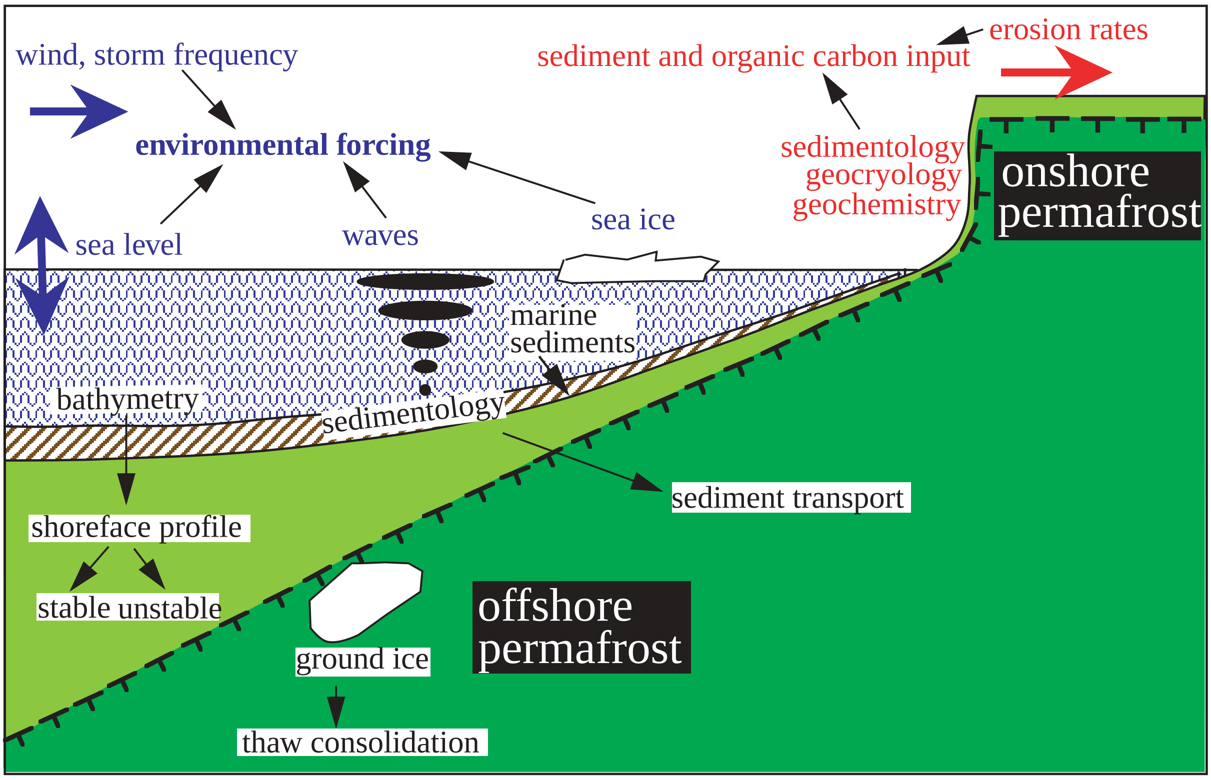

Figure 1. Coastal dynamics as a function of environmental forcing, coastal morphology, and onshore and offshore permafrost characteristics.

The Arctic Coastal Dynamics (ACD) program is a multi-disciplinary, multi-national forum to exchange ideas and information. The overall objective of ACD is to improve our understanding of circum-Arctic coastal dynamics as a function of environmental forcing, coastal geology and cryology and morphodynamic behavior. Figure 1 schematically summarizes the relevant parameters and processes. In particular, the ACD program proposed to:

- establish the rates and magnitudes of erosion and accumulation of Arctic coasts;
- develop a network of long-term monitoring sites including local community-based observational sites;
- identify and undertake focused research on critical processes;
- estimate the amount of sediments and organic carbon derived from coastal erosion;
- refine and apply an Arctic coastal classification (includes ground ice, permafrost, geology, etc.) in digital form (GIS format);
- compile, analyze and apply existing information on relevant environmental forcing parameters (e.g. wind speed, sea level, fetch, sea ice etc.);
- develop empirical models to assess the sensitivity of Arctic coasts to environmental variability and human impacts;
- produce a series of thematic and derived maps (e.g. coastal classification, ground-ice, sensitivity etc.);

The project elements were formulated at a workshop in Woods Hole in November 1999 carried out under the auspices of the International Permafrost Association (IPA), its working group on Coastal and Offshore Permafrost and its Coastal Erosion subgroup (Brown and Solomon 2000). As a result of the workshop a metadata form for the selection and establishment of key monitoring sites was developed. A consistent and generalized coastal classification scheme was established based on morphology and materials. Consensus was reached on direct and indirect methodologies for estimating ground-ice volumes and presentations of data on maps. Finally, a suite of standard tools and techniques for development of long-term coastal monitoring sites was recommended.

During the Arctic Science Summit Week in April 2000 in Cambridge, UK, and at the request of the IPA, the Council of the International Arctic Science Committee (IASC) approved funding for a follow up workshop to develop a Science and Implementation Plan for ACD. The resulting international workshop, held in Potsdam (Germany) on 18-20 October 2000, produced a phased, five-year Science and Implementation Plan (Figure 2).

The participants selected Volker Rachold to be the official IASC Project Leader. Hans Hubberten, Head of the AWI Potsdam Department, agreed to establish an ACD project office at AWI-Potsdam with a secretariat headed by Volker Rachold to maintain international communications including the web site (http://www.awi-potsdam.de/www-pot/geo/acd.html) and an electronic newsletter. The secretariat is assisted by the International Steering Committee (ISC) consisting of

- Felix Are, St. Petersburg State University of Means and Communication
- Jerry Brown, International Permafrost Association, Woods Hole
- George Cherkashov, VNIIOkeangeologia, St. Petersburg
- Mikhail Grigoriev, Permafrost Institute, Yakutsk
- Hans Hubberten, AWI, Potsdam
- Volker Rachold, AWI, Potsdam
- Johan Ludvig Sollid, Oslo University
- Steven Solomon, Geological Survey of Canada, Dartmouth

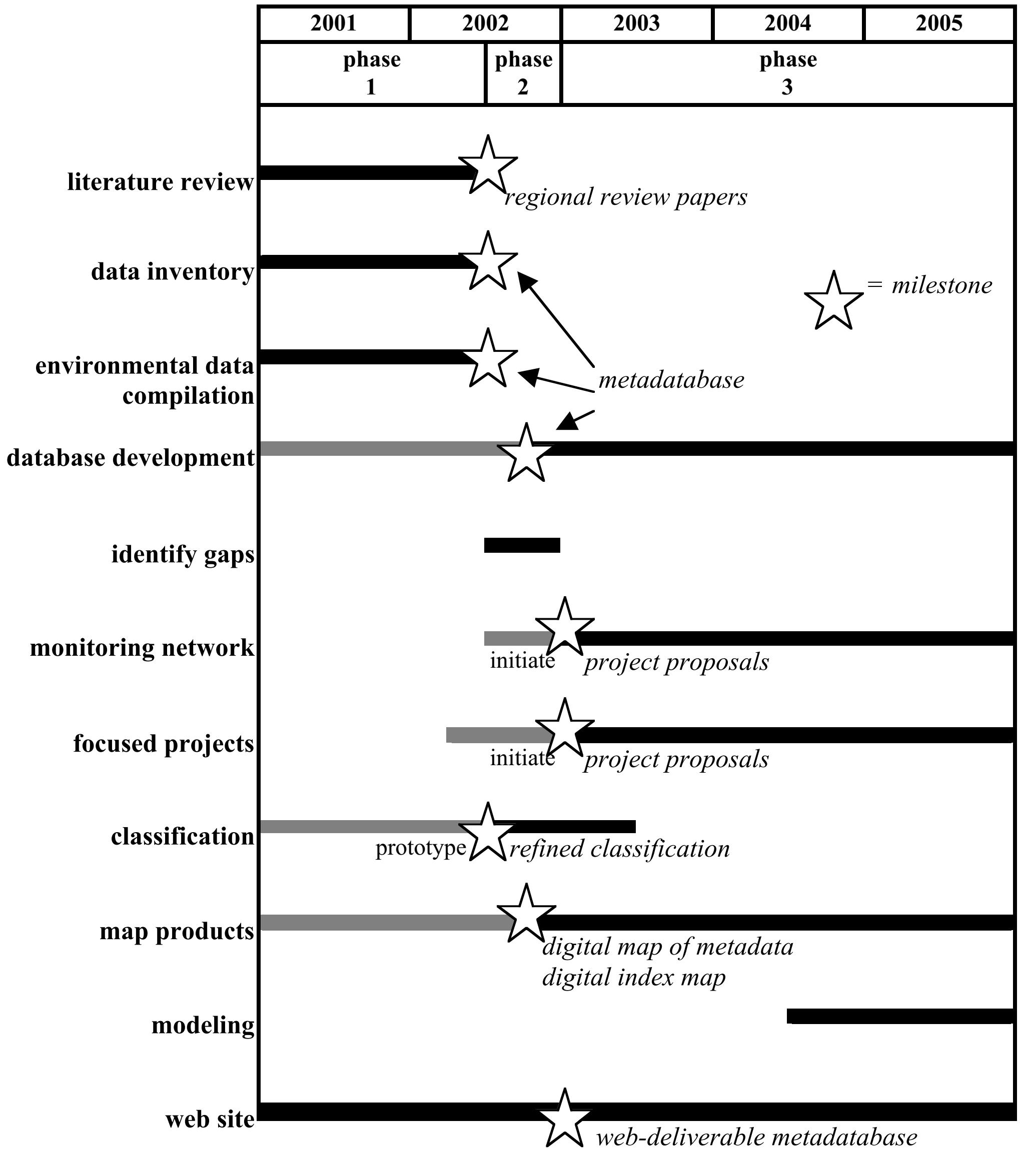

Figure 2. Main elements of the ACD Science and Implementation Plan, schedule and milestones.

The Science and Implementation Plan (IASC Arctic Coastal Dynamics, 2001) was made available at the ACD web page and submitted to the IASC Council for review, approval and advice on future directions. At the Council Meeting during the Arctic Science Summit Week in Iqaluit, Canada (April 22-28, 2001), IASC officially accepted the ACD project and approved funding for the 2nd ACD workshop in Potsdam, November 26-30, 2001. The main objective of the 2nd ACD workshop was to review the status of ACD according to phase 1 of the Science and Implementation Plan. During the first part of the workshop status reports of the ACD working groups and several papers dealing with different aspects of circum-Arctic coastal dynamics were presented. During the second part the workshop, progress of the ACD working groups was discussed and, based on these discussions, the next steps were identified in the ACD Steering Committee meeting. The results of the workshop including ca. 30 extended abstracts were published in the journal *Reports on Polar and Marine Research* (Rachold et al. 2002).

According to the results of the 2nd ACD workshop, emphasis is currently on developing a circum-Arctic estimate of sediment and organic input from coastal erosion to inner shelf.

Several papers on this topic have recently been completed (Brown et al., in press; Grigoriev and Rachold, in press; Jorgenson et al., in press; Rachold et al., in press [a]). The studies indicate that coastal erosion forms a major source not only of the sediment input but also of the total organic carbon (TOC) input to the Arctic seas. The comparison between riverine and coastal TOC input, based upon a combination of detailed field studies carried out in the Laptev and East Siberian Seas during the last several years (Grigoriev and Rachold, in press) and on a review of the existing literature, is shown in Figure 3 (Rachold et al., in press [a]). It has to be noted that the data given in Figure 3 are the best currently available estimates, but may include errors ranging from ca. 30 % for the Laptev and East Siberian Sea (Grigoriev and Rachold, in press) to one order of magnitude for the other seas.

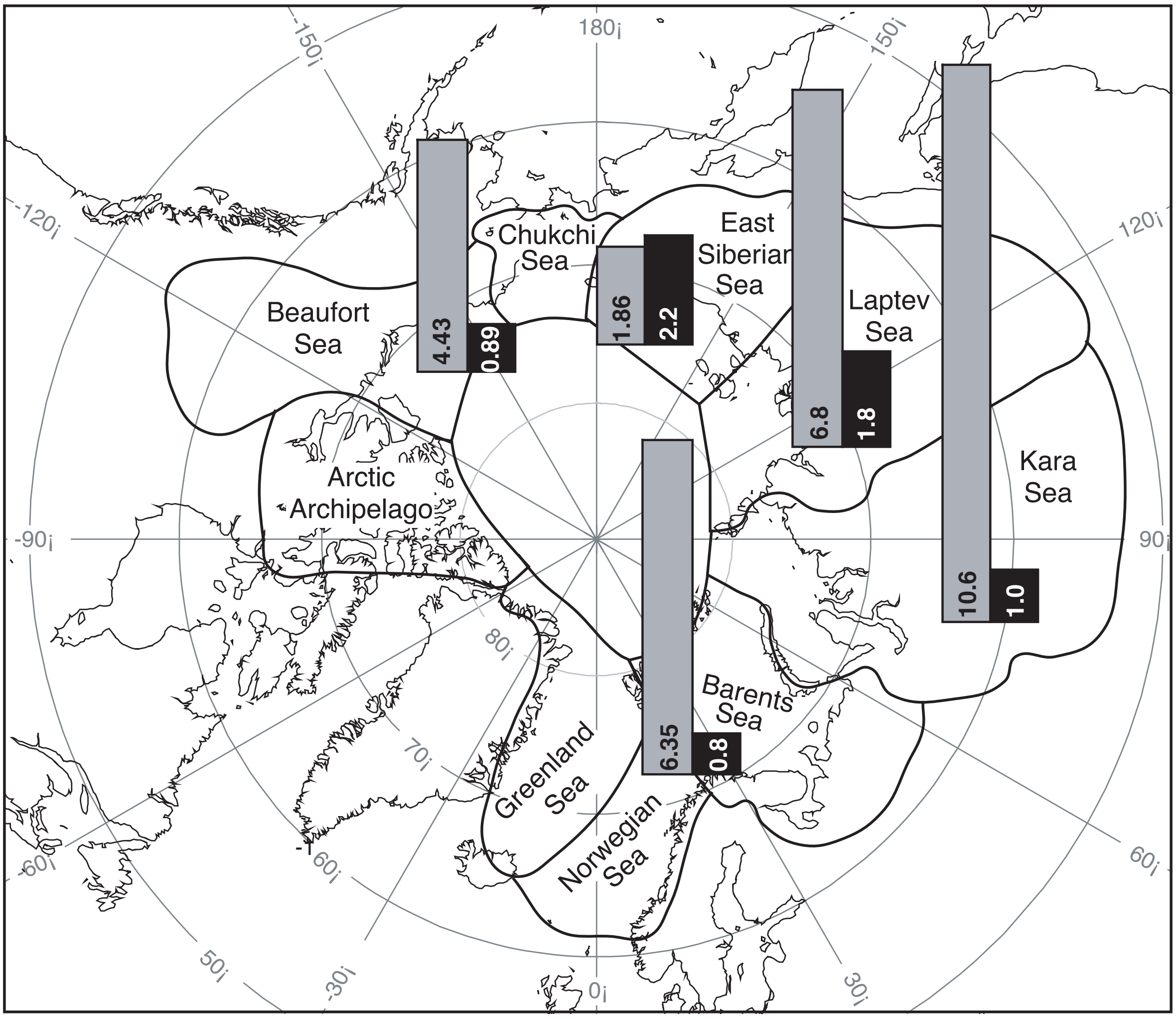

Figure 3. Riverine and coastal TOC input (10^6 t C yr^{-1}) to the Arctic Ocean (Rachold et al. in press [a]). Grey bars refer to river input and black bars to coastal input. Note that the sum is shown for Beaufort and Chukchi Sea and that Barents Sea input data include White Sea. The drainage systems are taken from http://www.R-ArcticNET.sr.unh.edu/.

The development of a reliable assessment of the sediment and organic input through coastal erosion involves classifying and segmenting the entire circum-Arctic coastline into common elements based primarily on morphology, ground-ice composition and erosion rates. Accordingly, a coastal mapping template (Table 1), which allows coastal scientists to record information about Arctic coasts, was developed during the 2nd ACD workshop in Potsdam, and modified during a small working meeting[1] at the AWI in Bremerhaven in October 2002. The segmented data will be entered into the PANGAEA data system (http://www.pangaea.de). Regional expert teams to perform the segmentation for the major Arctic seas were identified during the Potsdam workshop. Figure 4 shows the areas by major seas, the length of their shorelines is given in Table 2. For the Laptev Sea a first version of the segmentation has already been completed (Rachold et al. in press [b]).

Table 1. ACD Coastal Classification Template.

field	*entry options*
primary_contact_person	provide name and email
regional_sea	Chukchi Sea=CS, East Siberian Sea=ESS, Laptev Sea=LS, Kara Sea=KS, Barents Sea=BS, Greenland Sea/Canadian Archipelago=GSCA, Beaufort Sea=BS
segment	
segment_name	text field
segment_no	number
segment_start_lat	decimal degrees (4 decimals)
segment_start_long	decimal degrees (4 decimals)
segment_end_lat	decimal degrees (4 decimals)
segment_end_long	decimal degrees (4 decimals)
segment_comment	yes=y or no=n (to be added if islands are included in the segment)
onshore (direction landward from the sea)	
onshore_form	delta=d, lowland(<10m)=l, upland(10-500m)=u, highland(>500m)=h, wetland=w
backshore (upper part of the active beach above the normal reach of the tides (high water), but affected by large waves occurring during a high water)	
backshore_form	cliff=c, slope=s, flat=f, ridged/terraced=r, anthropogenic=a, complicated=x
backshore_elevation	in meters
backshore_material_1	lithified=l, unlithified=u
backshore_material_2	mud-dominated=m, sand-dominated=s, gravel-dominated=g, diamict=d, organic=o, mixtures= e.g mg, sg
backshore_comment	text to be added if backshore_form=r or backshore_form=x
shore (strip of ground bordering the sea which is alternately exposed, or covered by tides and/or waves)	
shore_form	beach=b, shore terrace*=t, cliff=c, complicated=x
beach_form	fringing=f, barrier=b, spit=s (to be filled if shore_form=b)
shore_material_1	lithified=l, unlithified=u
shore_material_2	mud-dominated=m, sand-dominated=s, gravel-dominated=g, diamict=d, organic=o, mixtures= e.g mg, sg
shore_comment	text to be added if shore_form = x
offshore	
depth_closure**	in meters (if available)
distance_2m_isobath	in meters (if available)
distance_5m_isobath	in meters (if available)
distance_10m_isobath	in meters (if available)
distance_100m_isobath	in meters (if available)
offshore_material	mud-dominated=m, sand-dominated=s, gravel-dominated=g, diamict=d, organic=o, mixtures= e.g mg, sg

[1] M. Grigoriev, J. Brown, S. Solomon, W. Pollard (McGill University, Montreal, PQ, Canada) and V. Rachold participated in the October meeting which was funded in large part by the Canadian Department of Foreign Affairs and International Trade.

Table 1. Continuation.

field	*entry options*
general	
ground_ice_1	low(2-20)=l, medium(20-50)=m, high(>50)=h
ground_ice_2	in % total volume of shoreline (best guess!)
ground_ice_comment	text to be added if ground ice template was filled out
change_rate	in meter/year (erosion=minus, accumulation=plus)
change_rate_interval	in years (years of observation, e.g. 1956-1999)
dynamic_process	erosive=e, stable=s, accumulative=a (interpretation, only to be filled out if change rate is not available)
dry_bulk_density	in t/m3 (if no data available use: clay=1.3, silt=1.5, sand=2, or mixtures, e.g. silty sand=1.8)
organic_C	in weight % (best guess!)
soil_organic_C	in kg/m2 (if available)
environmental	
glacier_ice	floating=f or grounded=g
sea_level_change	in centimeters per hundred years (if available) (negative for submergence)
tidal_range	in meters (if available)
meteorol_tidal_range	in meters (if available) (positve and negative storm surge)
mean_freezeup_date	Julian day (if available)
mean_breakup	Julian day (if available)
open_water_length	days (if available)
landfast_ice_min	in km (if available)
landfast_ice_max	in km (if available)
open_water_max	in km (if available)
open_water_mean	in km (if available)
open_water_min	in km (if available)
data_sources	text (provide the sources or references(citation) of used information, i.e. published, unpublished observations or reports)
comments	text (space for additional comments)

*shore terrace = a terrace made along a coast by the action of waves and shore currents, it may become land by uplifting of shore or lowering of the water; **depth_closure = maximum storm wave base

Table 2. Shoreline lengths of the Arctic seas based on World Vector Shorelines (excluding islands).

	Sector	**Shoreline length (km)**
CS	Chukchi Sea	5,203
ES	East Siberian Sea	3,500
LS	Laptev Sea	7,931
KS	Kara Sea	10,790
BS	Barents Sea	6,176
GSCA	Greenland Sea/Canadian Archipelago	4,378
CBS	Canadian Beaufort Sea	3,787
USBS	US Beaufort Sea	1,958
	total	**43,723**

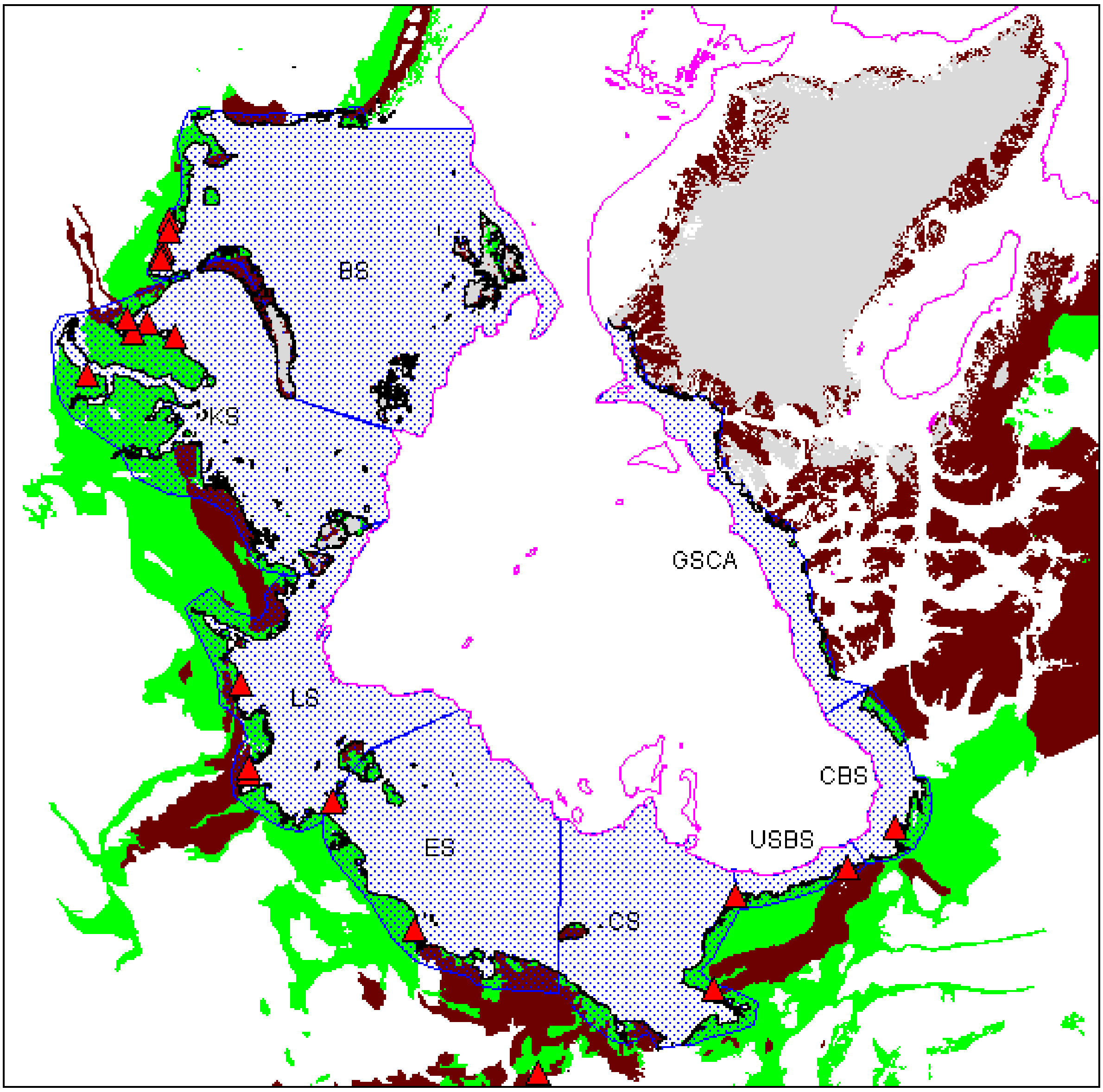

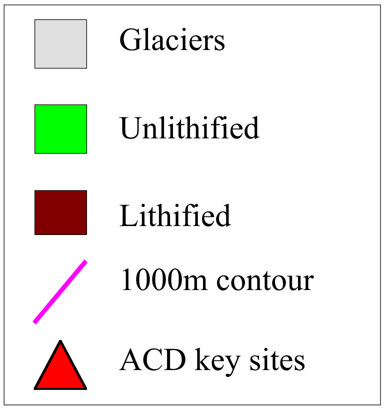

Figure 4. ACD segmentation of the Arctic coastline by major seas. The metadata for the ACD key site are given in Appendix 1. Terrain units are based on the digitized version of the IPA permafrost map (Brown et al 1997).

References

Are, F.E. (1999) The role of coastal retreat for sedimentation in the Laptev Sea. In: Kassens, H., Bauch, H., Dmitrenko, I., Eicken, H., Hubberten, H.-W., Melles, M., Thiede, J. and Timokhov, L. (eds.) Land-Ocean systems in the Siberian Arctic: dynamics and history. Springer, Berlin, 287-299.

Brown, J., Ferrians, O.J. Jr., Heginbottom, J.A. and Melnikov, E.S. (1997) Circum-Arctic map of permafrost and ground-ice conditions, U.S. Geological Survey Circum-Pacific Map CP- 45, 1:10,000,000, Reston, Virginia.

Brown, J. and Solomon, S. (eds.) (2000) Arctic Coastal Dynamics – Report of an International Workshop, Woods Hole, MA, November 2-4, 1999. Geological Survey of Canada Open File 3929.

Brown, J., Jorgenson, M.T., Smith, O.P. and Lee, W. (in press) Long-term rates of erosion and carbon input, Elson Lagoon, Barrow, Alaska. Proceedings of the 8th International Conference on Permafrost. Zürich (Switzerland), 21-25 July 2003.

Grigoriev, M.N. and Rachold, V. (in press) The degradation of coastal permafrost and the organic carbon balance of the Laptev and East Siberian Seas. Proceedings of the 8th International Conference on Permafrost. Zürich (Switzerland), 21-25 July 2003.

IASC Arctic Coastal Dynamics (ACD) (2001) Science and Implementation Plan, International Arctic Science Committee, Oslo, April 2001.

Jorgenson, M.T., Macander, M., Jorgenson, J.C., Ping, C.P. and Harden, J. (in press) Ground ice and carbon characteristics of eroding coastal permafrost at Beaufort Lagoon, northern Alaska Proceedings of the 8th International Conference on Permafrost. Zürich (Switzerland), 21-25 July 2003.

MacDonald, R.W., Solomon, S., Cranston, R.E., Welch, H.E., Yunker, M.B. and Gobiel, C. (1998) A sediment and organic carbon budget for the Canadian Beaufort Shelf. Mar. Geol. 144, 255-273.

Rachold, V., Grigoriev, M.N., Are, F.E., Solomon, S., Reimnitz, E., Kassens, H. and Antonow, M. (2000) Coastal erosion vs. riverine sediment discharge in the Arctic shelf seas. International Journal of Earth Sciences (Geol. Rundsch.) 89, 450-460.

Rachold, V., Brown, J. and Solomon, S. (2002) Arctic Coastal Dynamics -Report of an International Workshop, Potsdam (Germany) 26-30 November 2001. Reports on Polar Research 413, 103 pp.

Rachold, V., Eicken, H., Gordeev, V.V., Grigoriev, M.N., Hubberten, H.-W., Lisitzin, A.P., Shevchenko, V.P., Schirrmeister, L. (in press [a]) Modern terrigenous organic carbon input to the Arctic Ocean, In: Stein, R. and Macdonald, R.W. (Eds.) Organic Carbon Cycle in the Arctic Ocean: Present and Past. Springer Verlag, Berlin.

Rachold, V., Lack, M. and Grigoriev, M.N. (in press [b]) A Geo Information System (GIS) for Circum-Arctic Coastal Dynamics. Proceedings of the 8th International Conference on Permafrost. Zürich (Switzerland), 21-25 July 2003.

Reimnitz E, Graves S.M., Barnes P.W. (1988) Beaufort Sea coastal erosion, sediment flux, shoreline evolution and the erosional shelf profile. U.S. Geological Survey. Map I-1182-G, and text, 22 pp.

2 Program and Main Results of the Workshop[2]

The third IASC-sponsored ACD workshop was held in Oslo, Norway, on December 2-5, 2002. Participants from Canada (3), Germany (3), Great Britain (1), the Netherlands (1), Norway (6), Russia (11), Switzerland (1) and the United States (2) attended. Of these five were young scientists supported by IASC. Two current INTAS projects provided support for six additional Russian participants. The Geography Department at the University of Oslo organized the local logistics for the workshop.

The objective of the workshop was to review the status of ACD according to the Science and Implementation Plan, with the main focus on the quantitative assessment of the sediment and organic carbon input to the Arctic Ocean through coastal erosion.

2.1 Program

During the first part of the workshop (Monday, December 2 and morning of Tuesday, December 3) 29 papers dealing with regional and/or circum-Arctic aspects of coastal dynamics were presented (the extended abstracts including several from those not attending are presented in Section 3):

- Beaufort and Chukcki Sea: 6 papers;
- Laptev and East Siberian Sea: 5 papers;
- Kara and Barents Sea: 9 papers;
- Norwegian and Greenland Sea: 3 papers;
- circum-Arctic processes, methods and techniques: 6 papers.

Based on the presentations and the regions and expertise represented at the workshop three regional working groups (WG) and two circum-Arctic WGs (focusing on GIS development and extraction and presentation of environmental data) were organized. The WGs met on Wednesday, December 4 and Thursday, December 5. Plenary meetings were held twice per day in order to discuss general questions and to exchange information on the progress of the working groups.

Western Russian Arctic (Barents and Kara Sea) WG

Leader: A. Vasiliev
Participants: D. Drozdov, A. Kizyakov, D. Pertednya, I. Streletskaya, S. Ogorodov, F. Rivkin and A. Vasiliev

Eastern Russian Arctic (Laptev, East Siberian and Chukchi Sea) WG

Leader: M. Grigoriev
Participants: F. Are, M. Grigoriev, H.-W. Hubberten, V. Ostroumov and V. Rachold

Canadian and Alaskan Beaufort Sea WG

Leader: S. Solomon
Participants: J. Brown, A. Mahoney, H. Lantuit and S. Solomon

[2] The complete program and the list of participants are given in Appendices 2 and 3.

Environmental WG

Leader: D. Atkinson[3]
Participants: D. Atkinson, J. Hölemann and A. Mahoney

GeoInformation System (GIS) WG

Leader: R. Ødegaard
Participants: D. Atkinson, D. Drozdov, B. Etzelmüller, H. Lantuit, I. May, V. Rachold, F. Rivkin, F. Steenhuisen and B. Wangensteen

A meeting of the teams involved in two ACD related INTAS projects was held in conjunction with the workshop on Sunday, December 1:

Arctic coasts of Eurasia: dynamics, sediment budget and carbon flux in connection with permafrost degradation. INTAS Open Call 2001-2329

Arctic coastal dynamics of Eurasia: classification, modern state and prediction of its development based on GIS technology. INTAS Open Call 2001-2332

participants: F. Are, G. Cherkashov, D. Drozdov, M. Grigoriev, A. Kizyakov, R. Ødegaard, V. Ostroumov, D. Perednya, V. Rachold, F. Rivkin, J.L. Sollid, I. Streletskaya, A. Vasiliev, B. Wangensteen

Finally, the results of the workshop and the next steps were discussed in the ACD Steering Committee meeting.

2.2 Main Results of the Working Group Meetings

The main task of the regional WGs was to continue the coastal segmentation and classification for their sectors. Additionally, representative photographs of coastal sites for each sector were selected for inclusion in a coastal photo library. These, and metadata forms for key sites will be incorporated into the IPA CAPS 2 CD ROM currently in preparation at the National Snow and Ice Data Center, Boulder, Colorado. The discussions of the two circum-Arctic WGs concentrated on the extraction and presentation of relevant environmental data and on technical aspects concerning the development of a circum-Arctic coastal GIS.

At the end of the workshop the WG leaders reported on the progress of their groups:

Western Russian Arctic (Barents and Kara Sea) WG

For the coast of the western Russian Arctic 40-45 photographs of typical shores were selected. The collection includes photographs of the ACD key sites in the Kara Sea and in the Barents Sea.

The segmentation of the coastline in the western Russian Arctic was almost completed during the workshop. However, the western segments of the Barents Sea have to be revised (responsible: D. Drozdov, S. Ogorodov for western Barents Sea and A. Vasiliev for Yamal

[3] David Atkinson, the leader of the Environmental WG, is financed through the IARC grant "Analysis of Coastal Meteorological and Oceanographic Forcing in the Arctic Basin".

Peninsula). White Sea and Kola Peninsula have not been classified yet. This region is located outside of the permafrost zone but should be included to calculate the sediment budget. The segmentation of the Taymyr Peninsula west coast is still in progress (50-60 % of the Kara Sea are completed) and will be finished by middle of 2003 (responsible: A. Vasiliev).

The final version of the segmentation and classification of the entire western Russian Arctic will be available at the next ACD workshop (November 2003, see below).

Eastern Russian Arctic (Laptev, East Siberian and Chukchi Sea) WG

For both Laptev and East Siberian seas ca. 15 coastal photographs and for the Chukchi Sea four photographs covering the ACD key sites in the eastern Russian Arctic and some additional sites were selected.

The segmentation of the Laptev Sea coast is practically finished, but the western segments (east coast of Taymyr Peninsula and Severnaya Zemlya Archipelago) have to be revised (responsible: H.-W. Hubberten, M. Grigoriev, deadline: May, 2003). For the East Siberian Sea 50-60 % of the coastline could be segmented, the segmentation of the remaining parts will be completed by middle of 2003 (responsible: M. Grigoriev, S. Razumov, S. Nikiforov, V. Ostroumov). A first approximation of the segmentation was performed for the coastline of the Chukchi. Literature sources and data of A. Kotov (Chukchi Scientific Center) will be used to perform the detailed segmentation and classification, which is anticipated no later than the next ACD workshop (responsible: M. Grigoriev, S. Razumov, D. Drozdov, A. Kotov).

Canadian Beaufort and U.S. Beaufort Sea and Chukchi WG

Much of the Canadian Beaufort Sea coastal segmentation and classification had been accomplished at the October meeting in Bremerhaven (see footnote on page 5). Discussions between Alaskan and Canadian scientists took place in order to maintain consistency across the border. Segmentation of the southern part of the Arctic Islands Archipelago (Banks Island) is underway as part of coastal vulnerability assessments in Canada and is expected to be completed by May 2003. The remainder of the Archipelago will be undertaken in conjunction with colleagues working on the Greenland coasts (Ole Humlum and Hanne Christiansen). The deadline for this segmentation was not set because key participants were not present. The working group also discussed recently initiated projects on the application of remote sensing to Arctic coastal mapping and process studies and ongoing work on landfast ice and ice/sediment interaction processes in the Barrow and Mackenzie regions.

The U.S sectors of the Beaufort and Chukchi seas have been divided initially into 45 and 15 segments, respectively, by Brown, and largely follows subdivisions made in earlier studies. The initial classification will be completed by July. Mahoney contributed a number of site photographs for the Barrow key sites and these will be added to for the other Alaskan sites.

Environmental WG[4]

The Environmental Working Group (EWG) discussed which environmental data should be included for output, how and in what time and spatial scales should the output be delivered, and what additional information is required to complete the output items. To become acquainted with what the field researchers consider of importance the EWG members met

[4] For additional details on environmental data extraction and presentation the reader is referred to the extended abstract of Atkinson and Solomon, this volume p. 19)

with the regional WGs. Additionally, the EWG output was discussed with the GIS WG to be consistent with the requirements and constraints of the final GIS structure.

The most important forcing elements considered by the regional WG members was the action of waves. Another important consideration identified was the impacts of meteorological or storm surges. The criticality of the presence of land-fast ice was also identified, as was the length of the open-water season. The importance of extreme events, and of specific sequences of events, was also identified. Based on such discussions the importance of moving beyond basic meteorological elements and into modelled elements became evident.

Various elements have been selected as relevant to the aims of the ACD project and will be output to the GIS. The first round will include basic meteorological elements as expressed in the form of various derived statistics. The second round will consist of process or temporal model results. To achieve this, various “modelling partners” have been identified either because they developed the relevant model or because they have specific knowledge that pertains to the issue under consideration. Element output layers and modelling partners (in parentheses) are listed in Table 3. Final output form will be in GIS layers, or in a format specified by the GIS technical personnel, delivered directly to the ACD secretariat. Issues that arise will be taken up with the GIS personnel there, or with members of the regional WGs.

The nature of this project includes a important exploratory aspect. Thus to accommodate unexpected results or observations, the EWG will continue to entertain suggestions for new environmental data layers until the deadline, as yet to be finalized, for the submission of new information to the ACD GIS database has been reached.

Table 3. Time line for delivery of environmental data. “Output” refers only to major element categories, and not specific data layers. Each category will consist of one or more specific data layers.

Date delivered by	Output (categorical only)
Jan 2003	Wind field
Jan 2003	Temperature
Jan 2003	Precipitation
Mar 2003	Open water season length
Mar 2003	Tidal ranges
Apr 2003	Surges (working with Proshutinsky)
May 2003	Land fast ice (working with Mahoney)
May 2003	Mean wave energy delivered to coast (working with Orogodov)

GeoInformation System (GIS) WG

It was decided that the ACD coastal segmentation database will be stored in the PANGAEA system (http://www.pangaea.de), which is the core database for “raw” data needed in the calculations of sediment and organic input. For analyses and other scientific purposes within the project the raw data will be exported from this system into different GIS and other processing software.

During the WG meetings Ian May (World Conservation Monitoring Centre) and Frits Steenhuisen (Arctic Center, the Netherlands) and new contributors to ACD, volunteered to produce a small web-based front-end to the PANGAEA system, which will be based on the ArcIMS software. This system will link the tabular data in PANGAEA to the World Vector Shoreline (WVS). The projection will be user defined and the segments will be allocated with a unique identifier. A regional area code should be included in this unique identifier together with a segment number. Tools will be available in this web system to perform corrections (e.g. split and move) and to define a coastal segment based on a polygon (e.g. complicated coast with several islands or barrier coast).

Only one person (the defined regional expert) will have the permission to carry out the segmentation for a predefined sector of the coastline. After the work in this system is completed the data will be transferred to the PANGAEA system for final quality control and permanent storage for the use within the ACD project. Once the data are stored there will be no system to update or change to the content of the database. However, the database will be modifiable through interaction with the database administrator.

The main deliverables from the ACD project will be:

- PANGAEA database (raw field data linked to the WVS with a unique identifier)
- ACD homepage with maps and figures (mainly bitmaps)
- Final product with different derived GIS features on CD-ROM

In addition to the technical details, the members of the WG discussed the issue of estimating coastal lengths based on the WVS. It was decided to initiate a small workshop to address this question. As a first step a review of existing literature on this subject will be finished in July 2003. The next step will be to develop a methodology, probably a statistical model, to be tested in one key area. This work should also include detailed information about the scale of coastal erosion measurements available in the project. Detailed validation data will be needed in representative coastal areas (digital maps scale 1:10000, air photos, high resolution satellite imagery and CORONA images).

2.3 Next Steps

Based on the presentations and on the results of the WGs discussions, the following next steps were identified in the Steering Committee meeting:

ACD Input for the New CAPS CD-ROM

The second version of the CAPS-CD (Circumpolar Active-Layer Permafrost System) will be completed for distribution at the 8th International Conference on Permafrost in July 2003. It was decided that the following ACD products will be submitted:

- Russian bibliography of ACD related literature containing ca. 550 references
- ACD metadata for key sites
- library of circum-Arctic coastal photographs of the ACD key sites and additional coastal sites containing ca. 120 photographs

The products will be available at the ACD web site as well.

Fate and Type of Eroded Organic Carbon

Organic carbon is supplied to the Arctic shelves and basins by rivers and rapid erosion of unlithified coastal materials. This information is important in order to understand the role of the Arctic in the global carbon budget; whether it is a source or a sink for carbon. The knowledge of the type of organic carbon (dissolved or particulate etc.) and its fate is essential to understand the role of coastal erosion in the carbon budget of the Arctic.

The participants agreed to study three key transects with regard of detailed organic carbon studies as a first step. The key transects, located in the Kara, Laptev and East Siberian seas, will be sampled during the summer activities in 2003. A sampling protocol will be developed.

U.S. Arctic Near-Shore Initiative

Planning of a new Land-Shelf Interactions program in the Arctic near shore is underway, and includes elements of the RAISE (Russian-American Initiative for Shelf-Land Environments) activities. In order to coordinate the effort with the ACD program, a summary of the ACD activities was provided to the planning group, headed by Lee Cooper.

Workshop Report

All participants and those unable to attend were invited to submit extended abstracts for the present workshop report.

ACD Publications

The presentations during the workshop documented that several studies are ready or almost ready for publication. Potential papers were identified and a preliminary table of contents for a special issue of a peer-reviewed coastal journal was proposed. The articles are expected to be ready for submission before the start of the summer field season. A series of ACD papers and extended abstracts will be published in the forthcoming publications of the 8th International Conference of Permafrost.

ACD Relevant Meetings in 2003

- ELOISE (European Land-Ocean Interaction Studies), Gdansk (Poland) 24-27 March 2003: ACD presentation by V. Rachold.
- Arctic Science Summit Week, Kiruna (Sweden), 31 March - 4 April 2003: ACD presentation at the IASC Council meeting by V. Rachold (and poster).
- Arctic Workshop, Tromsø (Norway), 3-5 April 2003: ACD poster.
- EGU/AGU (European Geophysical Union / American Geophysical Union), Nice (France), 6-11 April 2003: ACD poster.
- Annual geocryology conference, Pushchino (Russia), 19-21 May 2003: ACD presentation by V. Rachold, Meeting of the ACD INTAS teams.
- 8th International Conference on Permafrost, Zürich (Switzerland), 21-25 July 2003: special session on coastal permafrost, a number of ACD papers, and distribution of the present journal to conference participants.
- ICAM (Arctic Margins Meeting), Halifax (Canada), 30 September - 3 October 2003: special session on Arctic Margins: Coastal and Marine Environmental Geosciences in a Changing Climate; Implications for Development chaired by S. Solomon and L. Johnson (ACD poster and presentation).

Next ACD Workshop

It was decided to organize the 4th ACD Workshop in St. Petersburg (Russia), November 2003, ideally to take place at about the same time as the WCRP Arctic Climate System Study (ACSYS) Final Conference and the Climate and Cryosphere (CliC) meeting. George Cherkashov, VNIIOkeangeologia, has received permission to host the workshop. The status of ACD will be reviewed and the tasks for the next phase of the five-year plan will be developed. In particular, the Steering Committee decided to expand the scope of ACD to cover human aspects and the impact of coastal dynamics on habitats and species. Additional participants to cover these aspects including participants representing AMAP, CAFF, ACIA, LOIRA, LOICZ, WCMC and HARC will be considered based on IASC recommendations.

Acknowledgements

The success of the workshop would not have been possible without the financial and logistic support through the International Arctic Sciences Committee (IASC), in particular, we would like to express our appreciation to Odd Rogne. The Geographical Department of Oslo University provided excellent logistics, special thanks go to Bjørn Wangensteen and Bernd Etzelmüller.

Additional financial support by the following organizations is highly appreciated:

- International Permafrost Association (IPA)
- Canadian Department of Foreign Affairs and International Trade (DFAIT) - Canada-Germany agreement
- INTAS (International Association for the promotion of co-operation with scientists from the New Independent States of the former Soviet Union): project numbers INTAS Open Call 2001-2329 and INTAS Open Call 2001-2332
- International Arctic Research Center (IARC): grant “Analysis of Coastal Meteorological and Oceanographic Forcing in the Arctic Basin”

Finally, we wish to thank the AWI Research Unit Potsdam for supporting the ACD secretariat and several other organization who financed our circum-Arctic coastal field work during the last years.

3 Extended Abstracts

A CIRCUM-ARCTIC ENVIRONMENTAL FORCINGS DATABASE FOR COASTAL MORPHOLOGICAL PREDICTION: DEVELOPMENT AND PRELIMINARY ANALYSES

D.E. Atkinson and S.M. Solomon

Geological Survey of Canada (Atlantic), Bedford Institute of Oceanography, P.O. Box 1006, Dartmouth, NS, Canada B2Y 4A2

Abstract

Understanding the relationship between climate, sea state, and geomorphology is crucial to interpretation of coastal physiography and establishment of predictive capacity, especially for susceptible, "ambulatory" coastlines. Recognizing this fact, the Arctic Coastal Dynamics (ACD) project initiated a climatic component with the following objectives: establishment of a meteorological forcings database based on NCEP/NCAR Reanalysis products; quality assessment of reanalysis data using in-situ data; development and analysis of relevant climatologies (*e.g.* storminess, ice); generation of high-resolution sea level model results; and analysis of spatial and temporal erosion/storminess variability and correlation.

Here we report on progress made toward the first two project objectives. Relevant model and in situ data have been accumulated and prepared for use; criteria for station selection will be reviewed. Quality assessment of the reanalysis data has been conducted for the circum-arctic region for relevant climatic parameters; results from this work will be presented. Finally, spatial and temporal patterns and trends in the data and comparisons will be discussed.

Introduction

The NCEP/NCAR Reanalysis project (NCEP: National Centre for Environmental Prediction; NCAR: Prediction/National Centre for Atmospheric Research) was undertaken to give to the science community accurate, high-resolution data sets for climatological work (Kistler et al. 2001). The data sets produced by this project, and other similar efforts (such as the European Center for Medium Range Weather Forecasting reanalysis project), are known generally as "reanalysis data" and will be referred to here as "NNR data". The Reanalysis project combines an NCAR weather forecasting model and observational data from various sources. The distribution of climate observing sites over the earth is non-uniform, which means the influence exerted by the model on the final reanalysis data result varies according to the location and the parameter under consideration. Given this, it is of interest to compare NNR data back to observed station data ("in situ" data) and to assess its ability to reproduce the observed record for a given time and place. This is especially important if the NNR data are to be used as the basis of analyses conducted in remote, data sparse regions, or if they are to be used as input to other models to derive secondary parameters, such as wave heights (e.g. Proshutinsky 2000, Swail and Cox 2000). Studies that have assessed NNR data for use in sea-state derivation, including Proshutinsky (2000), who examined reanalysis data in the context of driving a storm surge model, and Swail and Cox (2000), who utilized NNR data to drive their north Atlantic wave model, have found that the NNR wind speeds are insufficient during times of observed high-magnitude events.

This paper presents limited results from a detailed comparison of NNR 6-hourly 10 mhag (meters height above ground) winds with observational hourly wind data from weather stations located throughout the circum-Arctic coastal region as well as inland stations from

Canada. Wind speed and direction will be treated separately. In situ data from inland stations were included to determine if discrepancies between observed and NNR data were due to some artefact of coastal proximity. Use of inland stations also offered the opportunity to assess correlation in mountainous terrain, in which stations are presumably heavily influenced by local topographic factors. Given what has been reported in the literature concerning other efforts to correlate NNR data with in situ data, it was anticipated that observed wind speeds would be under-estimated by NNR wind speeds. Thus, another objective of this work was the identification of consistent patterns to the underestimation and development of objective (i.e., computer-based) correction algorithms so the NNR data could be used to satisfactorily drive models generating other environmental data, while minimizing operator intervention.

Data

Specific NNR data elements used for this work consisted of the 6-hourly 10 mhag u and v components of wind. In situ data were obtained from government run surface weather stations. Station selection was guided by ACD project interests, and decisions were based on the following criteria: proximity to designated “ACD monitoring sites”, proximity to coast, length of record, uniform spatial distribution, and proximity to major rivers. Data preparation consisted of an initial extraction of suitable data elements for the required time period (1950 – 2000) and interval (6 hourly), separated into files by station. Station locations were then compared to NNR grid point locations. The nearest grid point location was identified and retained, and data for the identified NNR grid point were extracted and merged with the station data file. These files were used for the correlation work in this paper.

Method

Correlation calculations for wind direction were performed using vector correlation methods and for wind speed, Pearson’s product moment (r) correlation was used. Analyses included all months and were conducted for two speed categories: all wind speeds (hereafter “all speed category”) and >10 m/s (hereafter “high speed category”). The 10 m/s cutoff was based upon the use of this value as a general “storm threshold” described in arctic coastal research (e.g. Solomon et al. 1994). For these types of analyses all available data in the period 1950 – 2000 were retained and for each station a single correlation was performed using a minimum of 30 data pair. Two types of correlation analysis are presented: time aggregate and time series. For the time aggregate analysis all data from a particular point are utilized for a given correlation calculation. For time series analyses all correlation results for a given year are averaged to produce a region-wide time series. The time series data were extracted and smoothed using local linear regression to examine the results for general trends over time and to compare them to a major mode of arctic climatic variability, the Arctic Oscillation.

Correction of systematic underestimation by NNR data of observed high-magnitude wind events was undertaken using an algorithm that searches the NNR data series for “events”, which are defined by various combinations of magnitude, curve profile, and length of time above a set threshold. These were compared to similar occurrences in the in situ data to determine how corrections should be applied.

Results

a. Time aggregate results

Overall results in which correlations were performed on data for the entire 1950 – 2000 period indicate that the NNR wind directions have good to very good correlation with in situ data, while wind speeds have moderate to poor correlations. Results are presented for the "all speed" and "high speed" categories (Fig. 1). Direction correlation was good for the all speed category (Fig. 1a), breaking down only in mountainous (e.g., the Yukon) or fiords areas (e.g., Greenland, Baffin Island), or areas in which a strong local forcing agent is at work (e.g., the north coast of Novaya Zemlya). Direction correlation improved noticeably for the high speed category (Fig. 1b). Speed correlation was moderate to good for the all speed category (Fig. 1c), with the best results inland and over areas of low topography, such as central interior Canada. Speed correlation decreased noticeably for the high speed category (Fig. 1d).

b. Time series results

Time series results showed distinct periods when speed and direction correlations were better (Fig. 2). Direction correlation (Fig. 2a) overall was good, and varied over a relatively small range (0.82 – 0.87). There was no overall trend apparent, although during the first decade of the series the correlation rose steadily and rapidly from an initial low value. Speed correlation (Fig. 2b) overall was poor to moderate, ranging between 0.24 and 0.38. Unlike the trend for direction correlation, speed correlation did possess a generally continuous rising trend over the entire period of record: rapid rise from 1950-1960, plateau 1960-1980, and rise 1980 – 2000.

Interestingly, the patterns of variation in both direction and speed correlations appeared to bear relationships with the trend in the index of the Arctic Oscillation. This included both exhibiting inverse correlation before 1965, both exhibiting the more recent high points (~ 1975 and 1990) and low points (~ 1980 and 1995), and in the case of speed correlation, a similar increasing trend since ~1970.

c. Correction

Attempts to correct NNR data proved moderately successful. Many events that had been underestimated were trapped and adjusted (e.g., Fig. 3). In some cases the corrections overestimate the observed, while in other cases the algorithm did not correct the NNR data. Most of the time, however, estimates improved the existing situation, i.e., that the NNR data sometimes underestimated wind magnitudes.

Discussion

The observed patterns in wind <u>direction</u> correlation are consistent with a model-derived wind field being unable to resolve small-scale fluctuations in lower-speed wind regimes (the latitudinal distance between grid points is ~200 km). The dominance of local-scale influences on the wind regime increases as wind speed decreases. The reverse is also true: as wind speed increases the factors influencing the wind regime also grow in scale until they are of a size that the NNR grid and modelled processes can resolve. This is why direction correlation improves at higher wind speeds in all but the most mountainous or fiord terrain (Fig. 1c). In the case of <u>speed</u> correlation, the large grid spacing and 6-hourly time step precludes the complete depiction of the small, strong low-pressure systems that occur in this region. It is because storms, in particular, are not modelled at their full magnitude that the greatest discrepancies occur during times of the largest magnitude winds (Fig. 1d). The correlation results also indicated that the land/sea interface is problematic for the NNR model to capture, as suggested by the fact that the best speed and direction correlations in the all speeds category (Figs. 1 a-b) tended to be clumped in the continental interior, in areas of low relief. This follows from the spacing between the grid points in the model which, at 200 km, precludes detailed portrayal of many features of the planetary surface.

The observed patterns in the time series results suggest the following. First, model functioning improved during the first decade of the reanalysis project, suggested by the rapid rise in both direction and speed correlation values (Figs. 2a-b). Second, the model has difficulty capturing variability associated with the Arctic Oscillation. This is suggested by the apparent correspondence between the patterns in both circum-arctic wide direction and speed correlation results and the Arctic Oscillation index. Between 1950 and ~1965 it appears as though the correspondence between the two is inverse, however this may also be attributed to the NNR results effectively "stabilizing" during this period, as per the previous conclusion.

The effort to undertake correction of NNR wind speed underestimation, while reasonably successful, does currently have two limitations. The first is that the occurrence of a large-magnitude wind event is not always reflected in the NNR record. Usually there was some response from the NNR data; however, sometimes there was not. If an event has no representation in the NNR record, it is impossible to make any sort of objective correction, and the event will be missed. The second limitation concerns the magnitude of correction that is applied. It has proven difficult to consistently estimate how much correction to apply because a given pattern in the NNR record can correspond to a variety of observed events. For this reason the correction parameter is fixed, which results in some underestimation and some overestimation, and some events being missed. However, the correction effort is still underway. It is likely that more region-specific corrections will yield more accurate results. Despite some shortcomings, overall the corrected NNR data provide a more realistically representation of the observed record. In terms of ACD project requirements, the corrected NNR wind field will prove adequate to generate the necessary derived environmental fields.

References

Kistler, Robert, Eugenia Kalnay, William Collins, Suranjana Saha, Glenn White, John Woollen, Muthuvel Chelliah, Wesley Ebisuzaki, Masao Kanamitsu, Vernon Kousky, Huug van den Dool, Roy Jenne, Michael Fiorino, 2001: The NCEP–NCAR 50–Year Reanalysis: Monthly Means CD–ROM and Documentation. *Bulletin of the American Meteorological Society*: Vol. 82, No. 2, pp. 247–268.

Proshutinsky, A. Yu., 2000. Wind field representations and their effect on shelf circulation models: A case study in the Chukchi Sea. University of Alaska, Fairbanks, Coastal Marine Institute. U.S. DOI. OCS Study, MMS 2000-011. 136p.

Solomon, S.M., D.L. Forbes and B. Kierstead. 1994. Coastal Impacts of Climate Change: Beaufort Sea Erosion Study. Geological Survey of Canada, Open File 2890, 1994, 85p.

Swail, Val R. and Andrew T. Cox. 2000. On the use of NCEP-NCAR Reanalysis Surface Marine Wind Fields for a Long-Term North Atlantic Wave Hindcast. Journal of Atmospheric and Oceanic Technology, 17, 532-545.

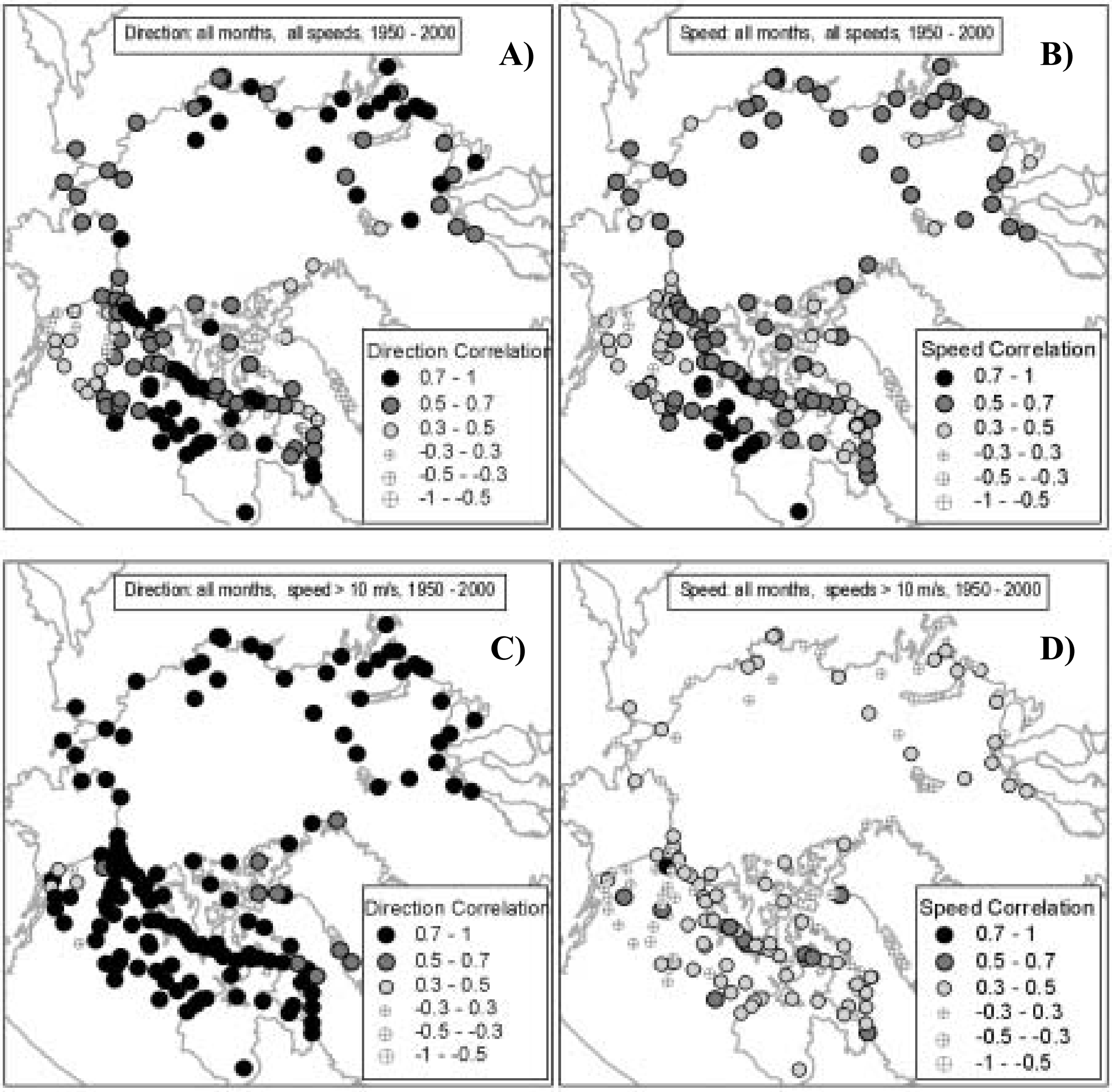

Figure 1. Time aggregate correlation results between wind directions and speeds from NCEP/NCAR 6hly reanalysis data and observed in situ data from weather stations: a) direction correlation results, 1950 – 2000, for all speeds over all months of the year, b) speed correlation results, 1950 – 2000, for all speeds over all months of the year, c) direction correlation results, 1950 – 2000, for high speeds (> 10 m/s) over all months of the year, d) speed correlation results, 1950 – 2000, for high speeds (> 10 m/s) over all months of the year.

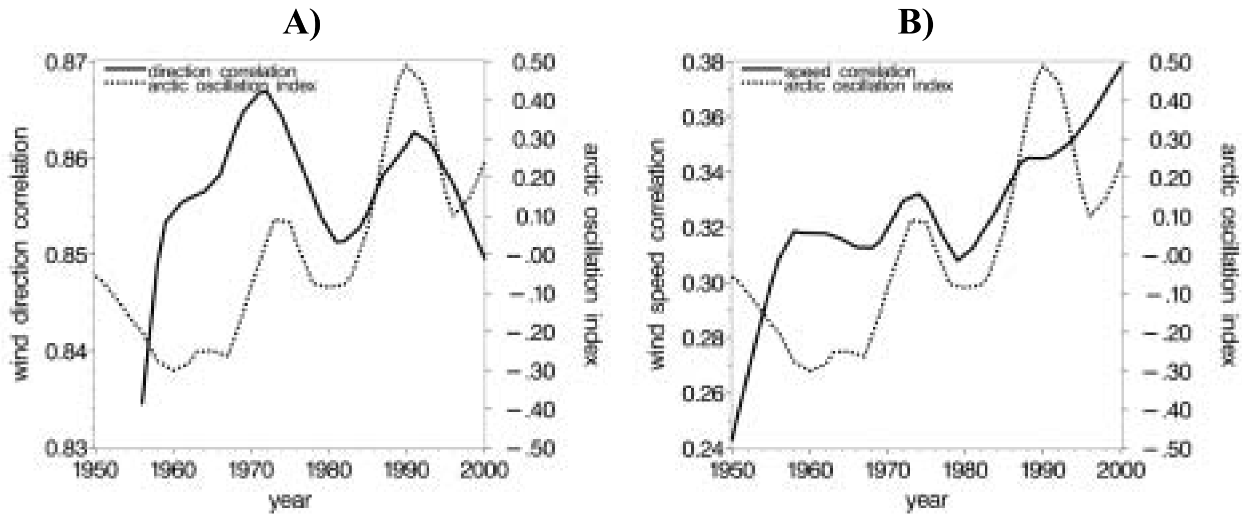

Figure 2. Time series of results of correlations performed between NNR data and circumpolar weather station data. a) Wind direction correlation, all months, and the annual index of the Arctic Oscillation. b) Wind speed correlation, all months, and the annual index of the Arctic Oscillation. All data series smoothed using a local linear regression technique (loess, smoothing factor = 0.25).

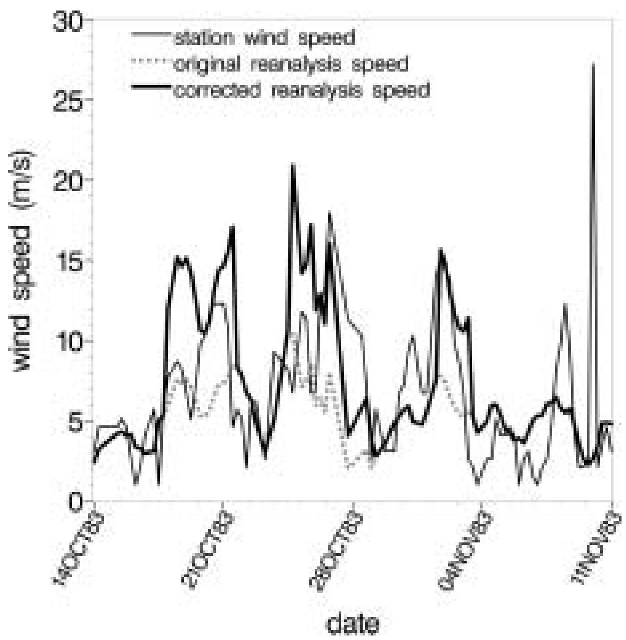

Figure 3. Example of results from the application of a correction algorithm to the NNR wind speed data.

CARBON ESTIMATES FROM TWO BEAUFORT SEA KEY SITES, ALASKA

J. Brown[1] and M.T. Jorgenson[2]

[1]International Permafrost Association, PO Box7,Woods Hole,MA, 02543, [2]ABR, Inc; PO Box 80410, Fairbanks, AK, 99708; email: tjorgenson@abrinc.com.

The Alaskan Beaufort Sea coastline is ~1783 km long and is dominated by low, organic-rich tundra bluffs faced by lagoons and their barrier islands (722 km), exposed tundra bluffs without barrier islands (462 km) and deltas with or without barrier islands (599 km). The present report estimates the annual organic carbon inputs from shoreline erosion from our two lagoon key sites; Elson and Beaufort Lagoons. Elson Lagoon is at the extreme western side of the Beaufort Sea and Beaufort Lagoon site is 60 km west of the Canadian border (Brown et al. 2003; Jorgenson et al. 2003). Previous investigations by the USGS estimated the sediment yield for a 344 km portion of the eroding Alaskan Beaufort coast (average rate of erosion of 2.5m/yr) to be 3.5 x 10^3 m^3/km for bluff erosion, and 3.8 x 10^3 m^3/km for offshore (submarine) sections (Reimnitz et al. 1988) These estimates used the ground ice-depth curve developed for the fine-grained sediments at Barrow; but no carbon estimates were provided for these earlier studies.

Low bluffs along Elson Lagoon consist of ice-rich, fine-grained sediments, surface and buried peats, and ice-wedges. A time series of erosion rates from 1949 to 2000 along the 10.8-km long reach of lagoon coast were determined by georeferencing aerial and high-resolution satellite imagery. Erosion rates for the period 1979-2000 were 47% higher (0.86 m/yr) than 1948-1979 (0.56 m/yr) and 23% higher than the 51-year average (0.68 m/yr). A total of 28 hectares of land was lost between 1979 and 2000 (Table 1). A sustained shift of storm surge-inducing winds at Barrow appears to correspond to the trend of increased erosion along the shores of Elson Lagoon. Using an average value of 50% ice volume (Sellmann et al. 1975), our initial estimates of annual sediment yield above sea level are 1.6 10^3 m^3/km for mineral sediment. Soil organic contents were based on available published soil map and carbon values for the principal soil units. We assigned carbon values of 50 kg/m^3 for these tundra soils (Bockheim et al. 1999, 2001). For the Barrow estimates we did not consider the carbon that occurs below the one-meter depth since the majority of soil and buried peats were observed to occur in this upper one-meter section. Based on the previously estimated ground ice contents, elevations, and erosion rates annual carbon input from the eroding shorelines (above water portion) is estimated at 63,500 kg C /km for this section of Elson Lagoon.

Coastal erosion over a fifty-year period, and permafrost characteristics of the shoreline associated with that erosion, were assessed at Beaufort Lagoon in northeast Alaska. Soil stratigraphy was obtained from two bank exposures on abandoned floodplain deposits and one exposure on a sand sheet deposit (Table 2). All exposures had a thin (10–11 cm) fibrous peat accumulation at the surface underlain by a thin (17–23 cm) eolian silt deposit. Below these surface layers were thick buried accumulations of disrupted, amorphous peat clumps extending as deep as 1.5 m. Moisture contents (% vol.) for soils with segregated ice ranged from 52.7% to 84.4% in frozen soils. The volume of excess ice from segregated ice in the entire profiles ranged from 12.3% to 49.7%. Volume of wedge ice ranged from 10% to 20%. Organic carbon stores were 48–79 kg C/ m^2 in the top 1 m, and 54–136 kg C/ m^2 for the entire portion of the banks above water level (1.7 to 3.3 m high). Photogrammetric analysis of aerial photography from 1948 and 1978, and IKONOS imagery from 2001, revealed a mean erosion rate of 0.5 m/yr for the 1948–1978 period and 0.5 m/yr for the 1978–2001 period along a 10 km stretch of coastline. Annual organic carbon input from the eroding shorelines (above water portion) ranged from 37,800 to 68,000 kg C/km of shoreline for the three sites.

Based on these two widely separated sites ~11 km in length, we estimate that the annual carbon input from eroding shorelines facing lagoons (722 km) along the Beaufort Sea Coast fall within the range of 37,800 to 68,000 kg C/km of shoreline. Rates of carbon input from exposed tundra bluffs are not yet available but probably are higher because of higher erosion rates. In contrast, deltas are flat, depositional environments that are accreting instead of eroding sediments and we assume the carbon input from shoreline erosion along deltas to be zero.

This report is based on two papers to be published in the proceedings of the Eighth International Conference on Permafrost, Zurich in July 2003. The following individuals collaborated in these investigations: Orson Smith, William Lee, and Oceana Francis, University of Alaska Anchorage; Matt Macander, ABR, Inc; Janet C. Jorgenson , U.S. Fish and Wildlife Service; Chien-Lu Ping, University of Alaska at Palmer; Jennifer Harden; U.S. Geological Survey, and James Bockheim, University of Wisconsin.

References

Bockheim, J.G., L.R. Everett, K.M. Hinkel, F.E. Nelson, and J. Brown, 1999. Soil organic carbon storage and distribution in arctic tundra, Barrow, Alaska. Soil Science Society of America Journal 63: 934-940.

Bockheim, J.G., K.M. Hinkel, F.E. Nelson, 2001. Soils of the Barrow region, Alaska. Polar Geography25: 163-181.

Brown, J., M.T. Jorgenson, O.P. Smith, and W. Lee, 2003. Long-term rates of erosion and carbon input, Elson Lagoon, Barrow, Alaska. in Proceedings, 8th International Conference on Permafrost, A.A. Balkema Publishers, Rotterdam, Netherlands (in press).

Jorgenson, M.T., M. Macander, J.C. Jorgenson, C-P. Ping, and J. Harden, 2003. Ground ice and carbon characteristics of eroding coastal permafrost at Beaufort Lagoon, northern Alaska in Proceedings, 8th International Conference on Permafrost, A.A. Balkema Publishers, Rotterdam, Netherlands (in press).

Reimnitz, E., M. Graves, and P.W. Barnes, 1988. Map showing Beaufort Sea coast erosion, sediment flux, shoreline evolution, and the erosional shelf profile (1:82,000). *U. S. Geological Survey Miscellaneous Investigations Series Map I-1182-G* and accompanying text. 22 pp.

Sellmann, P.V., J. Brown, R.I. Lewellen, H. L. McKim and C. J. Merry; 1975. The classification and geomorphic implications of thaw lakes on the Arctic Coastal Plain, Alaska. U.S. Army CRREL Research Report 344, 21pp.

Table 1. Annual sediment and carbon losses due to erosion, Barrow, Alaska (modified from Brown et al. 2003).

Segment	Segment Length (km)	Mean Elevation (m)	Photo Interval	Area Lost (ha)	No. Years	Mean Width Lost (m)	Mean Width Lost (m/yr)	Annual Sediment Input* (10^3 _ m^3/km)	Annual Carbon Loss in Top 1 m (kg/km)
A	-2.9	2.1-	1979-00	4.4	21	18	0.86	0.9	43,000
B	2.0	3.3	1979-00	2.8	21	13.7	0.65	1.1	32,500
C	3.4	2.9	1979-00	6.4	21	18.8	0.9	1.3	45,000
D	2.5	-1.8	1979-00	14.6	21	57.7	2.75	2.5	137,500
A-D	10.8	2.5	1979-00	28.2	21		1.27	1.6	63,500

*assumes 50% of mean bluff height is ground ice.

Table 2. Annual sediment and carbon losses at Beaufort Lagoon, northwestern Alaska (modified from Jorgenson et al. 2003).

	Transect 1	**Transect 2**	**Transect 3**
Bank height above water (m)	1.7	3.3	2.1
Mean thaw depth – tundra (cm)	38.2	37.9	39.2
Mean thaw depth – foreshore (cm)	100	119	46
Mean thaw depth - lagoon (cm)	nd	177	73.5
Cumulative organic thickness (cm)	32	60	29
Maximum organic depth (cm)	>82	60	85
Total amount of excess segregated ice (%)	12.3	49	49.7
Total amount of wedge ice (%)	10	20	15
Total volume of all excess ice (%)	21	59	57
Total organic carbon in top 1m; excluding ice wedges (kg C/m 2)	48	79	49
Total organic carbon in entire bank to water level; excluding ice wedges (kg C/m 2)	60	170	76
Total organic carbon in entire bank to water level, including ice wedges (kg C/m 2)	54	136	65
Total mineral sediments in entire bank to water level; including ice wedges (kg C/m 2)	794	998	871
Average erosion rate 1948-2001(m/yr)	0.7	0.5	1
Annual organic carbon input (kgC/m of shoreline)	37.8	68	65
Annual organic carbon input (kgC/km of shoreline)	37,800	68,000	65,000
Annual mineral sediment input (kgC/km of shoreline)	555,800	499,000	871,000

INVESTIGATIONS OF COASTAL DYNAMICS AT THE ACD KEY SITES IN THE WESTERN RUSSIAN ARCTIC (2001-2002 FIELD WORK)

G.A. Cherkashev, B.G. Vanshtein, Yu.G. Firsov and M.V. Ivanov

VNIIOkeangeologia, St-Petersburg, Russia

Precise geodetic and bathymetric measurements allowing to evaluate coastal retreat rates are of great importance for studying coastal dynamics.

The coastal survey conducted by our team included the following investigations:

- Determination of position and height of major fixed elements which can be used for the connection with both earlier conducted and following observations of coastal dynamics;
- Reconnaissance studies of existing geodetic points in the study area and determination of their precise coordinates in the WGS-84 system to calculate corrections providing the opportunity to use topographic and navigation maps as well as aerial photographs of the last years;
- Detailed tacheometric survey of the thermoerosional coast with precise fixation of the coastal scarp top and other morphostructures;
- Detailed survey of the bottom topography from the water level to the 10 m isobath at thermoerosional coasts using a NAVSTAR portable satellite device in differential regime and a digital echosounder;
- Determination of the current coastline position (i.e. water level, upper edge of the beach, upper edge of the coastal scarp) at the extended sections of both retreating and accumulative coasts using high-precision satellite equipment.

Following the ACD strategy field investigations should be implemented at specific key sites which are characteristic for the entire coastline. In the western Russian Arctic these key sites have been chosen in the Kara Sea (south-western coast of the Yamal Peninsula and Yugorsky coast) and in the Barents Sea (north-western coast of the Kolguev Island). In this paper we present some results of these investigations.

1. The Marre-Sale key site (69°43’N, 66°49’E) is situated at the south-western coast of Yamal Peninsula (Kara Sea). Earlier hydrographic investigations at this site were carried out in 1970. The subbottom topography was mapped from the pack ice. The depths were connected to the level of a fixed element which was installed at the polar station in 1952. A marine navigation map at a scale of 1: 25 000 was published in 1990. Systematic observations of coastal dynamics at the Marre-Sale key site were initiated by the Institute of Earth’s Cryosphere RAS in 1978 and were conducted on a coastal section of ca. 4.5 km length. More than 60 observation ranges were arranged perpendicular to the coast. The results of these observations constituted the digital data base on coastal dynamics for the last 22 years. It was observed that coastal retreat rates cyclically vary in time (Vasilyev et al. 2000) with periods of 20 years. A correlation between sea wave energy and coastal retreat rates has been noted. In the context of the ACD program the scales of observations at the Marre-Sale key site were expanded and, particularly, observations were conducted not only at thermoerosional but also at accumulative coastal sections. Preliminary studies carried out in 2001 included the observations using modern geodetic and GPS technologies in addition to conventional studies.

The study area was significantly extended and covered not only thermoerosional but accumulative types of the coasts located 40 km southward of the site. The observations at the coastal area of 4.5 km length showed that the total coastal retreat between 1941 and 2001 accounted for 147 m. Repeated observations of the upper edge of the coastal scarp conducted in 2002 using GPS and an electronic tacheometer exhibited a maximum coastal edge displacement of 6 m per year in the northern part of the site with an average displacement of 1.9 m. The most affected are inflections of the edge lines where the capes are cut off and gully mouths are deepened.

2. The same investigations were conducted in 2001 at the key site located in the Shpindler area on the Yugorsky coast (south-western Kara Sea). The studied offshore area of the site was 1.6 km^2, the onshore area 0.3 km^2. The coastal survey fixing the average multiyear coastline and the upper and lower edges of the coastal scarp was carried out over 3 km.

3. During the field season of 2002 coastal investigations were carried out at the key site on the north-western coast of Kolguev island (Barents Sea), southward of Sauchikha River mouth. The studied area of the offshore site was 1.3 km^2, of the onshore site 0.2 km^2. In addition, a coastal segment of 12 km length was surveyed in respect of the position of the average multiyear coastline and the upper and lower edges of the coastal scarp.

The field observations in 2001 and 2002 resulted in the elaboration of jointly used hardware and software components, i.e. electronic tacheometer DTM-350, GeoExplorer 3 satellite device and a small-scale echosounder installed in the Zodiak-type sloop. The coastal segments were surveyed using a water level database of stations of the Russian Arctic containing information on sea level fluctuations from the 1960-80s. The accuracy of the coastal scarp contours is 0.1-0.3 m and the accuracy of the determinations of the current position of the sea level relative to the average sea level is 2-3 m. The positions of the points and contours were determined in the international coordinate system (UTM) and the elevation was recorded in national elevation system (Baltic).

All collected information on the offshore and onshore topography of the sites is available in digital form that allows to create 3D digital elevation and bathymetry models and enables the subsequent analysis of coastal dynamics by means of GIS-technologies. Thus, during the field seasons of 2001 and 2002 key observations were conducted and the three key sites were prepared for future studies of coastal dynamic in the western Russian Arctic.

CHARACTERIZATION OF COASTAL POLYNYAS IN THE ARCTIC WITH REMOTE SENSING TECHNIQUES AND COMPARISON WITH NUMERICAL MODEL INVESTIGATIONS

S.T. Dokken

Norwegian Computing Center, Sverre.Dokken@nr.no.

Coastal polynyas in the Arctic basin from the winter period are characterized using ESA European Remote Sensing satellite (ERS)-1/2 Synthetic Aperture Radar (SAR). A SAR polynya algorithm is used to delineate open water, new ice, and young ice, and to define the size and shape of polynyas. In order to extract radiometric and contextual information in the ERS SAR PRI images, three different image classification routines are developed and applied. No in situ data have been available for verification of the polynya shapes and sizes, but one of the ice classification routines has been verified earlier using ground truth data. The SAR polynya algorithm is demonstrated to be able to discriminate between the polynya and the surrounding ice area for 85 analyzed cases. The results from the SAR algorithm are compared to passive microwave data (a recent Polynya Signature Simulation Method (PSSM)) and a numerical polynya model (NPM) forced by National Center for Environmental Predictions (NCEP) wind fields and air temperatures. The PSSM calculates the polynya shape and size, and delineates open water and thin ice. For polynyas of all sizes it has a correlation of 0.69 compared to the SAR images. For polynyas with widths greater than 10 km the correlation increases to 0.83. The NPM computes offshore coastal polynya widths, heat exchange, and ice production. Compared to SAR data, it overestimates the maximum size of the polynya by about 15% and has a correlation of 0.71 compared to the analyzed SAR PRI images. The polynyas in our main investigation area, located at Franz Josef Land, are found to be primarily wind driven. The surrounding large-scale ice drift and tidal currents have little effect on the polynya behavior. The presentation will demonstrate that the SAR polynya algorithm in combination with the NPM is a powerful tool for investigating and characterizing polynyas and other coastal sea ice openings at various scales in the Arctic.

THE LANDSCAPE MAP OF THE RUSSIAN ARCTIC COASTAL ZONE

D.S. Drozdov, G.V. Malkova (Ananjeva) and Yu.V. Korostelev

Earth Cryosphere Institute SB RAS, Vavilov str, 30/6, 74a., Moscow, 119991, Russia, Email: ds_drozdov@mail.ru

The landscape map of the Russian Arctic coastal zone (scale 1:4 000 000) is prepared using the principle based on separation of landscape unit types. This principle is widely used by the authors and their colleagues for preparing landscape, geocryological and environmental-geological maps of northern territories (the chief of these projects is E.S. Melnikov). At the first stage, the basic landscape forming features of the natural environment that influence on-shore, exogenic processes are sorted. These main features are the following:

- The location of the territory in a particular natural-climatic zone or subzone (for example, in arctic tundra, in northern forest-tundra, or in central taiga etc.).
- The location of the territory in units of altitude zonation (for example, in plains, plateau and mountains).
- The genetic and main morphological attributes of relief (for example, landscapes of marine plains and terraces, glacial landscapes, erosive denudation landscapes of mountains and piedmonts etc.).
- Lithological and petrographic composition of the sediments and rocks (clay, sand, debris material, karst and non-karst bedrocks etc.).

The overlay of all these maps results in a final landscape map that can serve as the basis to characterize modern geological processes. The units on the obtained landscape map can be used to estimate boundaries of common ranges. In the analysis of the landscape map the boundaries of natural-climatic zones are most important, the boundary of ground types are least important.

The described technique of preparing landscape maps was first tested in preparation of the Circumpolar Permafrost Map project (carried out by International Permafrost Association IPA), and the Circumpolar Arctic Vegetation Map project (chief of the CAVM project, D.A. Walker, USA). For the present project more attention is paid to the low lying marine and alluvial landscapes directly along coastal line.

For a topographic base, the digital, circumpolar Lambert projection map is used. Rivers, lakes and sea coast are present within the landscape polygons. The scale of information on the obtained landscape map of the Russian Arctic coastal zone is 1:4 000 000. An eight-digital index permits presentation of all kinds of information on each landscape site. In preparing the landscape map the author's own materials obtained in the field from various northern regions were used. Also satellite images and cartographic materials of appropriate or larger scale were employed. The following maps used were:

Churinov M.V. (ed.) et al., 1972. The Engineering-geological map of the USSR (scale 1:2 500 000). Moscow, GUGK[State comity on geodes and mapping of the USSR].

Ganeschina G.S. (ed.), Adamenko O.M. et al., 1976. The map of the Quarternary (surface) Geology (scale 1:2 500 000). Moscow, GUGK.

Gudilin I.S. (ed.) et al., 1980. The landscape map of the USSR (scale 1:2 500 000). Moscow, GUGK.

Melnikov E.S. (ed.) et al., 1999: The landscape map of the Russian permafrost (scale 1:4 000 000). Moscow, Earth Cryosphere Institute SB RAS.

This study is supported by INTAS (N 2332).

THE SPATIAL DISTRIBUTION OF COAST TYPES ON SVALBARD

B. Etzelmüller[1], R.S. Ødegård[2] and J.L. Sollid[1]

[1] Department of Physical Geography, University of Oslo, Norway, [2] Gjøvik College, Gjøvik, Norway

Introduction

In connection with an oil spill protection program in the Barents Sea a major part of the coast of Svalbard was mapped with regard to geomorphological coast types and coastal fauna (Dep. of Physical Geography, Univ. of Oslo and Norwegian Polar Institute, unpublished). In collaboration with the Norwegian Polar Institute the coast maps were produced in a scale of 1:200,000 at the Department of Physical Geography, University in Oslo, led by Prof. J.L. Sollid. All geomorphological information was digitized, and a Geographical information system of Svalbard's coast was established. In this extended abstract paper, digital spatial analyze techniques were used to depict the spatial distribution pattern of different coast types on Svalbard. A coastal zonation of Svalbard is suggested based on geomorphological parameters.

Setting

The Svalbard archipelago is located between 74°N and 81°N and 10°E and 35°E (Fig. 1), and comprises a total area of approximately 63,000 km^2, where more than 60% of the land area is glaciated. The archipelago consists of the islands Spitsbergen, Nordaustlandet, Barentsøya, Edgeøya and a range smaller islands. The climate is relatively mild, seen in relation to the high latitude. At the Spitsbergen west coast annual mean temperature of -6°C to -8°C are measured (Hanssen-Bauer et al. 1990). Besides some taliks beneath the accumulation area of the glaciers the whole island has continuous permafrost conditions, with measured permafrost depth of 500 m, decreasing to ca. 100 m in the coastal areas (Liestøl 1977; Isaksen et al. 2001). The coastal water areas are usually covered with sea ice throughout the wintertime, with a maximum in April. Off the west coast sea ice belt open water is possible during the wintertime (cf. Vinje and Kvambekk 1991)

The geology of Svalbard displays all the main geological systems from Precambrian to Quaternary (Fig. 2). Pre-Devonian rocks consist mainly of hard metamorphic rock types, located on Nord-Austlandet and along most of the west-coast of Spitsbergen. Devonian conglomerates, sand- and siltstones dominate in northern Spitsbergen, while often fine-grained sedimentary rocks from the Mesozoic and Tertiary covers most of central Spitsbergen and the islands of Edgeøy and Barentsøya. During the Quaternary time period Svalbard was glaciated several times. During Weichsel maximum the ice reached the continental shelf (e.g. Mangerud et al. 1992).

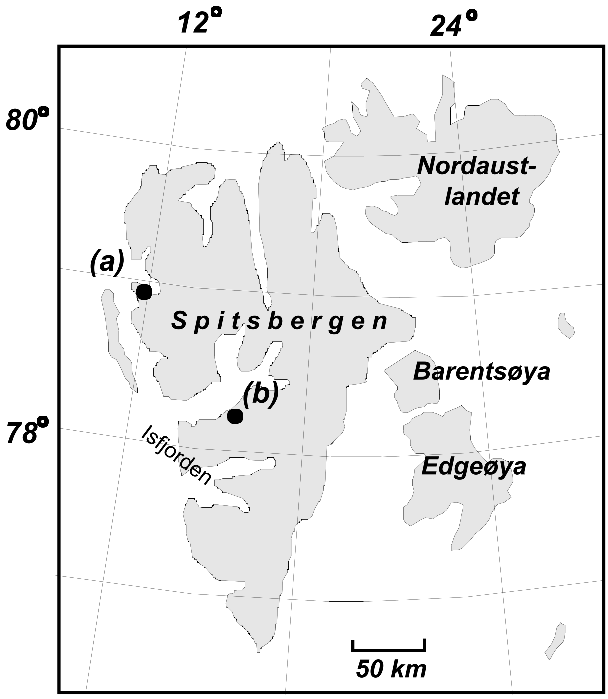

Figure 1. Key map over the Svalbard archipelago. (a) Ny-Ålesund, (b) Longyearbyen.

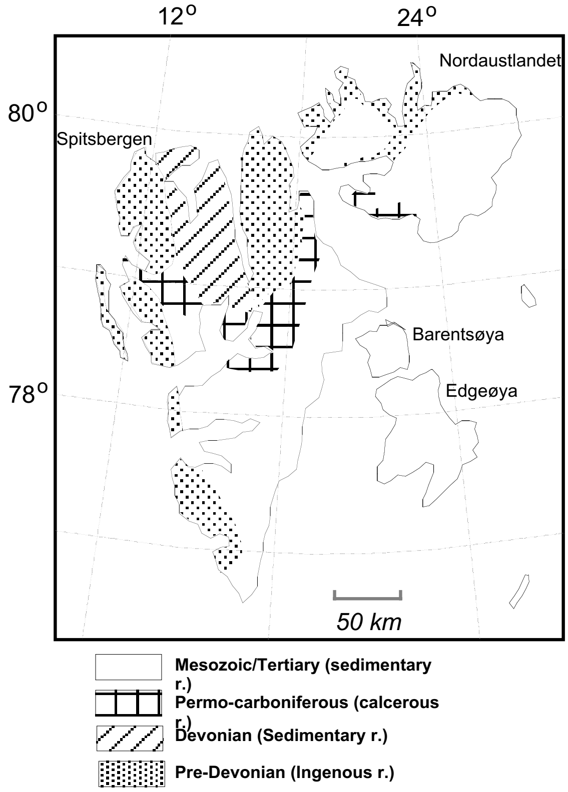

Figure 2. Simplified geological sketch over Svalbard.

Methods

The classification system of the coast maps is based on grain-size distribution of beach sediments and geomorphological parameters as differences in bedrock- and unconsolidated sediment cliffs and abrasion platforms in connection to rock shores (Table 1). A comparable system was used on the Norwegian mainland (Klemsdal 1979). In order to make the system operate for Svalbard conditions, there were applied some corrections, especially in relation to grain-size parameters and rock cliffs (see also Owens et al. 1981; Harper and Sawyer 1983).

The coastal types and grain size of beach sediments were mapped using vertical air photos in scale 1:30,000 and 1:50,000. Additionally, helicopter-borne video pictures, which are available along most of Svalbards coast at the Dep. of Phys. Geography, Univ. of Oslo, were used. The coast maps are based on the topographic maps 1:100,000 (©Norwegian Polar Institute). Mapping accuracy and coast type generalization is approximately in the range 300 m to 500 m. The classification is based on five classes of grain-size distribution and 14 parameters for different geomorphological types. Beach sediments in front of rock cliffs are mapped as well (Table 1).

The coastal maps were digitized using the GIS ARC/INFO (ESRI). Digitizing was based on the topographic maps in scale 1:100,000. Totally ~6000 km coast line was registered in that scale. The coast line was split into segments, containing an unique code which attributes the coast types (Fig. 3). Additionally, the coast segments contain information on bedrock geology. The coastal GIS developed within this project offers the possibility to analyze frequency or coast length relationships interactively, both by selecting certain geographical regions in relation to location, bedrock geology or wave energy exposure.

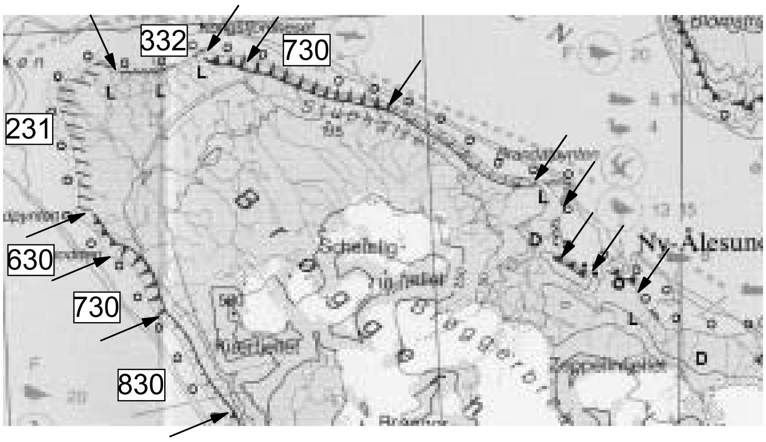

Figure 3. Detail from a coast map 1:100000 (Forlandsundet, western Spitsbergen, Ødegård et al. 1987). An unique code represents coast types, grain size and special coast forms (see Table 1). Total 3400 coast segments were registered and more than 6000 km coast line was digitized (in scale 1:200000).

Some Results and Discussion

Unconsolidated sediments dominate in the shore zone of Svalbard: 74% of the shore line is classified as unconsolidated material or unconsolidated beach material (narrow beach) in front of bedrock cliffs. About 40% of the shore embodies exposed bedrock as cliffs (27%) or rocky shore (13%). However, active cliffs in unconsolidated or ice-rich sediments are rare. Coast with glaciers calving in the sea is 12%, not taking the glacier areas of Nordaustlandet into account (Fig. 4b). The grain size of the unconsolidated sediments is dominated by gravel to coarse gravel (Fig. 4a). Finer material is found in connection to deltas developed in the innermost fjord areas, while boulder rich sediments are mostly found in areas with hard rock types (northwestern Spitsbergen, Hinlopen) or shores affected by talus development (Isfjord). The coastal pattern indicates coarse sediment production in the coastal zone, probably mostly due to frost weathering (see also Ødegård and Sollid 1993; Ødegård et al. 1995). Most active material translocation is related to inner fjord areas and glacier fronts connected to melt water river outlets and outwash planes.

By analyzing the occurrence of different coast types, certain patterns can easily be identified. E.g., the outermost western coast of Spitsbergen consists of a different frequency of coast types than the eastern coast of Spitsbergen along Storfjorden (Fig. 5a). There, wide sediment beaches and calving glaciers dominate. The first indicate low wave action and good supply of sediments. This area has long lasting sea ice. The west-coast is exposed, and dominated by beach ridges and rocky shores, calving glaciers are mostly lacking. Higher wave energy, building beach ridges, and low material supply dominate this coast. Another pattern is related to bedrock geology. When regarding grain size distribution on coast types frequency as a function of bedrock type, we can observe a clear grading from hard metamorphic pre-Devonian bedrock towards intermediate Mesozoic sedimentary bedrock to softer Tertiary types (Fig. 5b). In hard bedrock areas grain size is coarser with most shores dominated by bouldary gravels. Unconsolidated sediment in the shore zone is 83% in pre-Devonian bedrock versus 98% in Tertiary bedrock types. If we assume active beach erosion in areas where we have low rock cliffs with beach material in front of, this types of coast we find in 35% of the coast stretches in hard bedrock, while the number is 71% in Tertiary rock types.

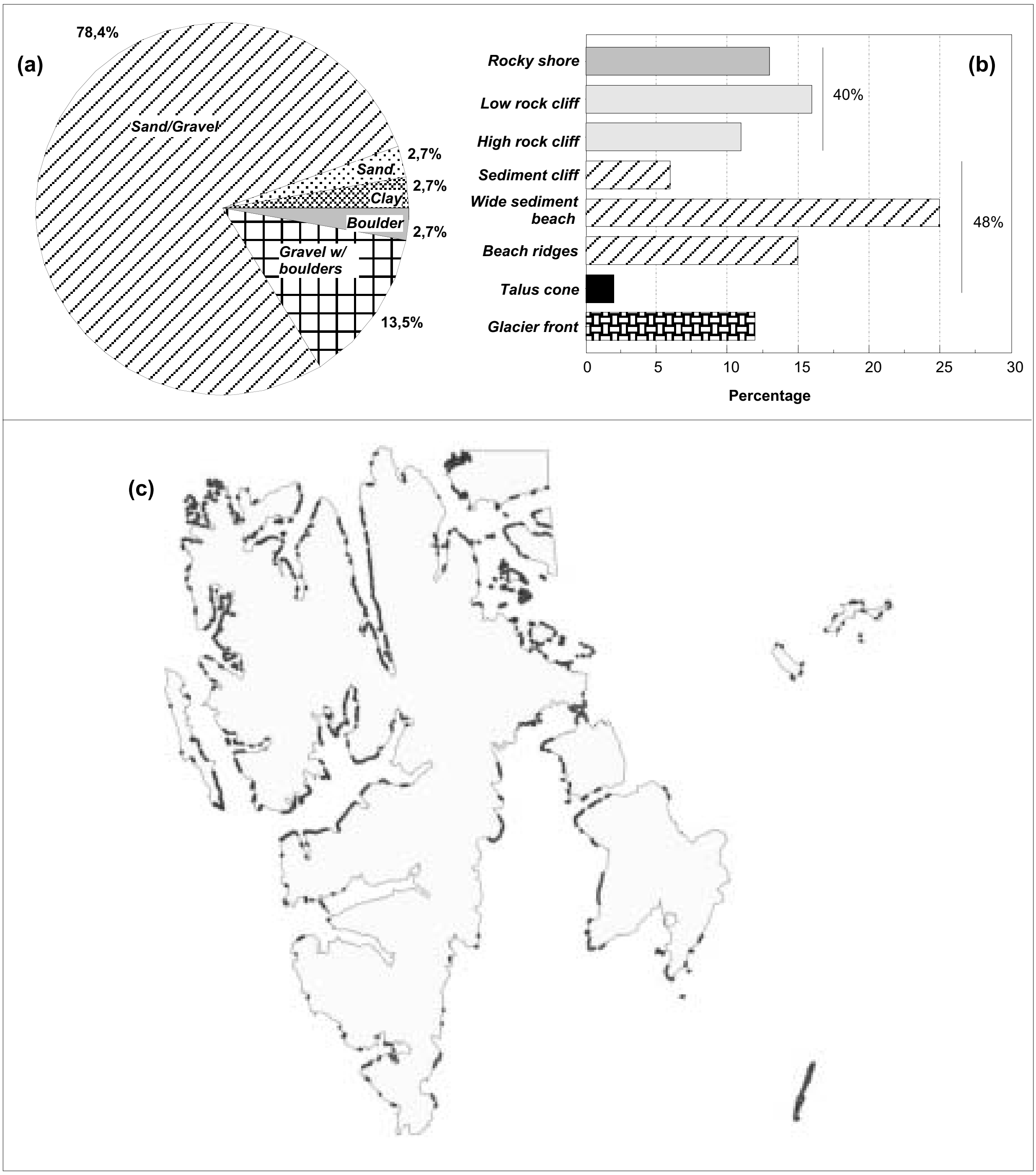

Figure 4. (a) Grain size distribution of unconsolidated sediments in the coast zone. (b) Frequency of geomorphological coast types on Svalbard. Calving ice cliffs are underrepresented as only parts of Nordaustlandet is within the analyses. (c) Spatial distribution of coastal cliffs in bedrock on Svalbard, indicating active zones of coast erosion. Active sediment cliffs are only identified at ca. 5% of the coast line.

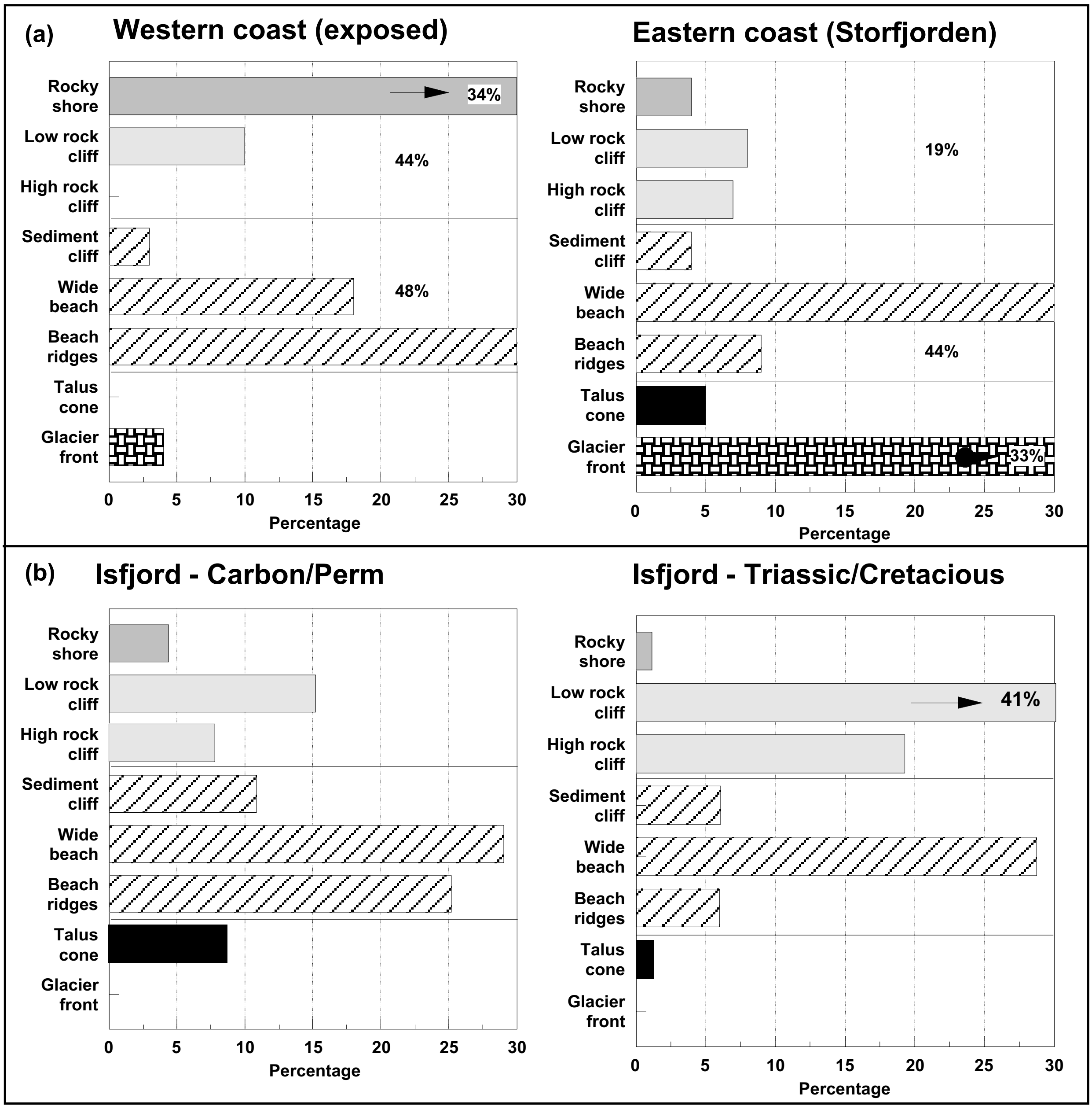

Figure 5. Frequency distribution of geomorphological coast types of certain areas on Svalbard. (a) Exposed western coast and eastern coast (Storfjorden) on Spitsbergen. (b) Coast types along Isfjorden within Permo-carboniferous (often calcareous) and tertiary rock types (mostly sedimentary, sand and silt).

The Coastal Zones on Svalbard

Svalbard is classified in different coastal regions. Eight coast classes on Svalbard were identified (Fig. 6):

1) *Wave exposed areas along the west- and north coast of Spitsbergen*. The area is dominated by rocky shore (> 30%), barriers and lagoons, indicating active marine transport processes along the coast. Calving glaciers and rock cliffs (< 15%) are seldom.

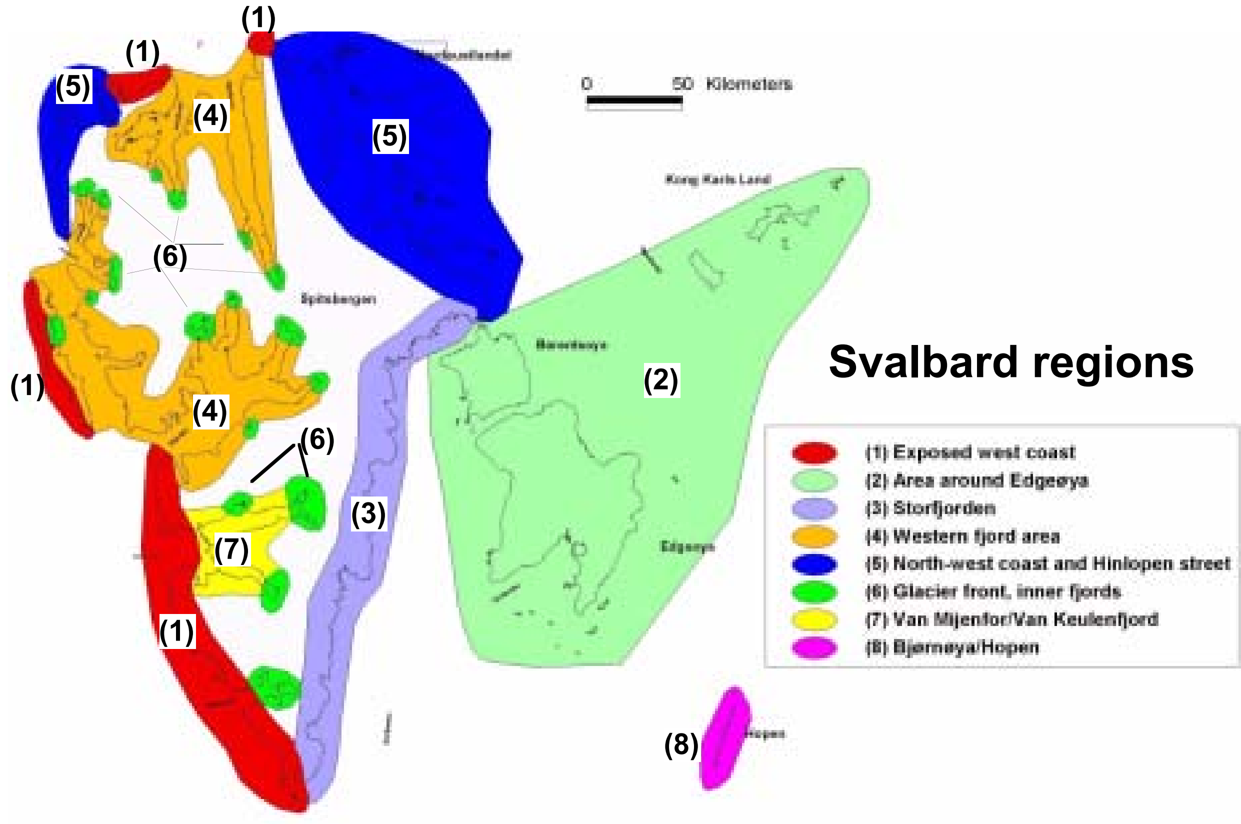

Figure 6. Proposed coastal regions on Svalbard, based on frequency analyses and subjective classification.

2) *Moderate wave exposed area at Barentsøya, Edgeøya and Kong Karls Land*. The coast is moderately exposed to waves because of land fast ice during most of the year, and active erosion in bedrock is supposed to be low.

3) *Coast dominated by calving glaciers - the Storfjorden area*: Glacier fronts and wide sediment beaches, showing lower wave action and sediment supply by the glaciers, dominate this area. Rocky shores and rock cliffs are more seldom.

4) *Coast dominated by rock cliffs with a narrow beach - the western fjord areas*: Rock cliffs behind a narrow beach, indicating active coastal erosion in bedrock, dominate the area. Grain size of the beach is often more sandy, reflecting the dominance of Mesozoic and Tertiary sedimentary bedrock in the area.

5) *Coast dominated by rock cliffs and rocky shore with low amount of beach sediments - the north-west coast of Spitsbergen/Hinlopenstretet*: This area is dominated by metamorphic rocks and sea ice exposition towards north and northeast. Grain size is coarser, and the amount of unconsolidated sediments in the shore zone is low. Rocky shore and rock cliffs are dominating. This area is one with the lowest frequency of coast types developed in unconsolidated material.

6) *The inner fjord areas*: These areas are dominated by glacier fronts or glacier meltwater outlets. There is an abundance of deltas and sand-rich sediments. These areas have the highest abundance of clayey beaches and wide tidal flats, and the shore zone is considered to be more subjected to rapid changes than elsewhere on Svalbard. Wide beaches dominate, cliffs are not frequent and rocky shores absent.

7) *Coast dominated by unconsolidated sediments - Van Mijenforden/Van Keulenfjord*: Sandy to gravelly beaches dominate this area, with 20% of the area being classified as sediment cliffs. This area is potentially prone to coast erosion. Sea ice cover duration is longer than in other fjord areas.

8) *Coast dominated by high rock cliffs - the islands of Bjørnøya and Hopen*: These islands are almost totally dominated by high rock cliffs, with 70% of the shore area. Sediment beaches are seldom.

This rough classification gives an overall indication of coast types, applicable both for coast management and erosion considerations. However, an objective, statistical analyses of coast type distribution on Svalbard (clustering, factor analyses etc) remains to be done.

Table 1. Coastal classification for Svalbard.

Classification based on grain size distribution		
1. Clayey beach	C	Grain size less than 0.063 mm, beach width 50-500 m in delta areas and 10-20 m in lagoons.
2. Sandy beach	S	Grain size between 0.063 and 2 mm. Beach width 10-20 m.
3. Gravelly beach	G	Grain size ranging from coarse sand to coarse gravel. Beach width 5-20 m.
4. Gravelly beach width boulders	GB	As (3), but with boulders.
5. Boulder rich beach	B	Grain size more than 28 cm. Beach width 5-10 m.
Classification based on geomorphological parameters		
1. Rocky shore / abration platform	Rs	Rocky shore without cliff development
2. Low cliff, in unconsolidated sediments	LcS	Cliff in unconsolidated material, < 5 m high
3. High cliff, in unconsolidated sediments	HcS	Cliff in unconsolidated material, > 5 m high
4. Low cliff in bedrock	LcR	Cliff in exposed bedrock, < 5 m high
5. High cliff in bedrock	HcR	Cliff in exposed bedrock, > 5 m high
6. Talus cone	Tc	Talus cone which reach sea page
7. Beach ridge	Br	Beach ridge in unconsolidated beach material
8. Wide sediment bach	Sb	Flat beach in unconsolidated material, > 20 m width, without beach ridge development
9. Stacks	St	Isolated coastal cliff, common on Bjørnøya
10. Calving ice front	If	Calving ice front in the sea/fjord
11. Tidal flat	Tf	Wide tidal flat.
12. Lagoon	La	
13. Delta	De	
14. Ice on the beach	Ei	Exposed ground ice or glacier ice in the shore zone.

References

Hanssen-Bauer, I., Kristensen Solås, M. and Steffensen, E.L., 1990. The climate of Spitsbergen. 39/90, The Norwegian Metereological Institute, Oslo.

Harper, J.R. and Sawyer, B., 1983. Coastal Analysis of the Long Beach Segment and Broken Islands Group,, Woodward-Clyde Consultants, Victoria BC, Canada.

Isaksen, K., Holmlund, P., Sollid, J.L. and Harris, C., 2001. Three deep alpine permafrost boreholes in Svalbard and Scandinavia. Permafrost and Periglacial Processes, 12(1): 13-26.

Klemsdal, T., 1979. Kyst-, strand- og vindgeomorfologi. Norsk Geografisk Tidskrift, 33: 159-171.

Liestøl, O., 1977. Pingos, springs, and permafrost in Spitsbergen. Norsk Polarinstitutt Årbok, 1975: 7-29.

Mangerud, J. et al., 1992. The last glacial maximum on Spitsbergen, Svalbard. Quaternery Research, 38: 1-31.

Owens, E.H., Taylor, R.B., Miles, M. and Forbes, D.L., 1981. Coastal Geology mapping: An Example from the Sverdrup Lowland, District of Franklin. Geological Survey of Canada, Paper 81-1B: 39-48.

Vinje, T. and Kvambekk, Å.S., 1991. Barents sea drift ice characteristics. Polar Research, 10: 59-68.

Ødegård, R., Etzelmüller, B., Vatne., G. and Sollid, J.L., 1995. Near-surface spring temperatures in an Arctic coastal rock cliff: Possible implications for rock breakdown. In: O. Slaymaker (Editor), Steepland Geomorphology. Wiley, Chichester, pp. 89-102.

Ødegård, R. and Sollid, J.L., 1993. Coastal cliff temperatures related to the potential for cryogenic weathering processes, western Spitsbergen, Svalbard. Polar Research, 12(1): 95-106.

Ødegård, R.S., Sollid, J.L. and Trollvik, J.A., 1987. Kystkart Svalbard A3 Forlandsundet 1:200000. Norsk Polarinstitutt and Unviersity of Oslo, Oslo.

THE GIS-BASED QUANTIFICATION OF THE SEDIMENT AND ORGANIC CARBON FLUX TO THE LAPTEV AND EAST SIBERIAN SEAS THROUGH COASTAL EROSION

M.N. Grigoriev*, M. Lack and V. Rachold****

** Permafrost Institute, Siberian Branch of the Russian Academy of Sciences, Yakutsk, Russia,** Alfred Wegener Institute for Polar and Marine Research, Research Unit Potsdam, Germany*

Coastal erosion forms a major source of the sediment, organic carbon and nutrient flux into the Arctic basin. Numerous publications about coastal characteristics of that area are available in the literature. However, the portion of sediment and organic carbon that is supplied to the shelf from each type of erosive coastal sections is known insufficiently. For a detailed evaluation of the main parameters and effects of coastal erosion in the Laptev and East Siberian Seas the review and analysis of our own, new data and published information concerning coastal dynamics, shore composition, lithology, morphology, hydrodynamics and permafrost features was carried out.

Based on the available data a preliminary database of coastal dynamics and an assessment of the coastal sediment and organic carbon flux to these Arctic Seas were created. The development of a coastal dynamics database is founded on a detailed segmentation of the studied coast according to the parameters indicated above. This segmentation is based upon the detailed classification of erosional and accumulative shores of the Laptev and East Siberian Seas. The results are incorporated in a digital map, which is the main component of the coastal database. The local (regional) database is organized in ArcInfo/ArcView GIS-format. These studies allow us to summarize cumulative data on coastal dynamics as well as to estimate the coastal sediment input for those seas where the influence of permafrost peculiarities is most important. A segmentation of the Laptev Sea coastline was performed as a first step towards a GIS-based quantification of the Arctic sediment and organic carbon fluxes resulting from coastal erosion.

At this stage a preliminary GIS-based database of the Laptev Sea coastal dynamics is available. All main coastal parameters including sediment and organic carbon flux are introduced to the database and characterized by average values within each of the 73 selected coastal segments. Our previous estimation of the annual coastal sediment and organic carbon input was 58.4 and $1.8 \bullet 10^6$ t yr^{-1} respectively. The new GIS-based quantification suggests similar values: 62.2 and $1.63 \bullet 10^6$ t yr^{-1}.

The East-Siberian Sea coast is not investigated in such details yet. Nevertheless, we can roughly quantify coastal sediment and organic carbon input as 66.5 and $2.2 \bullet 10^6$ t yr^{-1}.

THE SENSITIVITY OF ARCTIC SHELF SEAS TO VARIATIONS IN ENVIRONMENTAL FORCING: 10 YEARS OF PROGRESS IN UNDERSTANDING THE "LAPTEV SEA SYSTEM"

J.A. Hölemann[1], H. Bauch[1], S. Berezovskaya[2], I. Dmitrenko[3], H. Kassens[4], S. Kirillov[5], T. Müller-Lupp[4], S. Priamikov[5], J. Thiede[1], L. Timokhov[5] and C. Wegner[4]

[1] Alfred Wegener Institute for Polar and Marine Research, Bremerhaven, Germany
[2] Russian State Hydrometerological University, St. Petersburg, Russia
[3] International Arctic Research Center, University of Alaska Fairbanks, Fairbanks, USA
[4] GEOMAR Research Center for Marine Geosciences, Kiel, Germany
[5] Arctic and Antarctic Research Institute, St. Petersburg, Russia

Environmental forcing factors, i.e. atmospheric circulation, sea ice cover and river runoff, mainly affect the shallow water environment of the Laptev Sea in the Siberian Arctic. Especially the predominance of cyclonic or anticyclonic atmospheric circulation over the Arctic influences the current system of the Laptev Sea and the distribution of river runoff on the shelf. As a consequence also the transport of sediments and the sedimentation processes on the shelf are strongly affected by different regimes of atmospheric circulation and ice cover. New data show that this effect starts as soon as the Laptev Sea flaw polynya opens up during winter.

The modern depositional environment was probably established during the last phases of the Holocene transgression that reached the southern region of the Laptev Sea between ~ 7 ka and ~ 5 ka. The flooded areas now form large shoals that are covered by relict sandy sediments. Modern sediment deposition on the inner and central shelf is mainly connected to depressions in shelf topography. But even in a depression near the major outlet of the Lena River, the average sedimentation rate of the last 5 ka was not higher than 30 cm/ky.

New long-term measurements with bottom-moored instruments give strong evidence that modern shelf sediment transport is mainly connected to the N-S running submarine valleys on the shelf of the Laptev Sea. In the submarine valleys of the eastern Laptev Sea suspended sediments are transported within in a distinct bottom nepheloid layer which is strongly influenced by the prevailing atmospheric circulation and the ice cover. In the Eastern Lena Valley the main transport direction is towards the central and inner shelf. This transport system can explain the higher average sedimentation rates (40 – 70 cm/ky) at the southern end of the Lena Valley.

Geochemical and mineralogical signatures of surficial sediments in the Laptev Sea, the absence of a bottom nepheloid layer in the western Laptev Sea, and the hydrographic conditions let us arrive at the conclusion that the dominant source for surficial sediments in the central and outer shelf region is the riverine input of the Lena River. In the course of the spring freshet of the Lena River more than 50 percent of the annual input of suspended sediments enter the still ice-covered southeastern Laptev Sea. The suspended matter is laterally advected in an under-ice flow into the southeastern Laptev Sea. In the course of two weeks the material started to settle. During phases of strong atmospheric forcing the settled sediments are resuspended again and transported in the bottom nepheloid layer into the submarine valleys. Seafloor erosion of the shoals can also add significant amounts of sediments to the central and outer shelf region as they are influenced additionally by waves.

Based on the available data it can be assumed that the significant amounts of sediments that enter the Laptev Sea due to coastal erosion are trapped in a longshore transport system which prevents sediment transport towards the central shelf. Export of inner shelf sediments to the outer shelf area and the Arctic basin is mainly bound to the short period of the autumn freeze-up when new ice is formed in coastal and inner shelf areas. New data indicate that the atmospheric conditions during the first phase of the freeze-up -when the newly formed ice floes are still very mobile - control the incorporation of sediments into the ice cover and the export of “dirty” new ice into the Transpolar Drift System.

In general the seasonal variability of salinity and temperature in the region of the inner shelf is higher than the variability in the central and outer shelf region. This is mainly caused by fast ice which covers the inner shelf from October to the end of July. An examplary process is the supply of salt-enriched, cold brines which form during the growth of the ice. The low hydrodynamic forces under the ice cover allow the dense brines to accumulate in morphological depression. This process should have direct consequences for the stability of submarine permafrost on the inner shelf. Therefore climate-induced changes of the spatial and temporal distribution of the fast ice cover should have strong impact especially for the inner shelf environment and the submarine permafrost.

THE EXPEDITION LENA 2002

H.-W. Hubberten[1], M.N. Grigoriev[2], F.E. Are[3] and V. Rachold[1],

[1] *Alfred Wegener Institute for Polar and Marine Research, Research Unit Potsdam, Germany,*
[2] *Permafrost Institute, Siberian Branch of the Russian Academy of Sciences, Yakutsk, Russia,*
[3] *St. Petersburg State University of Means of Communications*

In this talk we present a summary of the Expedition LENA 2002, which was carried out within the framework of the Russian-German cooperation SYSTEM LAPTEV SEA 2000. From end of June to middle of September 2002 a group of ca. 30 Russian and German scientists, which were divided into 3 teams, focused on modern processes and the environmental history of the Laptev Sea coastal region (Fig. 1). Team 1 was based on the Island Samoylov in the central part of the Lena Delta and concentrated on the quantification of trace gas fluxes from permafrost-affected soils. Team 2 focused on the investigation of modern periglacial processes and their manifestation in ancient permafrost deposits. Modern features were studied in the surroundings of the city of Tiksi and geocryological field studies of natural exposures and detailed sampling of permafrost sections were performed along the coastline of the New Siberian Islands. For the expedition to the New Siberian Island the RV "Pavel Bashmakov" was used. Team 3 studied several key locations along the coast of the New Siberian Island in regard of coastal dynamics. Geodetic measurements of the coast lines (position of the cliff base and shoreline) were carried out, detailed shoreface profiles were obtained by echosounding and sediment sampling was performed. The team was based aboard "Pavel Bashmakov" together with team 2.

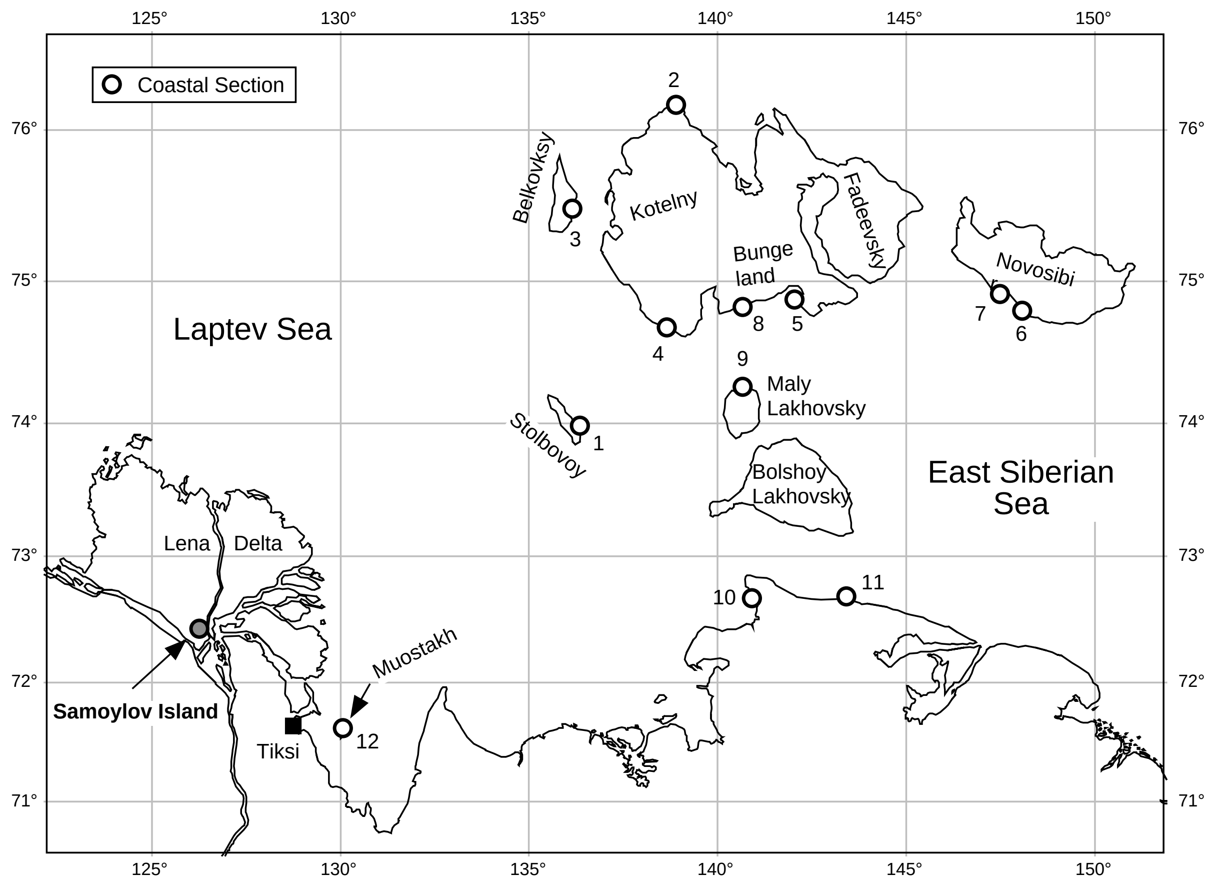

Figure 1. Location map of the expedition LENA 2002.

COASTAL PROCESSES IN THE SOUTHEAST CHUKCHI SEA, ALASKA: LANDSCAPE HISTORY AND THE FUTURE

J.W. Jordan

Department of Environmental Studies, Antioch New England Graduate School, 40 Avon St., Keene, NH 03431

The coasts and marginal lowlands of the southeast Chukchi Sea are geologically diverse and record a wide range of responses to Holocene climate and sea level change. The rich human history of this region spans the last 5000 years and provides a long-term view of human-environment interactions in the Arctic. Sea level has been slowly rising throughout this period (Jordan and Mason 1999; Mason and Jordan 1993) but coastal geologic features and the distribution of archaeological sites indicate that this trend has been modulated by shifts in climate that have influenced both marine and terrestrial systems (e.g. sea ice regime, wave dynamics, permafrost table, shoreline erosion rates, sediment mobility).

Long-term monitoring of coastal change is facilitated by an irregularly-spaced network of 26 shoreline change monitoring stations established between Cape Prince of Wales on Bering Strait and the village of Kivalina, between Kotzebue and Point Hope. Station data collected within the boundaries of Bering Land Bridge National Preserve (BELA) and Cape Krusenstern National Monument (CAKR) indicate that shoreline erosion is active along more than 80% of the shoreline. Retreat rates average less than 1.75 m yr^{-1} in the monumented reaches, but vary at several temporal and spatial scales depending on exposure, lithology, and importantly, the presence or absence of development or infrastructure. The rates and economic severity of coastal retreat are greatest at present at the village of Shishmaref, where late summer and fall storms have destroyed a 15 year-old seawall and have undercut several structures. The magnitude and frequency of these storms appear to exceed those calculated from historic data: 1.5 – 2.0 m event every 8 to 10 years (Jordan 1990). Present research focuses on developing an index of coastal change sensitivity (Pethick and Crooks 2000) for reaches in the southeast Chukchi Sea, establishing key coastal monitoring stations (one each in BELA and CAKR, see Fig. 1) and increasing the density of sector monitoring stations, and refining the record of eustatic and relative sea level change through field-based investigation of coastal environments. The integration of this effort with data from historical sources and community input will be critical for rational and sustainable economic development in the region.

Two key sites for monitoring coastal environmental change, one each in BELA and CAKR, have been designated BELA Site 1 and CAKR Site 1 and are shown in Fig. 1.

CAKR Site 1: Lat. 67° 03'/ Long. 163 ° 18' BELA Site 1: Lat. 66 ° 21'/ Long. 165 ° 40'

References

Jordan, J.W., 1990. Late Holocene evolution of barrier islands in the southern Chukchi Sea, Alaska. Masters Thesis, University of Alaska, Fairbanks.

Jordan, J.W., and Mason, O.K., 1999. A 5000 year record of intertidal peat stratigraphy and sea level change from northwest Alaska. Quaternary International, 60:37-47.

Mason, O.K., and Jordan, J.W., 1993. Heightened north Pacific storminess and synchronous erosion of northwest Alaska beach ridges. Quaternary Research, 40: 55-69.

Pethick, J.S., and Crooks, S., 2000. Development of a coastal vulnerability index: a geomorphological perspective. Environmental Conservation. 27:359-367.

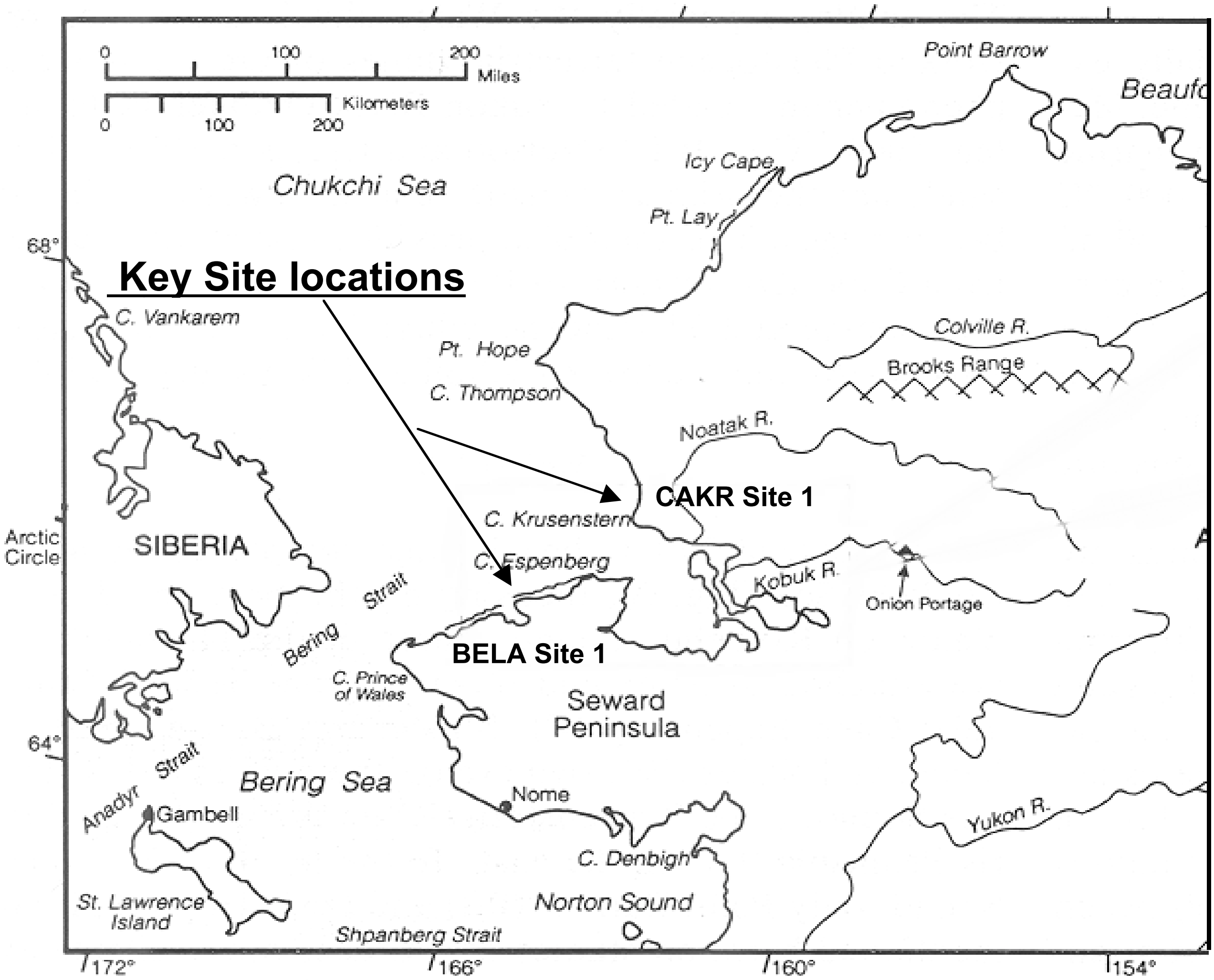

Figure 1. Southeast Chukchi Sea, showing location of key coastal monitoring sites.

CHARACTER OF THE COASTAL DESTRUCTION AND DYNAMICS OF THE YUGORSKY PENINSULA COAST

A.I.Kizyakov[1], D.D.Perednya[2], Yu.G.Firsov[3], M.O.Leibman[1] and G.A.Cherkashov[3]

[1]Earth Cryosphere Institute SB RAS, Tyumen; [2]Moscow State University, Faculty of Geography; [3]Institute for Geology and Mineral Resources of the Ocean (VNIIOkeangeologia), St-Petersburg

The coastal zone of Yugorsky peninsula is represented by a hilly plain, gradually lowering from Pai-Khoi ridge to the Kara sea. The western portion of the coast is characterized by rocky cliffs. Starting at Pervaya Peschanaya river (7 km east of Amderma town) eastward terraced surfaces are built of Quaternary sandy-clayey deposits. Coastal bluffs have a binomial geological structure: clayey deposits are overlain by sandy sequences. An important element of the geological structure of the study area is tabular ground ice. Some sections enclose two ice layers. A coastal section of ca. 36 km length is considered in this study. At least 7 sites 0.2 to 1 km long have tabular ground ice exposures within specific forms of coastal destruction – thermodenudational cirques. Ice wedges are less common and play a minor role in coastal evolution.

The key site in the central part of Yugorsky peninsula represents the hilly plain with heights of 35-55 m above sea level, with sandy-clayey deposits enclosing two layers of tabular ground ice. Coastal bluffs have a relative height from 12 up to 29 m, thermocirque scarps are up to 32 m high. Coasts are of erosion-thermodenudation type, wave-erosion niches are not formed. Numerous ravines and gullies are formed at the terrace edges. Sandy-clayey material is transported through the canyon-like ravines and loaded on a rather narrow beach, forming sandy-silty fans. These fans are wave-eroded. They are washed away most actively by the storm surges. This material is involved in alongshore drift directed west-to-east.

The development of thermocirques in the coastal zone increases the volume of erosion per meter of a shoreline due to a concentrated sediment flux through a narrow exit. The fans formed on the beach at the thermocirque “mouth” are, as a rule, built of clayey deposits. Compared with sandy deposits, the clays are washed away slower. The catchment of thermocirques is larger, the scarps are curved and thus longer than the shoreline for the smooth-faced bluffs. The thawing of tabular ice results in material flows and overlying blocks collapse. Lateral thermoerosion develops in the bottom of thermocirques providing channels for mudflows along the frozen base, carrying suspended matter derived from the ice and enclosing deposits.

In the course of three field trips in 1999, 2001 and 2002, the structure of the coastal zone was under study at Shpindler Urochishche: 69°43_ N and 62°42_ E (Cherkashov et al. 1999). In 2001 a comprehensive topographical survey was undertaken in joint effort with VNIIOceangeology Institute at a key site 2 km west of Khubtyakha-river estuary, and a monitoring network established at a thermocirque scarp edge. In 2002 the first measurement was made and the change in the contour of the edge and its retreat were determined (Fig.1). The retreat was irregular through the edge and ranged from 30 up to 325 cm. The average retreat for a 256 m long scarp edge was 1,6 m. The summer of 2002 was cool and started late, therefore measurements conducted in mid-August did not give maximum retreat values per year because the process was on-going until September.

The dynamics of long-term thermocirque growth was revealed based on comparisons of the field survey of modern outlines of a thermocirque scarp edge and the interpretation of aerial photographs of 1947, scale 1:60000. The most actively retreating scarp in the years 1947 to 2001 was analyzed and retreat rate determined to be 0.6-1 m/yr, while the coastal bluff retreated at 1.3-1.6 m/yr.

The topographic survey allowed to compile a digital model of the relief in SURFER software which gave an instrument to reconstruct the topography of the area prior to thermocirque formation and calculate the sediment input from the thermocirque during 54 years. The sediment input from the thermocirques normalized to the shoreline appeared to be approximately 3 times as high as from the smooth-faced coastal bluffs. Thus, active thermocirques provide the significant contribution to the sediment discharge into the frontshore zone though locally.

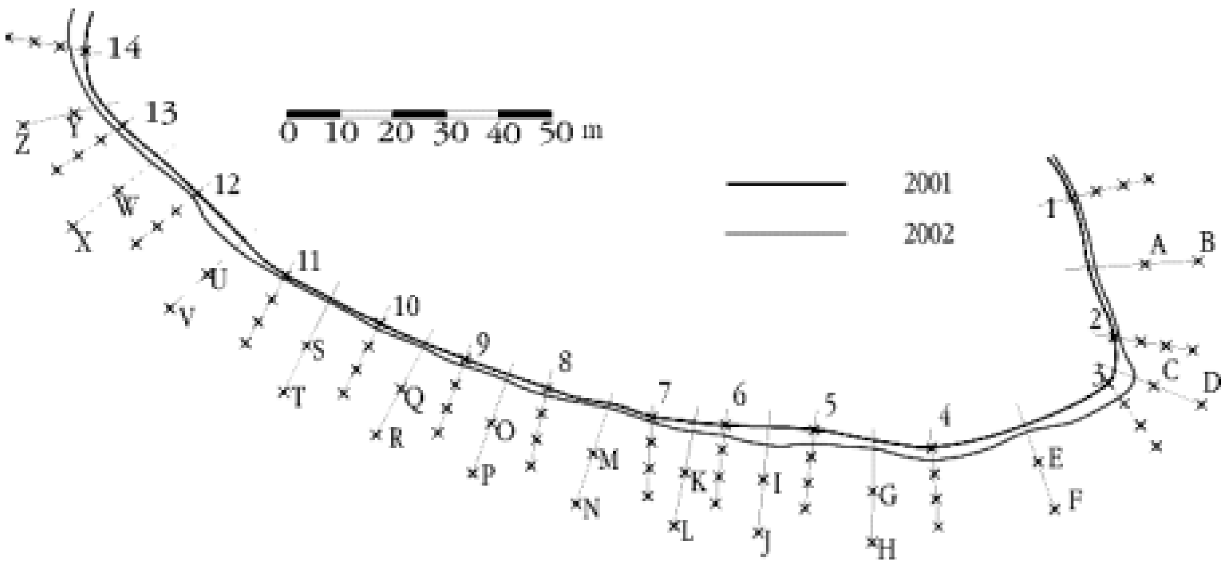

Figure 1. Scheme of the thermocirque scarp retreat in 2001-2002, key site «Shpindler».

To compare the coasts of different type, a rather low terrace of clayey and icy deposits was considered. The interviewing of the local inhabitants allowed to conclude, that the shoreline there retreated for the last decades with a rate of about 3 m/yr. Therefore in 2002 another observation network was established to monitor the coast of 10-12 m height. The stakes cover 110 m of the coastal bluff.

As a whole, Yugorsky coast represents a combination of sites with smooth-faced bluffs retreating practically parallel to themselves, and sites with thermocirques, where the scarp edge invades deep into the land by 200-400 m from the backshore. In the second type of coasts, the zone of mutual influence of the sea and land is considerably increased, the complex of thermodenudation processes and sediment discharge becomes complicated. Out of 36 km of considered coast, river estuaries cover 1 km, thermocirques about 2 km, and smooth-faced bluffs cover 33 km.

The work was performed within the framework of the INTAS projects, grants 01-2329 and 01-2211.

Reference

Cherkashov G.A., Goncharov G.N., Kizyakov A.I., Krinitsky P.I., Leibman M.O., Persov A.V., Petrova V.I., Solovyov V.A., Vanshtein B.G., Vasiliev A.A. Arctic Coastal Dynamics in the Areas with Massive Ground Ice Occurrence. Arctic coastal dynamics workshop, Woods Hole, 1999, pp.5-6.

MONITORING OF THE ONEMEN BAY COAST (CHUKOTKA)

A.N. Kotov and O.D. Tregubov

Chukchi Scientific Center

Onemen Bay coast has been studied annually since 1989. Special genetic and facial heterogeneity of sediments composing coastal cliffs are found using cryofacial approaches of analysis. It essentially affects dynamics of breaking down of the coast.

A 2.5 km section of late Pleistocene and Holocene ice-complex sediments is exposed north of the Cape Rogozhny (Kotov 1991). The late Pleistocene sediments are composed of sections of brown fine-grained, sand between 10 and 18 m thick. The average weighted diameter of the sand grains range between 0.06 and 0.14 mm. The content of water-soluble salts is 0.036 –0.05 % per 100 g of sediment. The cryogenic composition of the deposits include several layers of syngenetic, repeated-vein ice (RVI) of width between 0.8 and 2 m and in vertical extent up to 14 m. The cryogenic texture of sands ranges from massive to basal and ataxitic. Volumetric ice content of sediments exceeds everywhere 60%.

The low geomorphological levels were formed in the Holocene along the creek valleys during the thermo-erosion partitioning of the Pleistocene surface into separate segments. They are folded by products of destruction of the late Pleistocene cryolitogenous sediments (deluvial-solifluction deposits) and by peat. The thickness of this deposits ranges from 2-3 m up to 7 m. The deposits are penetrated throughout by RVI up to 2 m in width. The lower ends of veins are hidden beneath the waters of Onemen Bay. The cryogenic texture rhythmically varies from massive up to basal and ataxitic throughout the profile. The last one is often accompanied by ice schlieres of up to 3 cm in thickness. Volumetric ice content of the Holocene deposits of the ice complex is 70 - 85%.

The extremely unstable pattern of destruction of the coast formed by the ice-complex deposits was observed during the past 13 years. The bottom of the coastal cliff was impacted by strong gales in 1989. This led to the exposure of the buried RVIs that occurred everywhere and to the active thermo-abrasion. During one year from 1m up to 4 m of the coastal cliff. Were destroyed But in 1991 the RVI exposures were completely covered by re-deposited sediments. The coastal destruction has proceeded only by forming of thermo-erosion ravines in the top of cliffs. Small exposures of thawing RVIs were observed in 1995 - 1997 when the average annual air temperature were 1 –2.7º C higher than the long-term average

The destruction of the coast composed of the ice complex (moraine) is sustainable over time. It is composed of pebbly-boulder deposits filled with loamy sand and loam. Large inclusions of ice are not found.. On such coastal cliffs the wave-driven niche is formed and coastal cliff destruction is gradual. Many boulders up to 1.5 m in diameter with characteristic glacial hatching are found in the sandy beach below the cliff.

Destruction of the coast to the east of Cape Rogozhny formed by glacial-marine deposits is unstable. It is the result of the formation of in thermokarst cirques in locations of sheet ice. During the observational period the first thermo-cirques were exposed in 1991. Afterwards only in 1996 were several thermo-circuses exposed because of the increase of annual air temperature. The initial state of in forming a thermo-cirque is disastrous. Sliding of huge amount of deposits takes place. Landslide tongue can penetrate up to 50 m into the water area of the bay (Kotov 2002). The glacial-marine deposits are composed of bluish-grey clay with infrequent admixture of sand and pebble, and rarely boulders. The content of the clay fraction (less than 0.005 mm) ranges between 52 and 87%. The amount of water-soluble salts reaches 0.493 % per 100 g of sediments.. The cryogenic texture changes from the bottom upward from ataxitic to irregularly wide netlike with thickness of schlieres up to 5cm. From the bottom upward cells of the net become less and schlieres of ice become thinner (1-2 mm). The glacial-marine deposits are overlapped by sandy sediments of the late Pleistocene ice complex with syngenetic RVI's. The latter ones are similar to the described above sediments (Kotov 1997, 2001).

The glacial-marine deposits include flat ice deposits (FID). When FID thaw through, the thermo-cirques emerged. FID are not a uniform layer. They are represented by separate structures located at different altitudes (from 2 to 9 m) above the bay level. The lower boundary of FID was not determined. It is covered by mud-streams at 1-5 m above the bay level. The maximal visible thickness of ice (7 m) was monitored in 1997. In one of thermo-cirques, two layers of ice were observed. They were devided by an 8-m thick glacial-marine deposit.

Thermo-cirques at the northern coast of the Onemen Bay emerged in August 1996 and were studied in detail. Size was: width 46m; height of the frontal wall 15m. The volume of the ground sliding down at a time exceeded 15000 m^3. Seven transects were set up along the perimeter of the thermo-cirque to monitor its development. The measurements on transects for September 1997 showed that: the frontal wall of a thermo-circus has receded 14.7 to 20.5 m; the width exceeded 1.5 to 5 m. The volume of ground removed during one year (the summer season of 1997) was about 10000 m^3. In 1998 the development of the thermo-cirque was terminated. There was a relative flattening out of the frontal wall and many mud-streams of a sod were found. In 2001 the thermo-circus was nearly completely covered by vegetation (Kotov 2002). The close relationships in dynamics of climatic parameters, active- layer thickness, and appearance of thermokarst cirques were found.

The detailed study of the deposits of the northern coast of Onemen Bay, including pollen spectra, hydrochemical and isotopic analysis of underground ice, dating of absolute age by C^{14}, allows the reconstruction of the history and paleogeographic conditions of their formation. It enables us to trace the dynamics of the coastline from mid Pleistocene to the present.

Starting in 2001 annual mapping of the northern Onemen Bay coastline using GPS has been organized. A total of 18 transects were established to measure the coastal dynamics. Shrubs from bottoms of an old vegetated thermo-cirques are sampled to determine their age using dendrochronological approaches.

The study is supported by INTAS, grant #2329.

References

Kotov, A.N. Kriolitologicheskoye stroenie ledovogo kompleksa v ust'e r. Anadyr // Kompleksnye geokriologicheskie issledovaniya Chukotki. Magadan: NEISRI FEB AS USSR, 1991. pp.5-18.

Kotov, A.N. Ledyanye zalezhi na severnom poberezhye zaliva Onemen (Chukotka) // Pozdny pleistocen i golocen Beringii. Magadan: NEISRI FEB RAS, 1997. pp.92-98.

Kotov, A.N. Osobennosty zaleganyja, sostava i stroyenia ledyanykh zalezhei plastovogo tipa na severnom poberezhye zaliva Onemen (Chukotka) // Materialy Vtoroi konferentsii geokriologov Rossii. MGU im. M.V. Lomonosova. June 6-8, 2001. T.1. Chast' 2. Litogeneticheskaya geokriologia. M.: Izdatelstvo MGU, 2001. pp. 218-225.

Kotov, A.N. The catastrophic destruction of the Onemen gulf shores, Chukotka // Extreme phenomena in cryosphere: basis and applied aspects. International conference. Abstracts. Pushchino, Rossia, 2002. pp. 245-246.

THE ARCTIC COASTAL CLASSIFICATION FOR ESTIMATION OF INDUSTRIAL EFFECTS

M.M. Koreisha, F.M. Rivkin and N.V. Ivanova

Production and Research Institute for Construction Engineering Survey, Okhruznoi proezd, 18, Moscow, 105187, Russia, f-rivkin@narod.ru

The analysis of modern engineering-geocryological conditions and geological processes on the Arctic coast of Russia is the methodological basis for classification. Thermo-abrasion, thermokarst, thermodenudation, thermal erosion, erosion, abrasion, deflation and others processes are considered as the main exogenous processes effecting the coast.

The classification has a matrix form that takes into account coastal morphology, the dominating processes of coastal formation, and engineering-geocryological conditions of the coast. As a result of matrix analysis on the natural conditions complex 19 types of the coasts were classified.

Such an approach allows the estimation of the consequences of industrial effect on the frozen rocks of the Arctic coast during construction and operation of gas pipelines and oil terminals with the consideration of their heat and thermomechanical effect.

The development of oil and gas deposits on the Arctic shelf and coast and construction of terminals (gas and oil) and pipelines will increase the natural destructive processes and inevitably increase industrial effect on the coastal zone of the Arctic. First it is revealed through the thermomechanical effect on the frozen ground on the coast and the shallow waters in the coastal areas of Arctic shelf.

The Arctic coast from a geocryological point of view represents a complex and dynamic zone, along with the permafrost deposits having low temperature, cooled saline rocks.

The specificity of industrial effect on the Arctic coast of Russia was considered as this basis of the classification. The main types of technogenic effect caused by construction and exploitation of spatial and linear objects are taken into account. All types of coasts are classified according to the intensity of exogenous processes changing the Arctic coast under technogenic effect.

The classifications are represented on the map in the form of GIS-version map at scale 1:8 000 000.

The task was carried out with partial INTAS 2332 support.

REMOTELY SENSED EVIDENCE OF ENHANCED EROSION DURING THE TWENTIETH CENTURY ON HERSCHEL ISLAND, YUKON TERRITORY

H. Lantuit and W. Pollard

Dpt of Geography and Centre for Climate and Global Change Research (C_GCR), McGill University, 805 Sherbrooke West, Montréal, QC, H3A 2K6

Introduction

Herschel Island, also known as Qikiqtaruk, is located in the northern part of the Yukon Territory, Canada. The island is situated at 69°36'N and at 139°O4'W. It lies approximately 60 km east of the boundary between Yukon and Alaska and 3 km north from the continental coast (Fig. 1). The island is located in the Southern Beaufort Sea, in the physiographic region of the Yukon Coastal Plain. The island is a moraine resulting from the late fluctuations of the pleistocene ice sheets and is mainly composed of marine, non-marine and mixed origin sediments (Bouchard 1974). Sediments are clays, clayey silts, silts and sands.

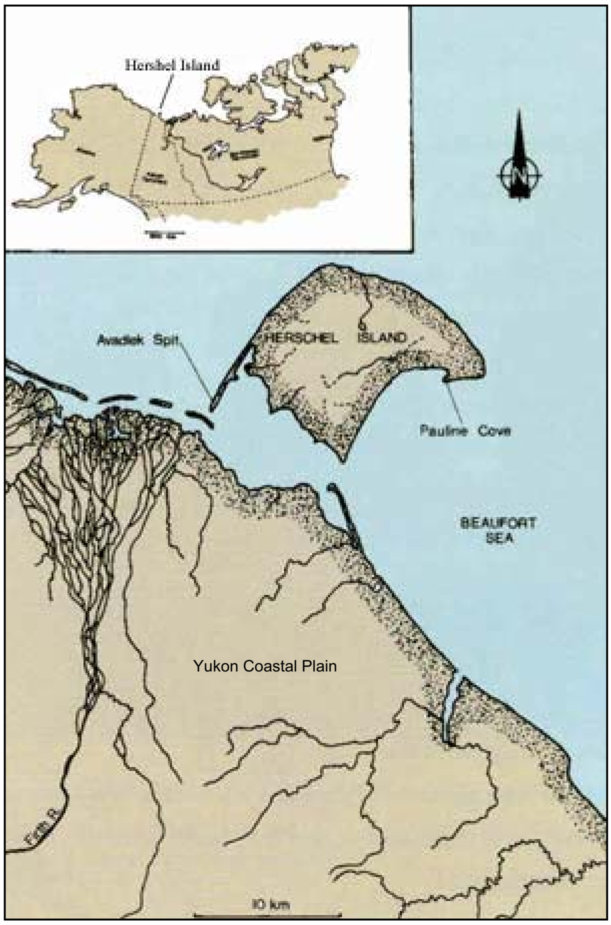

Figure 1. Herschel Island Location.

Recent attention has been given to the tremendous coastal retreat occurring in the area, which is assumed to be the most ice-rich area of the Canadian Arctic (Pollard and French 1980). Harper (1991) documented an average coastal retreat rate of 1.0 myr^{-1}, with some peak locations at 18myr^{-1} for the 1944-1970 period. Solomon (2002), in this issue documents average coastal retreat rates of –1 to –5myr^{-1} for the 1970-2000 period using the locations referenced by Harper (1991) in his study.

Global warming is believed to dramatically increase certain processes responsible for enhanced coastal erosion in the Arctic. McGillivray et al. (1993) showed that a longer open-water season, warmer sea temperatures and a reduced sea-ice extent would lead to greater storminess frequency, and hence, to enhanced erosional processes.

Few studies have documented the shoreline evolution on a large scale basis for the 1970-2000 period on Herschel Island. The purpose of this study was, then, to propose and update linear costal retreat rates in Herschel Island for the most recent period using the locations referenced by McDonald and Lewis (1973) in their study of the 1944-1970 shoreline evolution.

Methods

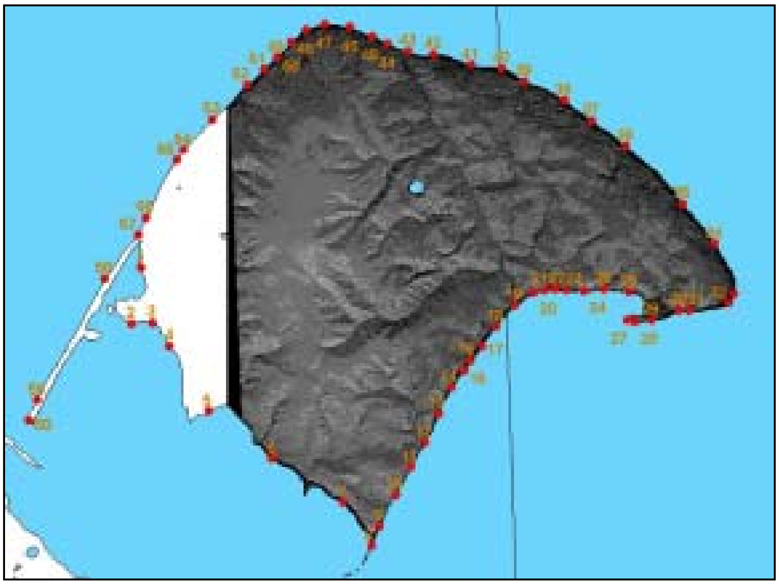

Figure 2. Study spots location. (Spots 1 to 7 are considered unexposed to ocean dynamics). The IKONOS image is displayed to show the matching area with McDonald and Lewis dataset (1973).

McDonald and Lewis (1973) used three airphoto series to document coastal retreat rates on Herschel Island, for 1944, 1954 and 1970. They established 60 study locations along Herschel island's shore and documented coastal retreat rates for these locations (Fig.2). We took for reference these points and calculated absolute coastal retreat distances and coastal retreat rates for the 1970-2000 period. The measurements were operated on the 1970 airphoto series and a 2000 ikonos image (1 meter resolution in panchromatic operating mode) approximately from the same period of the year (i.e late August).Fixed inland features (mainly tundra polygons edges) were identified and used to measure coastal evolution between the 1970 and 2000 shoreline. No rectification of optical distortion or terrain displacement was undertaken on the 1970 airphoto series. The 2000 ikonos image was displayed in geographic coordinates. As a result, the uncertainty of the measurements was roughly estimated at ±10%.

Results

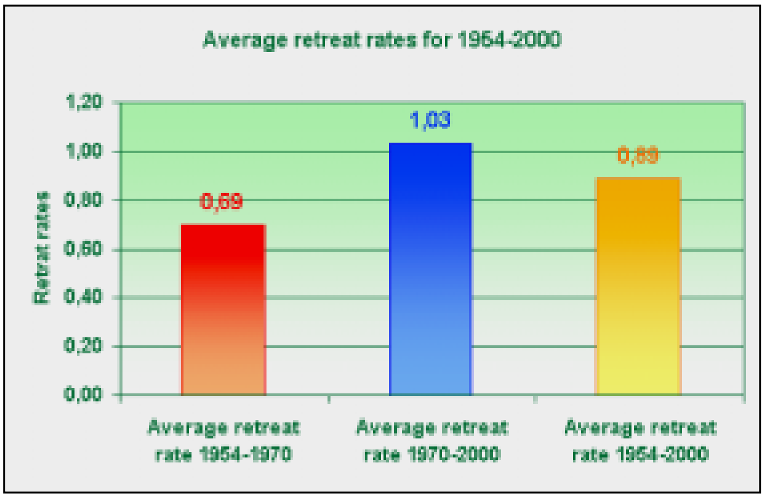

Figure 3. Average coastal retreat rates computed for the 1954-1970 period (red), 1970-2000 period (blue) and 1954-2000 period (yellow).

Absolute retreat distances and coastal retreat rates were computed for the locations displayed on both the airphoto series and the satellite image. An average coastal retreat rate was calculated for locations exposed to ocean dynamics for the 1970-2000 period and was compared to McDonald and Lewis (1973) calculations for the 1954-2000 period. Results are displayed in Fig. 3.

The average retreat rate for the 1970-2000 period was found to reach 1.03 myr^{-1}, as opposed to an average retreat rate of 0.69 myr^{-1} for the 1954-2000 period. It represents a 50% increase of coastal retreat over 28 years. Shoreline change along the exposed coastal areas for the 1970-2000 period varied from –64m to +108m (negative changes are erosional).

Results were computed and displayed in a GIS in order to detect the spatial patterns of erosion (Fig.4).

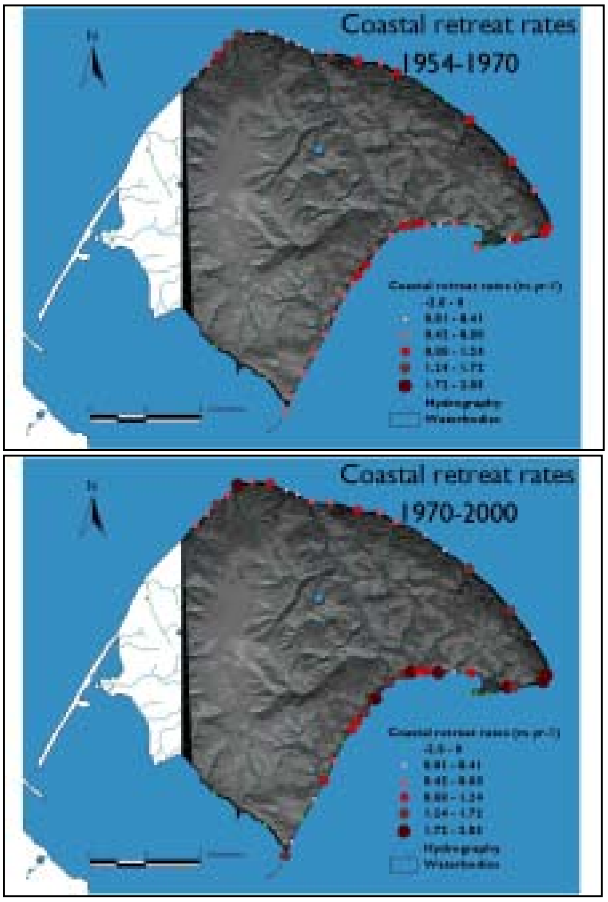

Figure 4. Mean annual coastal retreat rates computed for the 1954-1970 and 1970-2000 periods.

The distribution of the strongest eroding shorelines is clearly heterogeneous. The important eroding locations on the island are reported for the northern tip of the island, for Collinson Head on the eastern tip, and in Thetis Bay on the south-west shore. Storms have been shown to be the most important eroding agent for the shorelines of the southern Canadian Beaufort Sea (Solomon et Covill 1995) and to typically originate from the North-West. However, on Herschel Island, the North-western shore is not particularly more sensitive to the erosion processes. The coastal retreat rates are comparable for shores oriented differently: For the 1954-2000 period, we interpolated a coastal retreat rate of 1.09myr^{-1} for the south-west-facing shore, a rate of 1.04myr^{-1} for the east-facing shore, 0.70myr-1 for the north-east-facing shore and 1.05 myr^{-1} for the north-west-facing shore. The wind regime on Herschel Island is characterized by an unusual strong south-west component, which is a potential explanation for the erosional pattern on the island. However, this phenomenon can't solely explain the homogeneity of the erosional pattern on the island. We'll see below that this pattern is closely linked to the location of the major retrogressive thaw slumps.

The dramatic increase shown by our results strongly differ from the evolution described by Solomon (2002), who demonstrates that the rest of the southern Canadian Beaufort Sea has undergone a relative increase of the erosional processes and that the "highest rates of retreat are associated with spits or low tundra bluffs which are directly exposed to waves and storm surges caused by the northwesterly wind storms." Herschel Island is mainly characterized by high bluffs fronted by very narrow beaches and coastal retreat rates have been proven to increase in an important way in such configuration. Neither the wind configuration, nor the geomorphology of the island coasts can, then, solely explain such dramatic increase.

Solomon (2002), in this issue, also noted that the shoreline retreat rates could be quite high in areas were high ground ice content have been identified. Pollard and French (1980) have used geomorphic proxies such as polygonal soils, palsas, pingos or retrogressive thaw slumps to detect and identify the type of ground ice. Bouchard (1974) has shown that ice content rates on Herschel Island are believed to be somewhat 20% higher than ice content rates on the rest of the Yukon Coastal Plain. We identified all the major retrogressive thaw slumps on Herschel Island, as well, as surfaces characterized by polygonal soils, compared our results with Pollard (1990)'s study of ground ice on Herschel Island and linked these surfaces to the erosion al pattern displayed on the maps (Fig.4).

Ninety percents of the greatest rates computed for the 1970-2000 period appear to be associated with retrogressive thaw slumps (see Fig.5). Most of the greatest eroding locations were already undergoing strong erosion during 1954-1970 period. Certain locations, though, were weakly affected by the erosion during the 1954-1970 period and displayed values amongst the most important for the 1970-2000 period. A simple comparative analysis of the two datasets has taught us that these spectacular increase corresponded always to the activation or the reactivation of a large retrogressive thaw slump. The map of coastal retreat rates evolution between the two periods (Fig.5) clearly establishes the link between retrogressive thaw slumps, and then, high ice content, and enhanced coastal retreat rates. Ninety percents of the greatest increase between the two periods are associated with retrogressive thaw slumps. Ground ice appears, then, to be a prime order factor in the evolution of coastal retreat, as noted earlier by Hequette and Barnes (1990) for the southern Beaufort Sea.

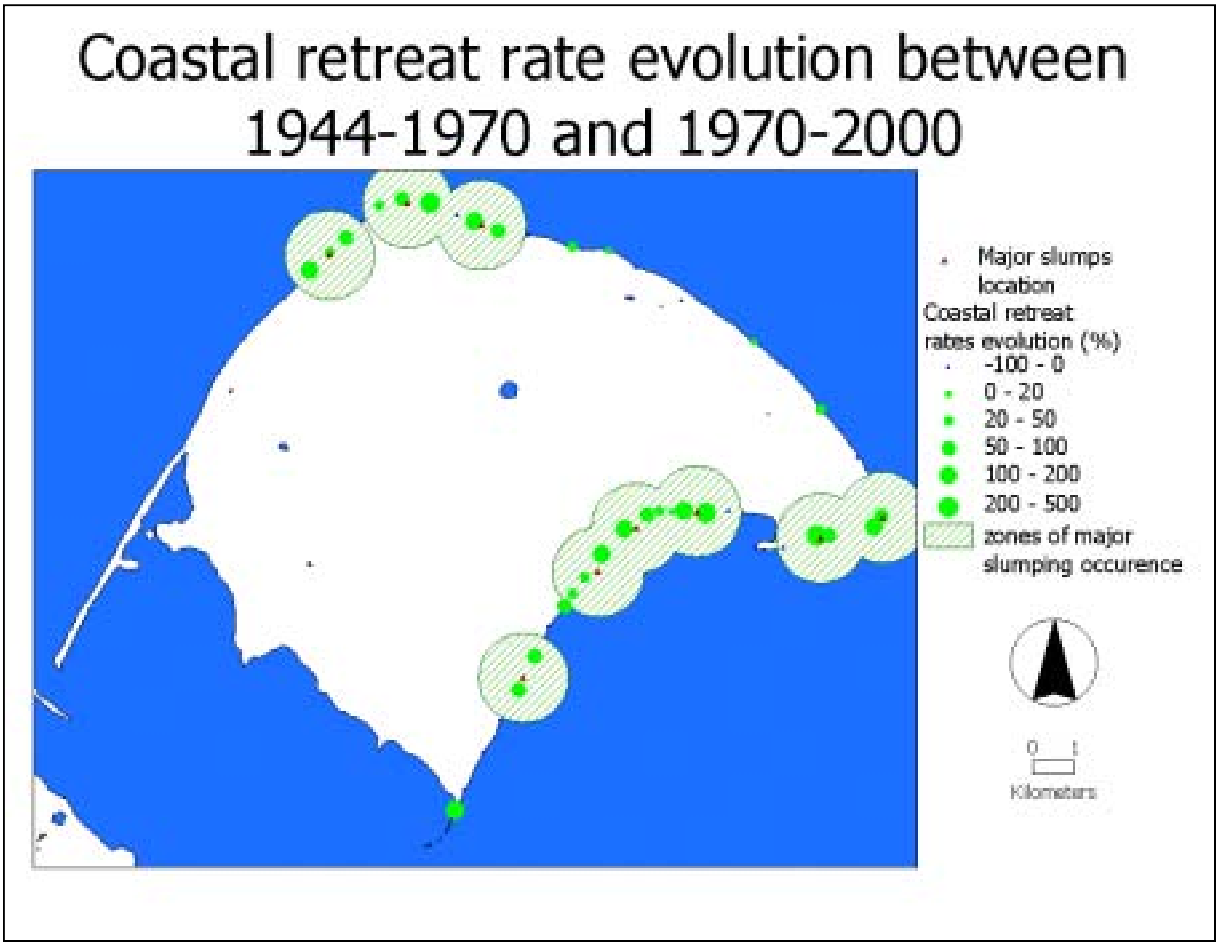

Figure 5. Coastal retreat rate evolution on Herschel Island between the 1944-1970 period and the 1970-2000 period. Note that the western tip of the island has not been included in the study.

One must note that a large part of the greatest increase between the two periods are not located exactly where the major slumps are, but in their close vicinity. A close examination of the airphotos and of the IKONOS image has led us to the conclusion that these cases correspond to the activation or reactivation of retrogressive thaw slumps. Some of these slumps have been proven to be dormant for more than a hundred years (De Krom 1990). It is critical, then to understand that this recent increase in the frequency of retrogressive thaw slumps occurrence can only be explained in terms of an important environmental change, which would include a change in the ocean dynamics and a change in the incoming radiation balance, as discussed by Lewkowicz (1991).

Conclusions

Shoreline erosion has been increasing dramatically over the 1954-2000 period on Herschel Island, Yukon Territory. Coastal retreat rate has been shown to change from 0.89myr^{-1} over the 1954-1970 period to 1.03myr^{-1} over the 1970-2000 period on the shorelines exposed to ocean dynamics. These changes are not compatible with the relative changes reported for the rest of the Beaufort Sea. The tremendous quantities of ground ice in Herschel Island which are associated with the huge retrogressive thaw slumps detected next to the major eroding areas are believed to be the driving factor for the outstanding erosion on the island. Further investigations are needed to map precisely the occurrence of ground ice on the island, to assess its precise role in the erosional processes and to interpolate a future evolution correlated to climate change.

References

BOUCHARD, M., 1974. Géologie des dépots meubles de l'île Herschel, Territoire du Yukon. M.Sc. Thesis, Montréal, Quebec, 70 pp.

DE KROM, V., 1990. Retrogressive thaw slumps and active layer slides on Herschel Island, Yukon. M.Sc. Thesis, Montréal, Quebec, 157 pp.

HARPER, J.R., 1991. "Morphology of the Canadian Beaufort Sea Coast" Marine Geology, **91**, 75-91.

HEQUETTE, A. and BARNES, P.W., 1990. "Coastal retreat and shoreface profile variations in the Canadian Beaufort Sea." Marine Geology, **91**, 113-132.

LEWKOWICZ, A.G., 1991. "Climatic Change and the Permafrost Landscape", in WOO, M.K. and GREGOR, D.J., 1991. Arctic environment: Past, Present and Future, proceedings of a symposium, Nov 14-15, 1991, Dpt. Of Geography, McMaster University, Hamilton, 91-104.

MCDONALD, B.C. and LEWIS, C.P., 1973. Geomorphic and Sedimentologic Processes of Rivers and Coast, Yukon Coastal Plain. Geological survey of Canada.

MCGILLIVRAY, D.G., AGNEW, T.A., MCKAY, G.A., PILKINGTON, G.R. and HILL, M.C., 1993. "Impacts of climatic change on the Beaufort sea-ice regime: Implications for the Arctic petroleum industry". Climate Change Digest CCD 93-01, Environnement Canada, Downsview, Ontario, 36pp.

POLLARD, W.H. and FRENCH, H.M., 1980. "A first approximation of the volume of ground ice, Richards Island, Pleistocene Mackenzie Delta, N.W.T." Canadian Geotechnical Journal, 17, 509-516.

POLLARD, W.H., 1990. “The nature and origin of ground ice in the Herschel Island area, Yukon Territory.” Proceedings, Fifth Canadian Permafrost Conference, Québec, 23-30

SOLOMON, S.M. and COVILL, R., 1995. “Impacts of the September 1993 storm on the Beaufort Sea”. Proceedings, 1995 Canadian Coastal Conference, 2, 779-795.

SOLOMON, S.M., 2003. “A new shoreline change database for the Mackenzie-Beaufort region, NWT, Canada”, this issue.

ALASKAN LANDFAST SEA ICE VARIABILITY AND EPISODIC EVENTS

A. Mahoney, H. Eicken and L. Shapiro

Geophysical Institute, University of Alaska Fairbanks, PO Box 757320, Fairbanks, Alaska, 99775 USA

Interest in the fast-ice regime of the Alaskan coast was prompted by the needs of coastal oil development, coincident with an increasing interest in the ice cover of the Polar Regions as a component of the climate system. In recent years, offshore development has forged ahead with an increased economic commitment, while concerns are rising both locally and globally about the response of the coastal ice to recent climate trends.

Of particular interest from the perspective of coastal processes are the duration of the landfast sea ice season and the occurrences of episodic events such as ice-shoves (referred to as an "ivu" by the local Iñupiat Eskimo) and break-out events, where the landfast ice becomes detached (See Figs. 1 and 2). Ice shoves are capable of considerable damage to property and infrastructure and are also able to rework beach material and deposit it beyond the reach of waves. This is thought to be the dominant depositional mechanism on some barrier islands (Reimnitz et al. 1990). The presence of open water and drifting floes in the nearshore zone, following an ice breakout event, presents an opportunity for considerable sediment working at a time of year when such processes are normally considered inactive.

Typically, the start of the landfast ice year is marked by in-situ formation of ice in sheltered regions of the coast. Ice typically forms later on exposed coastlines through the advection of ice from offshore. The landfast ice may go through several periods of detachment and reformation before it stabilizes around the middle of winter. The onset of spring sees melt ponds forming on the ice cover and flooding by rivers, where present. As melt progress the ice cover becomes weaker and floating in places where it may previously have been

Figure 1. Berm of beach material pushed up in front of advancing ice during an ice shove on June 18 2001 at Barrow, Alaska.

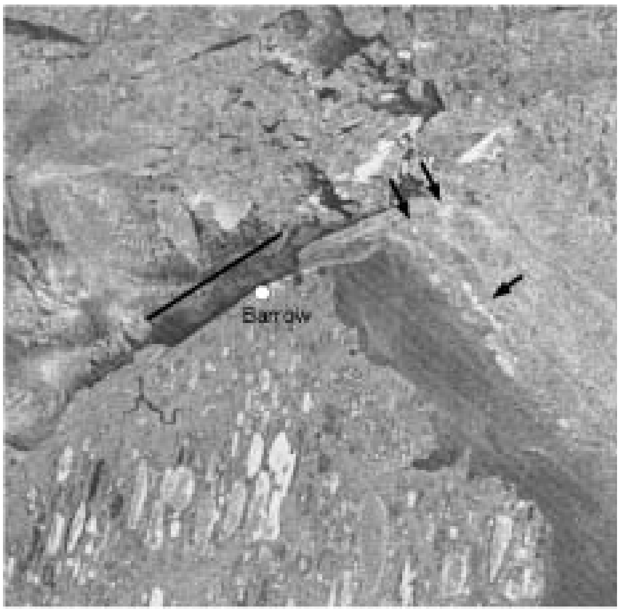

Figure 2. Radarsat scene showing an ~20 km section of landfast ice broken away from the coast near Barrow, Alaska in mid-December 2001.

grounded. On exposed coasts the ice is then removed by offshore wind and current forces, while in sheltered regions, the ice may melt in-situ. Periodic events may affect the landfast ice during this development, sometimes with lasting consequences for the ice cover such as is discussed later.

In this study we examine over 305 AVHRR scenes and field data from 1998 to 2001 describing the development of the landfast ice in the Alaskan Arctic from formation in the fall through to melting and break-up in the spring. Key events were identified and compared with the previous studies made in the 1970's (Barry et al. 1979; Shapiro and Metzner 1989). The methods used to identify events in the earlier studies are not the same as those used here and so the nomenclature for the events is not identical.

Recent reports suggest the ice-year in the Arctic is shortening, but the three years forming this study suggest that this is not necessarily the case. Rather, the timing of events within the ice-year have changed and the landfast ice experiences a shorter stable period, while the overall length of time landfast ice is present remains much the same (see Fig. 3).

The most marked difference is in the stabilization of the ice cover. The mean date of stabilization of the landfast ice in winter, after which little or no further deformation takes until spring, was approximately two weeks earlier in Barrow and one week earlier along the central Alaskan Chukchi coast. The fast ice of the Beaufort Sea apparently stabilizes earlier, but it is felt this may be due to misidentification of landfast ice in AVHRR imagery and further field data is required in this region. The dates of "freeze-up" and the events in the latter part of the landfast ice year appears notably unchanged

Examination of the interannual variability of events in the 1998-2001 period suggests that dynamic (rather than thermodynamic) processes may be responsible for the observed changes. Fig. 4 shows the range of dates of occurrence of each event relative to its mean. It is clear that the events with the greatest date range are those that are governed by predominantly dynamic processes such as stabilization and river break-up. The least variability is observed in those events dominated by thermodynamic processes such as ice formation in sheltered regions and the appearance of melt ponds.

Although only three years of data are presented here, the events of the 2001-2002 ice year support these observations. These data have not been included, partly because they are not completely analyzed yet, but also because of the difficulty of fitting them into the scheme of the current data. In Barrow, the landfast ice saw no stable period with two wintertime breakouts in December (Fig. 2) and March. Whether these changes in the landfast ice evolution are an ongoing trend or part of a natural oscillation within the Arctic is unclear, but nevertheless there are immediate implications. The time during which the sea ice is suitable for traveling on is shortened, yet the hindrance to shipping is not lessened.

Furthermore, the susceptibility of the landfast ice to episodic events is likely to be higher. The current and previous two ice years have seen an apparently unprecedented number of ice breakout events. In June 2001, the ice was pushed on-shore over a length of at least 20 km during an ivu event. Based on aerial photography, remote sensing and ground observations we examine the extent and variability of the shove as well as large scaling forcing. It comes to light that the thermal regime of the ice was fundamental in governing its response to onshore stress and such events may become more common if unstable ice conditions become more prolonged.

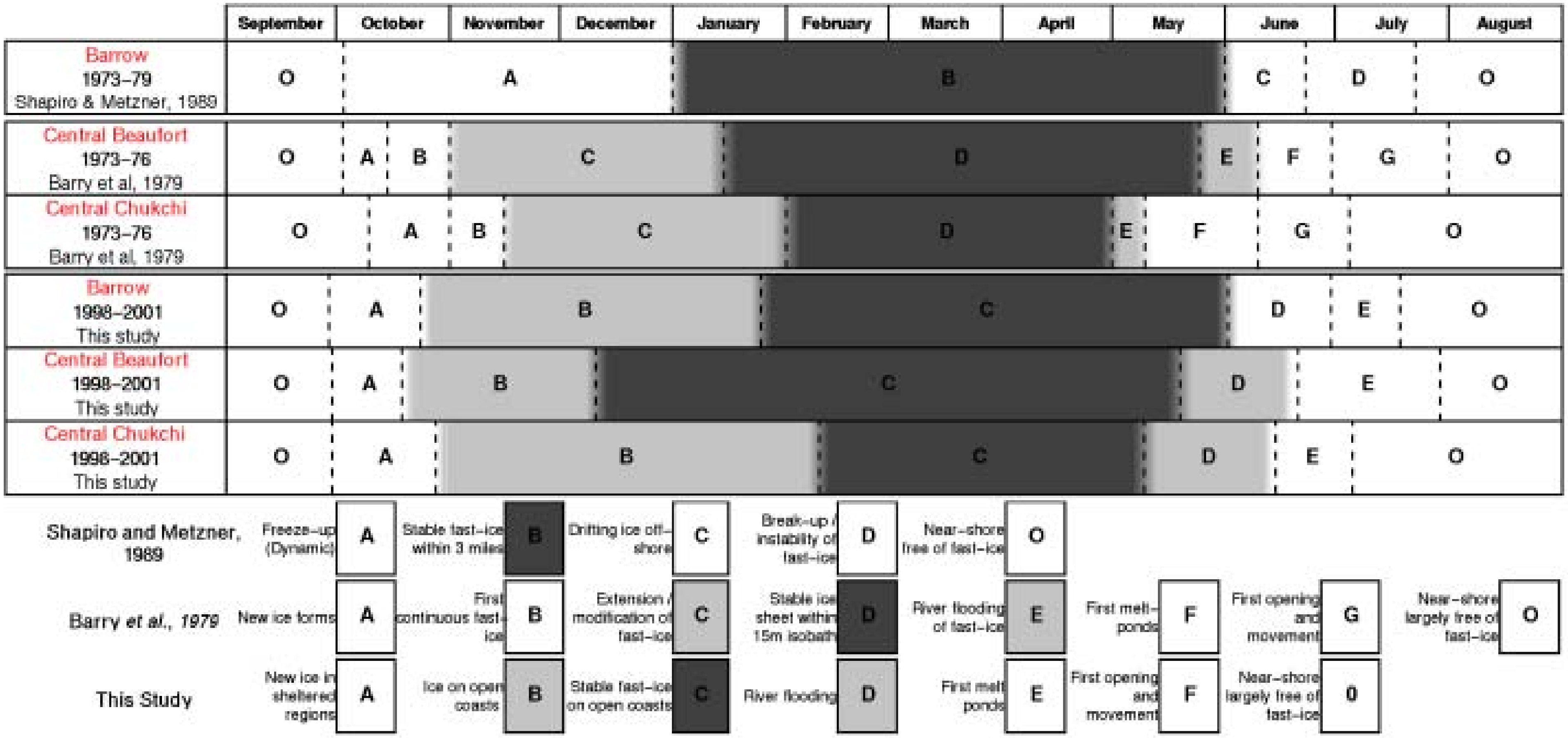

Figure 3. Comparison of recent observations of the timing of events within the landfast ice year along the Alaskan Arctic coast with those of approximately 25 years ago. The beginning and end of the ice year on all parts of the coast are show remarkably little difference. However, the duration of the stable period shows a significant reduction at Barrow and on the central Chukchi coast. The difference on the central Beaufort coast is thought to stem from difficulty identifying landfast ice from satellite imagery.

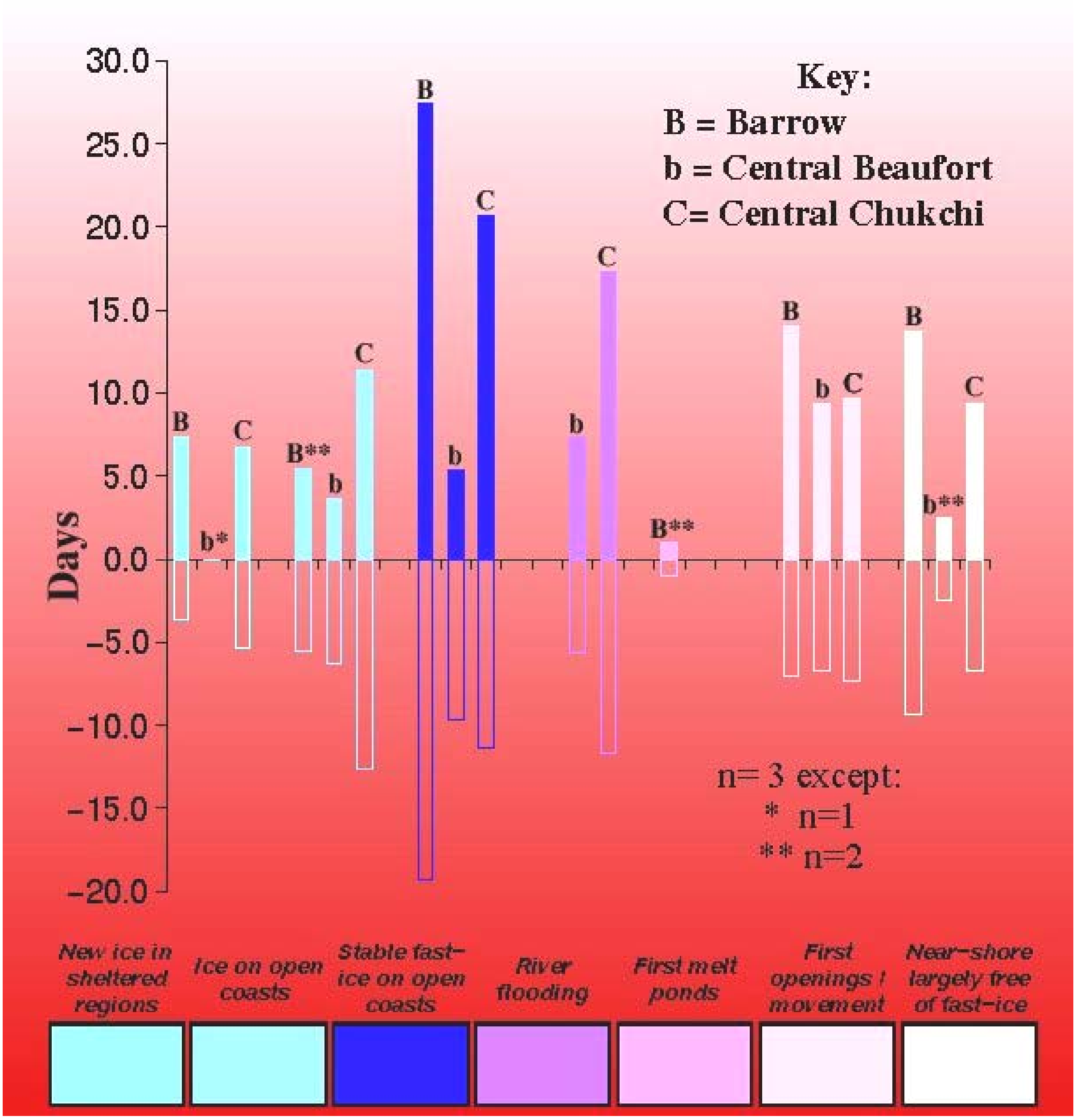

Figure 4. Earliest and latest occurrences of events within the landfast ice year relative to the mean date of their occurrence.

COASTAL RESEARCH IN THE AREA OF THE GEOCRYOLOGICAL STATION "CAPE BOLVANSKIY", IN THE ESTUARY OF PECHORA RIVER

G.V. Malkova (Ananjeva), D.S.Drozdov, M.Z. Kanevskiy and Yu.V.Korostelev

Earth Cryosphere Institute SB RAS, Russia, e-mail galina_malk@mail.ru

The "Bolvanskiy" geocryological station is located at Cape Bolvanskiy at the mouth of Pechora River at its inflow into the Barents sea. Cape Bolvanskiy juts far out into the sea and is bounded on the east and west by two bays. This area corresponds to the hilly eroded surface of IV glacial-marine plain with heights from 25 m up to 100 m above sea level.

The research on the coast and coastal processes in the area of the station began in summer 2000. The sites along about 18 km of the Pechora sea coast were surveyed and 10 observational profiles, located perpendicularly to the coastal bluff, were established.

In the study area the erosive-denudational types of coast prevail, except in the mouths of streams running to the sea where the erosive-accumulative types occur. The height of the coast varies from 2 up to 25-30 m and the slope angle reaches 45-90^0. We have allocated three basic types of deposits composing the coastal sections: 1) mainly peaty; 2) mainly sand; and 3) mainly sandy-loamy and loamy. The loams contain large quantities of bouldery material. All ground is perennially frozen. They have, as a rule, relatively low volumetric ice-content (no more than 0.2 without including polygonal-wedge ice). The increase of the ice-content (0.3 –0.4) is characteristic of the top 2-3 meters of sandy-loamy and loamy sections. The peat bogs contain the most ice-rich deposits, and they also have thick ice wedges. The width of ice wedges reaches 2-3 m, their depth is determined by the thickness of peat and can reach 5 m in depth.

The width of the beach at the inflow period reaches 5-10 m, and rarely 20 m. The beach is composed of bouldery material with mixed mineralogical composition. The width of the inflow-outflow (tidal) zone reaches 300 m. The sea floor here is sandy. The average height of inflow reaches 0.6 m. Permafrost under the sea is absent.

The most favorable conditions for the development and activation of coastal erosion appear when the tide is accompanied by the strong northeast winds. The base of slopes is undermined by the storm waves. The undermining of the coastal bluff breaks the equilibrium of the slopes and provokes the activation of slumping and sliding processes in the middle and upper parts of the slopes.

However, the formation of deep thermoerosive niches in the permafrost is not common, as the most ice-rich deposits lie usually in the upper part of coastal benches. The other reason is that the base of benches is blocked by a thick layer of sediments that were displaced downhill under the influence of slumping and slumping processes.

During our observations within the last two years we found no features of active coastal thermoerosion along the coast of the Pechora sea in the area of Cape Bolvanskiy. The retreat of the coastal bluffs top edges was stationary at six of the ten observational profiles; changing from several cm up to 40 cm per one year. The displacements of the active-layer ground blocks downslope (up to 6 m) were observed at several sites. The retreat of the coastal bluff occurs mostly as a result of slope erosion, slumping and sliding processes. The influence of coastal erosion was observed only at the base of the slopes at three observational profiles and located at the sites with the narrowest strip of the beach.

Thus, the coastal destruction in the area of Cape Bolvanskiy presently occurs under the influence of such processes as water and wind erosion, slumping, sliding, thermoerosion, thermodenudation etc.

This work is supported by INTAS (N 2332).

PHOTOGRAMMETRIC ANALYSIS OF COASTAL EROSION ALONG THE CHUKCHI COAST AT BARROW, ALASKA

W.F. Manley, L. Lestak, and J.A. Maslanik

INSTAAR, CIRES, and Aerospace Engineering, University of Colorado, Boulder, USA, email: William.Manley@colorado.edu

A variety of empirical and modeling approaches are being taken to assess the history and risk of erosion and flooding along the Chukchi Sea coast near Barrow, Alaska. Part of a broad assessment of climate impacts for the North Slope (nome.colorado.edu/HARC), this study utilizes softcopy photogrammetry and GIS to quantify coastal erosion over the last five decades.

We conducted a preliminary analysis of aerial photography for 1948 and 1997 (Fig. 1). The scanned photos were orthorectified and co-registered with PCI Geomatics to 0.5 m pixel resolution, using Ground Control Points (GCP's) previously acquired for this project with Differential GPS (instaar.colorado.edu/QGISL/barrow_gcp). The 1948 and 1997 shoreline and bluff-line positions were then digitized and overlaid. Locational accuracy is about 3.2 m for shorelines and 3.8 m for bluff lines, considering errors due to orthorectification, digitizing, and transient waterline shifts from tides and wave setup. Accuracy for corresponding erosion rates, averaged over the 49 year period, is thus 0.07 m/yr and 0.08 m/yr respectively.

Shoreline erosion is spatially variable, with 1948-to-1997 shoreline displacement averaging 20.7 m for the three areas shown in Fig. 2, equating with a time-averaged rate of 0.42 ± 0.07 m/yr. Net erosion rates reach 0.57 m/yr southwest of Barrow and 0.92 m/yr west of Barrow, with net progradation of about 0.1 m/yr for part of the Browerville shoreline (Fig. 2). Similarly, the nearshore bluff at Barrow has retreated on average 26.3 m over the intervening five decades, reaching a maximum retreat rate of 0.74 ± 0.08 m/yr. These erosion rates are approximately half those calculated for the ice-rich, peaty shorelines along Elson Lagoon, east of Barrow (Brown et al. 2003). They nonetheless are representative of the high rates of coastline erosion threatening many arctic settlements (cf. Hopkins and Hartz 1978; Reimnitz et al. 1988; Jorgenson et al. 2002; Smith 2002).

This analysis documents a significant hazard for the Barrow community. We plan to extend the analysis in space and time (SW of Barrow to Point Barrow, with additional photography for 1955, 1964, 1979, 1984, and 2002) to address such questions as: Which environmental factors control spatial variability in erosion? Is erosion accelerating due to climate change? Have mitigation efforts during the 1990's been effective at slowing erosion? Are the low-gradient gravel beaches northeast of Browerville experiencing progradation due to longshore drift of eroded materials? And with continued mitigation efforts, can we expect significant damage to buildings and infrastructure within the coming few decades?

References:

Brown, J., Jorgenson, T., Smith, O., and Lee, W., 2003, Long-term rates of erosion and carbon input, Elson Lagoon, Barrow, Alaska: Proceedings, 8th International Conference on Permafrost, A.A. Balkema Publishers, Rotterdam, Netherlands.

Hopkins, D.M., and Hartz, R.W., 1978, Coastal morphology, coastal erosion, and barrier islands of the Beaufort Sea, Alaska, U.S. Geological Survey, Open-File Report 78-1063, 54 p.

Jorgenson, M.T., Jorgenson, J.C., Macander, M., Payer, D., and Morkill, A.E., 2002, Monitoring of coastal dynamics at Beaufort Lagoon in the Arctic National Wildlife Refuge, northeast Alaska: Arctic Coastal Dynamics, Report of an International Workshop, Ber. Polarforsch. Meeresforsch., v. 413, p. 22-28.

Reimnitz, E., Graves, S.M., and Barnes, P.W., 1988, Beaufort Sea coastal erosion, sediment flux, shoreline evolution, and the erosional shelf profile, U.S. Geological Survey, Map I-1182G.

Smith, O.P., 2002, Coastal erosion in Alaska: Arctic Coastal Dynamics, Report of an International Workshop, Ber. Polarforsch. Meeresforsch., v. 413, p. 65-68.

Figure 1. Orthorectified 1997 aerial photography of Barrow and Browerville, showing the 1948 shoreline position, as well as the location of close-up panels in Fig. 2.

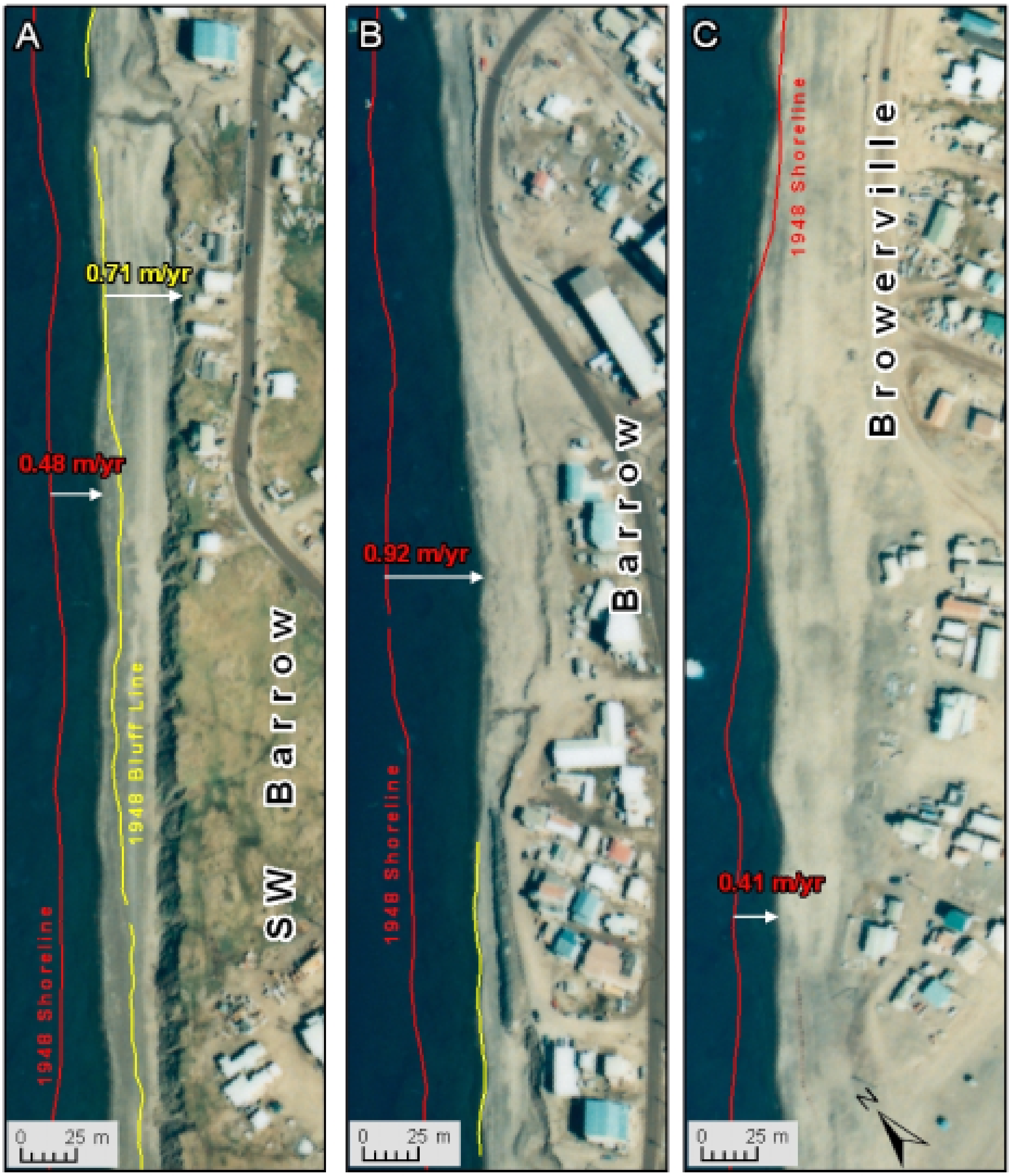

Figure 2. Coastal strips of the 1997 orthophoto mosaic, showing the position of the 1948 shoreline and bluff line. Also shown are shoreline and bluff-line erosion rates for selected areas.

CURRENT COASTAL RESEARCH IN CANADA'S WESTERN ARCTIC

G. Manson[1], D. Forbes[1], J.C. Lavergne[2], M. Craymer[2], J. Hines[3], H. Swystun[4] and T. Milne[5]

[1]Geological Survey of Canada, PO Box 1006, Dartmouth, NS, Canada, B2Y 1E5, [2]Geomatics Canada, 615 Booth St., Ottawa, ON, Canada, K1A 0E9, [3]Canadian Wildlife Service, 5204 50th Avenue, Suite 301, Yellowknife, NWT, Canada, X1A 1E2, [4]University of Northern British Columbia, 3333 University Way, Prince George, BC, Canada, V2N 4Z9, [5]Centre of Geographic Sciences, 50 Elliot Rd. RR#1, Lawrencetown, NS, Canada, B0S 1M0

Relative to other Canadian shorelines, those fringing the Beaufort Sea appear to have particularly high erosion rates due to the presence of ice-bonded, fine-grained sediments and rising relative sea level (RSL). East of Banks Island, shorelines become generally more rocky. Field observations, tide gauge records and ice-loading model results indicate that relative sea level regimes change from rising, through stable, to falling, suggesting decreasing erosion rates from the Mackenzie Delta towards the Coronation Gulf (Fig. 1). In several related and ongoing studies, we conducted fieldwork in the summers of 2001 and 2002 to measure rates of land motion, to revisit and establish coastal change monitoring sites, and to map coastal wetlands and snow goose and swan nesting habitat.

RSL is a function of changes both in land elevation (the isostatic component) and in sea level (the eustatic component). Measurements of both components are required to determine changes in relative sea level due to climate change. To measure land motion, continuous dual-phase GPS monitoring sites have been established at Resolute (NU), Inuvik, Sach's Harbour and Holman (NWT) and epoch sites (where measurements are taken annually over periods of days to weeks) have been established at Mould Bay and Kugluktuk. Land motion results will be used to validate of an ice-loading model and to assist in future model development. To measure sea-level, a tide gauge was established by the Canadian Hydrographic Service at Holman and efforts are underway to establish or re-establish other tide gauges at key locations (Fig. 2). Depending on rates of change, these instruments may take years or decades to produce statistically significant results; in the meantime, the GPS sites act as base stations for precise surveying and the tide gauges provide information on water levels relevant to shipping and communities prone to flooding during storm surges.

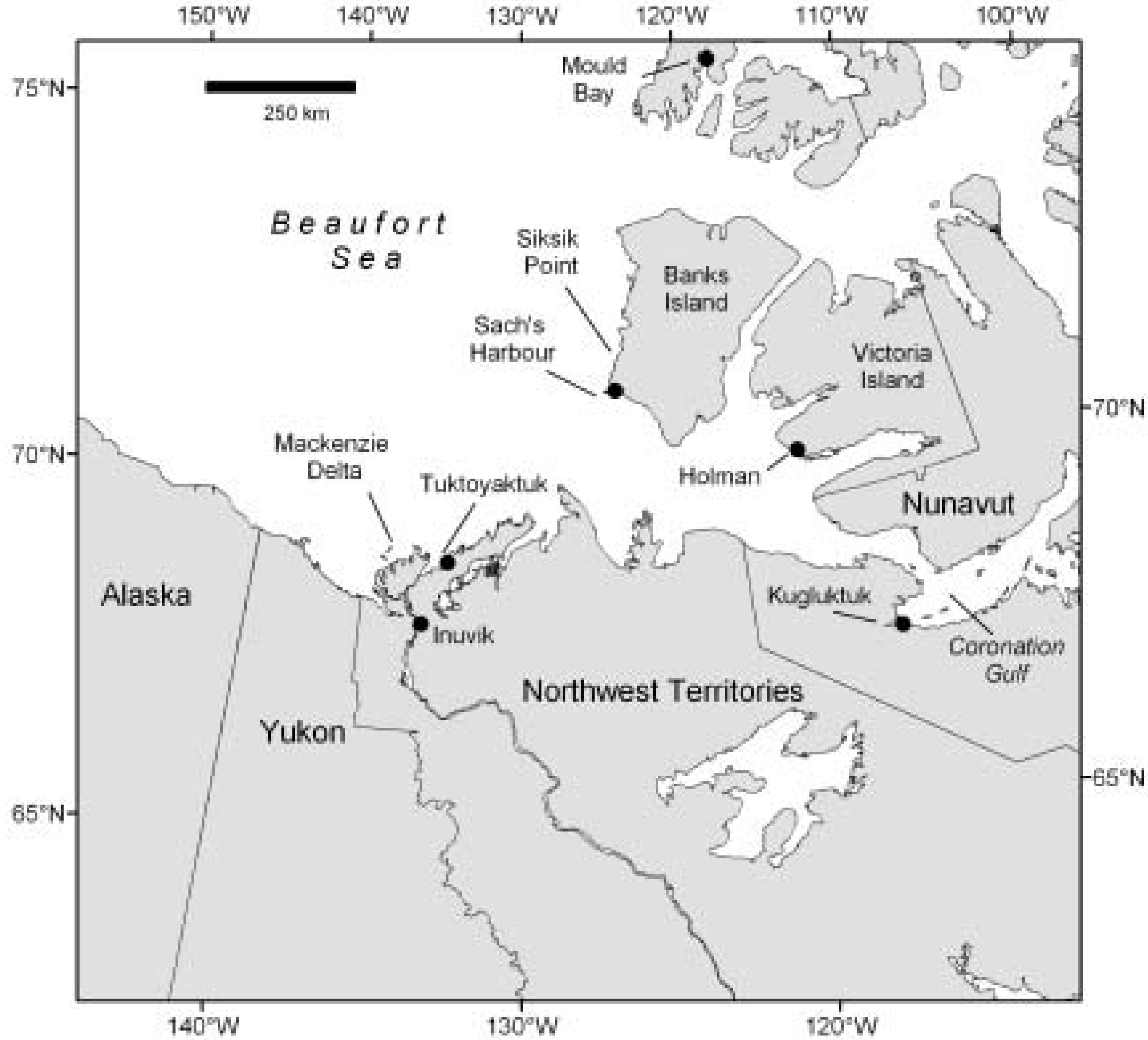

Figure 1. Map of locations in which field work was conducted.

In 2002, erosion monitoring sites on the outer Mackenzie Delta, and at Tuktoyaktuk, and Holman were revisited and new sites were established on the west coast of Bank's Island and at Sach's Harbour and Kugluktuk. Real-time kinematic (RTK) GPS with centimetre accuracy was used to collect cross-shore and alongshore profiles. These profiles were continued offshore using an echosounder with decimetre resolution mounted onboard various small boats and positioned with RTK GPS.

Several approaches were used to position and store observations of coastal wetland plant communities for mapping goose and swan habitats. Three scenes of QuickBird satellite imagery (totalling approximately 375 km^2) were collected at Tuktoyaktuk, Kugkluktuk and an area of western Banks Island at Siksik Point. Launched in October 2001, QuickBird is a passive pushbroom sensor collecting one panchromatic channel (450 – 900 nm) with 0.7 m spatial resolution and four multispectral channels with 2.8 m spatial resolution in the blue, green, red and near-infrared spectral regions (450 – 520 nm, 520 – 600 nm, 630 – 690 nm and 760 – 890 nm, respectively). From satellite ephemeris alone, the spatial accuracy of QuickBird imagery is purported to be 23 m which, with the exception of community mapping conducted by the territorial governments, is thought more accurate than base maps in the Canadian Arctic. Digital orthophotography with accuracy of 3 m exists for the Mackenzie

Delta and will be used to geocorrect the Tuktoyaktuk scene. In the community of Kugluktuk (Fig. 3), imagery will be geocorrected to the community maps.

The described research will contribute to other ongoing projects with national and international scope. These include a national assessment of the vulnerability of shorelines to changing climate, development of climate change adaptation strategies for Canadian coastal communities, implementation of intergrated coastal zone management and Canada's Oceans Act and contributions to the Arctic Coastal Dynamics Project and the Intergovernmental Panel on Climate Change.

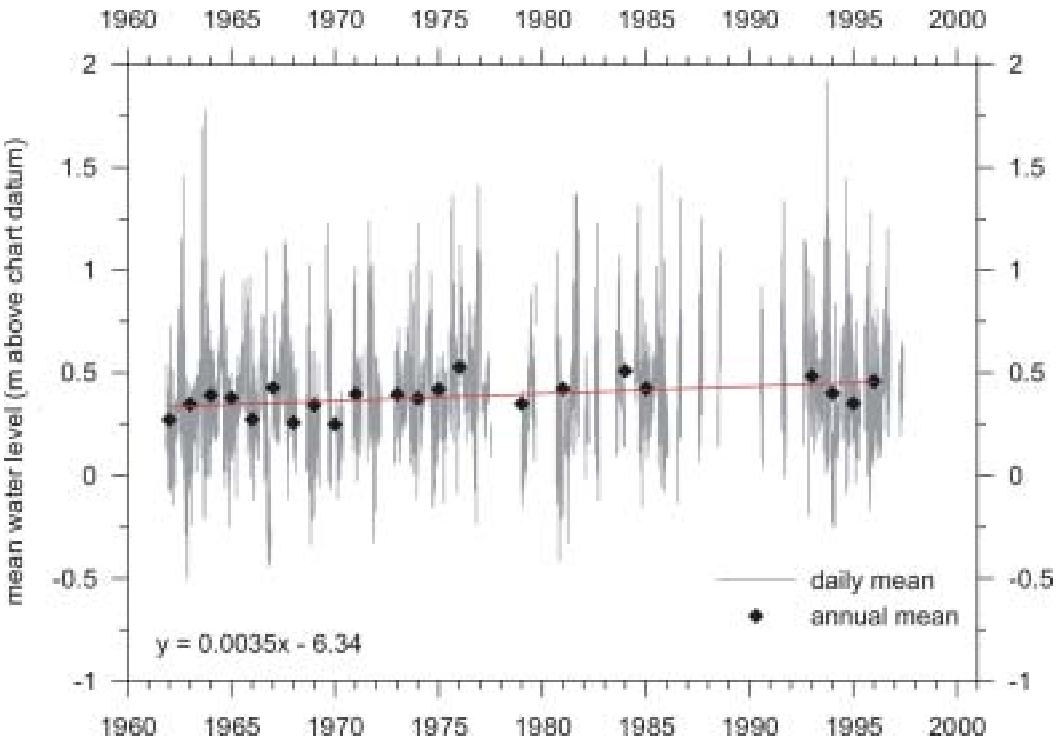

Figure 2. The tide gauge record from Tuktoyaktuk showing daily and annual means. Regression of annual means for years with nearly complete data from 1961 to 1997 gives a statistically significant ($\propto = 0.05$) rate of relative sea-level rise of 3.5 mm/a.

Figure 3. Panchromatic QuickBird imagery showing part of a mosaic of the Coppermine River delta and community of Kugluktuk. The inset (area of box) shows raised beach deposits intersected by gullies and ice wedge polygons.

THE FIT-FOR-USE OF THE GEBCO COASTLINE TO ESTIMATE COASTAL LENGTH – A CASE STUDY FROM SPITSBERGEN

R.S. Ødegård [1], B. Wangensteen[2] and J.L. Sollid[2]

[1] Gjøvik University College, P.O.Box 191, N-2802 Gjøvik, Norway, [2] Department of Physical Geography, University of Oslo, P.O. Box 1042 Blindern, N-0316 OSLO, Norway

The fit-for-use of the GEBCO coastline to estimate coatal length has been investigated for an area in Kongsfjorden, Svalbard (79˚ N, 12˚ E). This is one of the key sites of the ACD project. Coastal length is basically a fractal problem. The dependency between map scale and obtained length will depend on the mapping technique used, post processing of the digital data and the complexity of the coast. A comparison of the GEBCO coastline with digital maps on the scale 1:100 000 and satellite imagery (Landsat) clearly shows the problems of estimating reliable coastal lengths in coastal dynamics applications. The two main problems are that the quality of the estimate is not known and that the quality needed in the ACD applications is not clearly defined.

The following strategy is suggested:

- Define user requirements for the ACD project depending on desirable accuracy of estimates made within the project.
- Test different methods to correct the estimates from the GEBCO coastline, based on reference from satellite imagery.
- Decide on a method based on validation from high accuracy digital maps or field control.

COASTAL DYNAMICS IN THE PECHORA SEA UNDER TECHNOGENIC IMPACT

S.A. Ogorodov

Faculty of Geography, Moscow State University, Moscow, Russia, ogorodov@aha.ru

Abstract

The geoecological situation in the regions of intensive industrial exploitation on the Pechora Sea coast, particularly Varandei area, is at an almost critical state. The technogenic impact causes the intensification of eolian and slope processes, thermoerosion and thermokarst. The stability of the coasts decreases, and the rate of their retreat grows. Industrial exploitation results in not only destruction of natural environments, but also, considerable material losses. Several housing estates and industrial constructions have been already destroyed in the course of abrasive cliff retreat. The damage will grow every year following the cliff retreat towards the center of the Varandei settlement. Oil terminal, airport and other industrial objects are endangered.

Introduction

Under natural conditions, the Pechora Sea coasts are relatively stable, but become rapidly destroyed under technogenic impact (Geoekologiya… 1992). The case in point is the Varandei industrial area where expeditious measures on protection of industrial and residential buildings are necessary. Technogenic impact upon the Varandei area activates abrasion because of improper exploitation that does not consider the peculiarities of coastal relief and dynamics (Novikov and Fedorova 1989; Ogorodov 2001a,b; Sovershaev et al. 2001). Coastal erosion of the Varandei area threatens the settlement, oil terminal and airport. Therefore, it is necessary to thoroughly analyze coastal morpholithodynamic schemes before the natural environments are disturbed.

Results and discussion

Two main morphogenetic complexes (Fig. 1) are distinguished within the studied area which has an extent of 90 km from the western extremity of the Pesyakov Island to the eastern extremity of the Medynskii Zavorot Peninsula.

The first complex represents a young marine accumulative terrace with an average height of 3-5 m formed during the Holocene transgression. The terrace occupies the Pesyakov and Varandei islands (that are, in fact, barrier beaches), Peschanka River mouth and Medynskii Zavorot Peninsula. Its width reaches 2-6 km. The terrace is formed by a fine sand unit underlain by peat-grass pillow. The cryogenic structure of the terrace sediments is characterized by small ice volume of 5-10% (Novikov and Fedorova 1989). The frontal, seaward, part of the terrace is covered by an avandune (dune belt of the barrier beach) reaching 5-12 m asl (Fig. 2). At the distal parts of the barrier beaches, the avandune turns into a series of ancient and young beach ridges corresponding to different stages in evolution of barrier beaches and barriers-spits. The barrier ridges have undergone considerable reworking by eolian processes. The inner parts of the terrace behind the dune belt represent a laida up to 2.5-3 m high with two levels corresponding to the surges of low and high recurrence.

At present, under natural conditions, most part of the Holocene terrace is being eroded at a rate of 0.5-2.5 m per year (Ogorodov 2001 a,b; Fig. 1). The abrasion coast (Fig. 3) has an erosion scarp cut in eolian-marine fine sands. Its height ranges from 1 to 6 m. Close to the zones of wave energy divergence, where the rate of abrasion is higher, the coastal bluff is well pronounced and remains nearly perpendicular during most part of the year. In the regions of sediment transit, due to denudation, deflation and slope processes the coastal slope is relatively gentle, about 20-50°. However, during years with extraordinary strong fall storms the slope is eroded and becomes steeper for a short period of time. Thermoabrasion does not, in fact, erode slopes of the Holocene terrace. The latter is destroyed due to relatively high average annual ground temperature, small ice volume and a considerable thickness of the layer of seasonal melting. Coastal erosion is determined by a combination of different factors including a deficit of coarse-grained beach-forming material (discrepancy between the grain size and hydrodynamic conditions), a not well developed profile of the submarine coastal slope, and a high gradient of the avandune slopes. Sediment material released due to erosion is accumulated at the distal parts of Pesyakov and Varandei islands and Medynskii Zavorot Peninsula, where the wave energy decreases. Here, the young beach ridges and high-water surge berms are formed (Fig. 1).

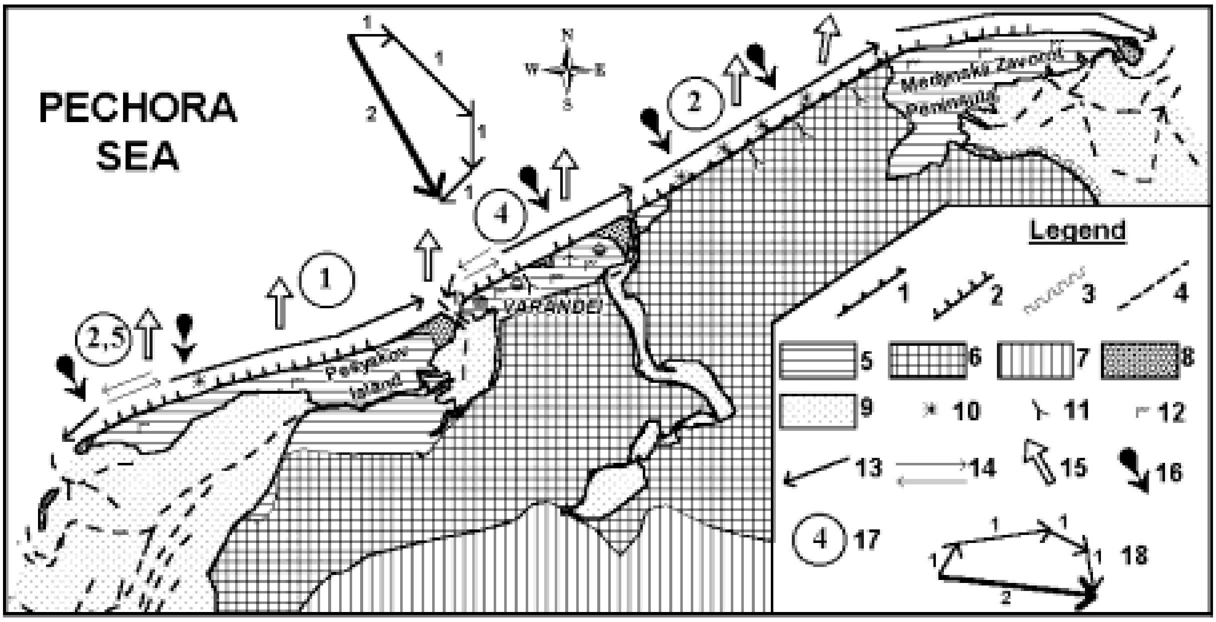

Figure 1. Morpholithodynamics of the Pechora Sea coasts near Varandei settlement. Key: Types of abrasion coasts: 1 – with thermoabrasion or abrasion-thermodenudation cliff in dense boulder loams; 2 – with wave-cut cliff in sand and peat beds with low ice content; 3 – dead cliffs. Elements of bottom relief: 4 – big channels of subaerial and hydrogenic origin. Types of terrestrial relief: 5 – marine transgressive terrace (QIV) with dune belt (up to 5-12 m asl) in the frontal part and laida (up to 2.5-3 m) in the inner part; 6 – alluvial-lacustrine terrace (QIII-IV) up to 5-15 m high with thermokarst dissection; 7 – glacial(ice?)-marine denudation plain (QII) (above 20 m high) with erosional dissection; 8 – free accumulative forms (QIV) (beaches with well-developed profile, high-water surge berms). Elements of morpholithodynamics: 9 – areas of lagoonal accumulation within tidal flats and bays; 10 – “clayey bench”; 11 – regions of active gully thermoerosion; 12 – regions of active deflation; 13 – average multiannual directions of sediment flows; 14 – areas of bilateral sediment flows; 15 – removal of fine-grained material along small discharge channels; 16 – release of the rock debris and pebbles from submarine coastal slope; 17 – measured average multiannual rate of coastal bluff retreat, m/year; 18 – energetic polygon plotted on the base of the hydro-meteostation Varandei data, where (1) – rhumb component of the wave energy flow; (2) – wave energetic resultant, 1 mm of the arrow length = 1 arbitrary unit of wave energy.

The second morphogenetic complex is represented by the 5-15 m high gently rolling lacustrine-alluvial (?) plain with numerous lakes (Fig. 1) usually referred to as the First terrace of the Late Pleistocene-Holocene age (Novikov and Fedorova 1989). The origin of this terrace has long been debated (Danilov 1978), but there is still no concrete evidence for its genesis. Also, the age of the terrace is still uncertain. Though this terrace occupies most part of the territory it reaches the coastline only between the Peschanka River and the base of the Medynskii Zavorot Peninsula. The surface of the terrace is covered with frost polygons and bogs. The base (terrace socle) of the terrace is composed of dense ice(glacial?)-marine loams and clays with inclusions (3-5%) of strongly weathered boulders, blocks, rock debris and gravel (_ of the section). The layer of sands and peat represents the upper _ part of the terrace section. The terrace sediments include ice wedges and massive ice beds.

Where the First terrace reaches the sea, the thermoabrasion coast (Fig. 4) has a cliff worked out in frozen dense boulder loams. The height of the abrasion cliff ranges from 3 to 10 m. Unlike the Holocene terrace, here thermoabrasion plays the main role in coastal erosion. At some places, typical thermoabrasion niches are present. Thermodenudation processes (i.e. thermoerosion, solifluction, slumping, suffosion) considerably affect the coastal dynamics supplying sedimentary material to the coast basement (Fig. 4). The abrasion cliff is surrounded by a narrow (10-20 m) pebbly-sandy beach that gradually turns into an abraded tidal flat (Fig. 5) – the so-called “clayey bench”. Due to specific granulometric composition of the sediments, the amount of beach-forming material produced by thermoabrasion is insufficient. The presence of landslides and mud-flows, as well as small beach width give evidence for the relatively low resistance of the coasts. The average rate of thermoabrasion coast retreat was estimated at 1.8-2.0 m per year (Novikov and Fedorova 1989).

About 300×10^3 m^3 of fine sand material are supplied to the coastal zone every year due to erosion of the Holocene terrace (Ogorodov 2001a). The thermoabrasion

Figure 2. Dune belt on the barrier beach separating laida from the sea, Pesyakov Island (photo of N.N. Lugovoi).

Figure 3. Wave-cut cliff near the Varandei oil terminal.

Figure 4. Thermoabrasion coast 30 km to the east-northeast of Varandei settlement (photo of N.N. Lugovoi).

coast supplies 130×10^3 of sand, 5×10^3 of coarse debris, 25×10^3 of peat and 120×10^3 of clay to the coastal zone. Parts of the sand and all clay material are accumulated below the 10 m isobath. All coarse debris and parts of the sand material are incorporated into alongshore drift and form beaches and beach ridges at the distal ends of barriers and spits. In the course of eolian transportation the fine-grained fraction is partly evacuated from the beaches towards the barriers and settles within the dune belt.

Coastal retreat is accompanied by erosion of the submarine coastal slope and the tidal flat due to abrasion (including thermoabrasion) (Fig. 5). This results in increasing water depths. As mentioned by Mel'nikov and Spesivtsev (1995), the presence of permafrost and, hence, thermoabrasion of the submarine coastal slope are typical only for thermoabrasion coasts. As a rule, permafrost is absent on the submarine coastal slope of barriers and spits. In the Varandei coastal region, the submarine coastal slope is mainly composed by the same clayey sediments (with inclusions of coarse grained material – 3-5%) that are exposed at the thermoabrasion part of the coast. A thin layer of sands in places overlying boulder loams is unable to protect the submarine coastal slope from abrasion during strong storms. Practically no beach-forming material is produced due to abrasion of the submarine coastal slope. Discharge and rip currents evacuate clay particles that move downslope in the form of suspension flows. The currents are restricted to numerous troughs that cut the lower part of the submarine coastal slope at a depths of 5-10 m. Coarse-grained material washed out from loams is mainly accumulated *in situ* forming a pebbly pavement at bottom swells. Where the shifting force of waves is sufficiently high, some fragments reach the coastline and take part in beach formation. For instance, pebbly beaches at the western extremity of the Pesyakov Island and eastern extremity of the Varandei Island were formed through this mechanism (Fig. 6). Coastal bluffs of these beaches are formed of fine sands solely. Using the method of Shuiskii (1986), we estimated the average layer of effective abrasion of the submarine coastal slope at 0.02 m/year. It slightly increases at tidal flats. As a result, the amount of sedimentary material supplied to the coastal zone is nearly equal to the amount of sediments released in the course of coastal erosion. However, as shown above, the amount of beach-forming material in this zone is extremely low.

Figure 5. Abrasion surface of tidal flat ("clayey bench"), 30 km to the east from Varandei settlement.

Figure 6. Pebbly beach on the eastern end of the Varandei Island.

Active exploitation of the Varandei industrial area started in the seventies. Varandei Island was subjected to the strongest technogenic impact. Here, the main industrial base was formed, and Novyi Varandei settlement for 3.5 thousand inhabitants was built. The well-drained dune belt of the Holocene terrace (first morphogenetic complex) composed by sand beds with low ice content was chosen as a place for the settlement, oil terminal and storehouses, because it seemed to be more stable from the engineering-geological point of view than the surrounding swampy tundra lowland (second morphogenetic complex).

The construction of the settlement and industrial base that was held practically at the edge of the abrasion cliff demanded repeated withdrawals of sand and sand-pebble sediments from the avandune and beach. This is absolutely unallowable for the zones of wave energy divergence (Fig. 1) (Popov and Sovershaev 1988), especially in the zones that has been eroded before.

Within the zone of industrial exploitation, the coastal bluff and the coastal zone experienced considerable mechanical deformations of the landforms because of transport ramps, mechanical leveling of coastal declivities and other technogenic disturbances (Novikov and Fedorova 1989; Sovershaev et al. 2001). Systemless use of transport and construction technique including caterpillars caused the degradation of the soil and plant covers of the whole dune belt of Varandei Island. Under conditions of deep seasonal melting, the dune belt formed of fine sands is subjected to deflation, thermoerosion and thermokarst. The extent and rate of these processes are so great that in places the surface of the island became 1-3 m lower than before the period of exploitation (Fig. 7). Deflation hollows and thermokarst depressions became widespread. Numerous deflation-thermoerosional gullies were formed in the abrasion cliff. As a result, the cliff becomes lower, its homogeneity is disturbed, the amount of sediments supplied to the coastal zone decreases and, finally, the coasts become less stable, and the rate of their retreat grows.

During the 2000 field season we measured the rates of deflation and thermoerosion on the specially equipped stations (Ogorodov 2001b). The averaged data of repeated measurements at more than 50 reference squares have shown that the thickness of the sand layer blown away by wind was 10 to 14 cm at technogenically-deformed territories. At the same time, eolian accumulation took place at the territories that are not affected by human activity. At the "erosional" station, we observed the formation of a big gully (up to 4 m deep) in the coastal bluff. Up to 400 m^3 of sand were removed from the gully itself and from its catchment area during the two weeks of snow melting in June.

Coast protection in the area close to Novyi Varandei settlement (the region of wave energy flow divergence and, correspondingly, formation of sediment flows) caused a decrease in sediment supply to the adjacent areas and, hence, their erosion.

Figure 7. During the period of exploitation, the surface of barrier beach on the Varandei Island became 1-3 m lower due to deflation, thermoerosion and thermokarst.

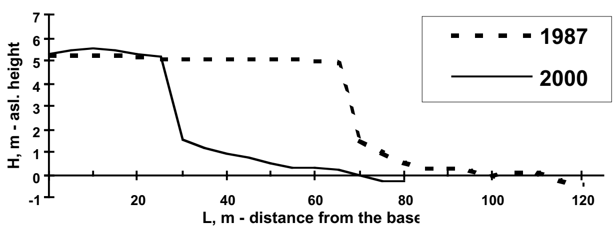

Figure 8. Dynamics of the coast near Varandei settlement.

After the earth-dam and bridge across the Promoi River branch were constructed in the eastern part of the Varandei Island, the height of the storm surges increased. The latter is an important factor of coastal dynamics. Previously, during high surges corresponding in time with tides water was partly flowing into the Promoi branch and then to the Varandeiskii Shar channel, thus lowering the surge height and decreasing its influence upon the coast.

Under existing conditions of intensive technogenic impact, the abrasion rate considerably increased in the middle-late seventies. In some years it was up to 7-10 m/year. The rate of coastal retreat slightly decreased, down to 1.5-2 m/year, after the coastal protecting construction was built near Novyi Varandei settlement. However, it remained high at the adjacent areas. Recent measurements during 1987-2000 (Fig. 8) have shown that the rate of coastal retreat in the region around the settlement increased and reached 3-4 m/year that is twice as high as in the regions that are not affected by human activity.

Conclusions

The geoecological situation on the Varandei Island is almost critical. The industrial exploitation of the territory resulted in not only the destruction of the natural coastal system, but also in considerable material losses. Due to rapid retreat of the abrasion cliff, several industrial and residential buildings were destroyed by October 2000. With further retreat of the coastal cliff towards the center of the settlement, the losses will grow from year to year. The oil terminal is endangered, because the distance between the coastal bluff edge and the nearest oil storage tank is less than 6 m (Fig. 3).

Active industrial exploitation of the Pechora region demands a well-thought-out strategy of the territory development and the finding of proper areas for new constructions. The negative example of the Varandei region requires a well-developed ecologically grounded approach to further exploitation of coastal regions.

After many years of investigations in the Pechora Sea region, the Research Laboratory of the Geoecology of the North, MSU, has worked out a unique methodology of morpholithodynamic research and created a database on the coastal morpholithodynamics of this area that will be a basis for solving both fundamental and applied problems arising in course of coastal reclamation.

References

Danilov, I.D., 1978. Pleistotsen morskikh subarkticheskikh ravnin (The Pleistocene of the subarctic marine lowlands. Moscow, Izd. MGU, 198 pp. (in Russian).

Geoekologiya Severa (Geoecology of the North), 1992. Solomatin, V.I. (ed.), Moscow, Izd. MGU, 270 pp. (in Russian).

Mel’nikov, V.P., Spesivtsev, V.I., 1995. Inzhenerno-geologicheskie i geokriologicheskie usloviya shel’fa Barentseva i Karskogo morei (Engineering-geological and geocryological conditions of the Barents and Kara shelf). Novosibirsk, Nauka, 197 pp. (in Russian).

Novikov, V.N., Fedorova, E.V., 1989. Destruction of coasts in the southeastern Barents Sea. Vestnik MGU, ser. 5, geografiya, 1, 64-68. (in Russian).

Ogorodov, S.A., 2001a. Morphology and dynamics of the Pechora Sea coasts. Proceedings of the Institute of Oceanology BAN, Varna, vol. 3, P. 77-86. (in Russian).

Ogorodov, S.A., 2001b. Functioning of the Pechora Sea coastal systems under technogenic impact. In: Sedimentologicheskie protsessy i evolyutsiya morskikh ekosistem v usloviyakh morskogo periglyatsiala (Sedimentological processes and evolution of marine ecosystems under marine periglacial conditions). Apatity, Izd. KNTs RAN, P. 82-90. (in Russian).

Popov, B.A., Sovershaev, V.A., Novikov, V.N., Biryukov, V.Yu., Kamalov, A.M., Fedorova, E.V., 1988. Coastal area of the Pechora-Kara Sea region. In: Issledovanie ustoichivosti geosystem Severa (Investigations of the geosystems stability in the North), Moscow, Izd. MGU, P. 176-201. (in Russian).

Shuiskii, Yu.D., 1986. Problemy issledovaniya balansa nanosov v beregovoi zone morei (Problems in investigations of sediment balance in the coastal zoneof the seas). Leningrad, Gidrometeoizdat, 239 pp. (in Russian).

Sovershaev, V.A., Ogorodov, S.A., Kamalov, A.M., 2001. Technogenic factor in development of coasts in the Varandei industrial area. In: Solomatin, V.I. (ed.) Problemy obshei I prikladnoi geoekologii Severa (Problems of the general and applied geoecology of the North). Moscow, Izd. MGU, P. 126-134. (in Russian).

DYNAMICS AND EVOLUTION OF BARRIER BEACHES IN THE PECHORA SEA

S.A. Ogorodov and Ye.I. Polyakova

Faculty of Geography, Moscow State University, Moscow, Russia, ogorodov@aha.ru

Abstract

The article discusses the main results of the complex investigations of barrier beaches in the Pechora Sea including coastal dynamics and accompanying exogenic processes (eolian transportation), lithological and micropaleontological studies of the sediment sequence and radiocarbon dating. We were the first to reconstruct sedimentation conditions and evolution of these big accumulative forms in the Pechora Sea. Stationary observations on coastal dynamics and the rate of eolian sedimentation allowed estimating the rate of barriers retreat. The mechanism of formation and evolution of dune belts on these barriers is described. The composition of diatom associations and lithological data give evidence for facial-genetic conditions of sedimentation during the accumulation of barriers. Radiocarbon datings corroborate the “young” age of the modern avandune ridges of the barrier beaches.

Introduction

Coastal accumulative landforms (spits, barriers, bay-bars) are widespread in the Pechora Sea among them big barrier beaches and barrier islands – Varandei Island, Pesyakov Island, Gulyaevskie Koshki Islands (Popov et al. 1988). These landforms are thought to be accumulated during the period of climatic optimum at the final stage of the Holocene transgression, when both the duration of the dynamically active period and the hydrodynamic activity were highest (Zenkovich 1957; Badyukova and Kaplin 1995). Clastic material from the upper shelf involved in onshore movement was accumulated in big coastal landforms. Where the wave resultant is nearly normal to the coastline, the typical barrier beaches and barrier islands were formed. Other accumulative forms of Holocene age, like the Russkii and Medynskii Zavorot Peninsulas, are usually considered as barriers-spits by specialists (Popov et al. 1988). Besides the transversal movement of load, alongshore sediment flows also plays an important role in their formation. A further lengthening of the barrier-spits results from the decrease in the alongshore wave energy flux and corresponding sediment discharge.

Where the waves are high enough to overflow the coastal accumulative forms, the latter are lower than 2.5-3.0 m. Over considerable stretch of the shoreline, eolian processes have built a thick dune belt (avandune) over barrier beaches and barriers-spits. Their absolute height averages 4-7 m, but some dunes are up to 10-12 m high. Some researchers take the average height of the dune belt as the height of the ancient coastal ridges formed during maximum of the Holocene (Flandrian) transgression (Avenarius 2001). Based on this assumption, the Middle Holocene sea-level highstand is estimated as 5-6 m above its present position, and the high fragments of accumulative forms are referred to as the Middle Holocene ones (Avenarius et al. 2001; Avenarius and Repkina 2001). Therefore, according to this hypothesis, the dune belt represents “fragments of paleo-barriers”, that could hardly be a justified assumption.

Detailed geological and geomorphological investigations of Varandei and Pesyakov islands carried out by the authors included observations on coastal dynamics and accompanying exogenic processes (eolian transportation), lithological and micropaleontological studies of the coastal sections and radiocarbon dating. This allowed us to carry out the first reconstructions of sedimentation conditions and evolution of big coastal accumulative forms in the Pechora Sea.

Results and discussion

Barriers of Varandei and Pesyakov islands have similar structure (Fig. 1). The shoreface of these accumulative forms is covered with the dune belt (avandune) up to 4-10 m high. In the zones of divergence of wave energy, an abrasion bluff formed on the marine slope of avandune evidences a relatively high rate of coastal retreat. At the places of sediment transit, the marine slope of avandunes is relatively gentle (about 20-50^{o}) due to less intensive wave activity and the influence of slope processes. However, during years of extremely strong storms it could become steeper for a period of time due to abrasion. A relatively narrow beach (20-100 m) leaning against the marine slope of the avandune gradually turns into the tidal flat.

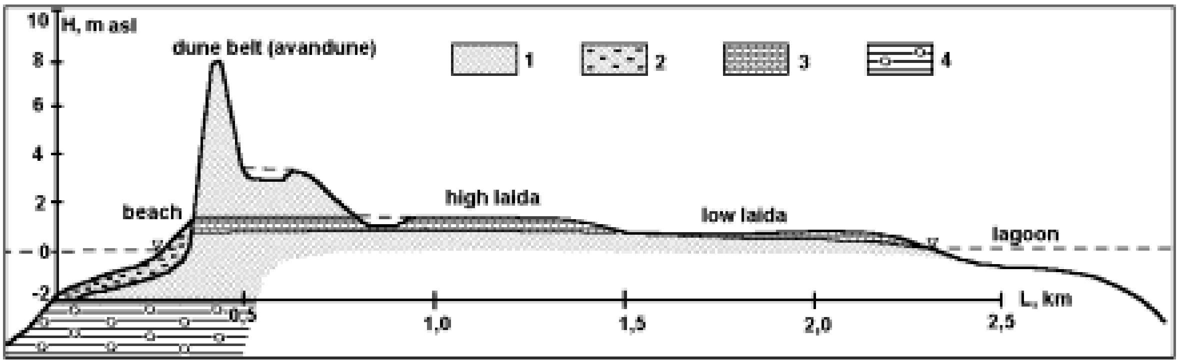

Figure 1. Geologic-geomorphologic transect of the barrier beach, Pesyakov Island. Key: 1 – fine-grained sands; 2 – sands with pebbles; 3 – "peat-grass pillow"; 4 – boulder clays and loams.

At the distal parts of barriers, the avandune becomes lower and is replaced by a series of inactive coastal ridges marking certain stages in evolution of accumulative landforms. Coastal ridges have been considerably reworked by eolian processes. Where the storm surge overwashes the barrier, the well-developed active coastal ridge is formed.

Laidas or high-water surge berms occupy the inner part of the barrier beach behind the dune belt. They are located at 2.5-3.0 m asl. Two morphological levels correspond to wind surges of low and high recurrence (Fig. 1).

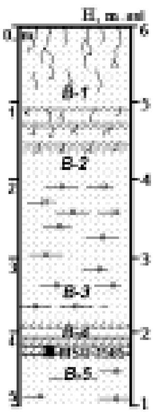

Figure 2. Composite section of the barrier beach, Varandei Island: **0-1,1 _** – sands, fine-grained, well-sorted, greyish yellow, with thin sub-horizontal layering, numerous plant roots. Spots of ferruginization and a thin organic-rich layer at the boundary with the underlying layer; **1,1-1,3 _** – sands, fine-grained, well-sorted, whitish yellow, with thin horizontal layering, inclusions of slightly decayed grass stems; **1,3-1,7 _** – intercalation of sub-horizontal undulated brown and black interlayers of "grass pillow" with interlayers of whitish yellow fine-grained and dusty sands, thickness of interlayers up to 5 cm; **1,7-3,9 _** – intercalation of whitish yellow and brownish yellow sands, fine-grained, well-sorted (sub-horizontal layering). Layering expresses itself by thin dark interlayers with semi-decayed plant debris and spots of ferruginization; **3,9-4,4 _** – "peat-grass pillow": semi-decayed remains of grasses and bog plants together with brownish sandy-clay material with greyish yellow interlayers of clayey fine-grained sands; **4,4-5,0 _ (apparent)** – fine-grained sands, grey, with plant debris, layering is absent; ***_-3*** – samples for diatom analysis; **MSU-1585** – sample for radiocarbon dating.

In general, barrier beaches of the Pechora Sea are relatively rapidly moving onshore because of shoreface abrasion, wave and eolian transportation of sand from the windward to leeward slope. Field observations on coastal dynamics carried out from 1969 till 2000 showed that the coastal retreat rates on Pesyakov Island, which is practically unaffected by human activity, equaled 0.5-2.5 m per year (Ogorodov 2001b). As a result, the so-called "fragments of paleo-barriers" with a width of 50 to 350 m must be completely reworked during 100-400 years. Thus, they could hardly be of Middle Holocene age even if assuming that the rates of coastal retreat have increased during the last century. Radiocarbon dating of wood (MSU-1585) from the lower part of the "peat-grass pillow" of the laida exposed in the basal part of coastal bluff (Figs. 1, 2) corroborates the extremely "young" age of the overlying sand layer.

Eolian processes play an important role in formation and evolution of barrier beaches in the Pechora Sea. This role has been previously underestimated. In case wind speed exceeds 12 m/s fine-grained sand material is evacuated from beaches and tidal flats. Observations revealed that during one storm a 3-5 cm thick sand layer could be blown away from the open beach surface (Ogorodov 2001a; Fig. 3). During the dynamically active period, deflation removes not less than 1 m^3 of sediments from one square meter of beach surface. Most part of eolian material removed from beaches and tidal flats is accumulated within the dune belt (avandune). Specific vegetation growing on avandunes protects it from deflation and favors intensive accumulation of eolian material. It should be noted, that the extent of the opposite eolian transportation – from the dune belt to the beach and tidal flats – is considerably less due to high anti-deflation stability of the dune belt.

Figure 3. Beach surface after severe storm wind, Pesyakov Island (photo of N.N. Lugovoi).

During fieldwork in 2000 we measured the rates of eolian sedimentation at specially equipped monitoring stations. Averaged data on repeated measurements carried out at more than 50 reference marks showed that the thickness of the sand layer accumulated during the two summer months ranged from 3-16 cm at a distance of 10 m from the avandune edge to 0.5-4 cm - at 100 m. These high rates of eolian accumulation are responsible for the considerable height and width of the dune belt previously mistaken for as "fragments of paleo-barriers".

Actually, the sediment sequence exposed in coastal bluffs of the barriers above 1.0-2.0 m is entirely represented by subaerial complex (Fig. 2): fine-grained sands with abundant grass remains and traces of soil processes. They are devoid of any pebbles, gravel and other coarse-grained debris. On the contrary, deposits of beaches, active coastal ridges and high-water surge berms in the Pechora Sea consist of less sorted sands with numerous pebbles, gravel, rock debris and single bivalve shells. Coarse-grained material originates from numerous exposures of boulder clays and loams on the submarine coastal slope (Fig. 1). No coarse debris was found in the barrier beach sediments from the cores recovered at considerable distance from the coastal bluffs. Laida deposits with characteristic peat-grass pillow are usually exposed below 1-2 m level. Laida deposits accumulated in the inner parts of the barriers under the influence of storm surges up to 2.5-3.5 m high do not give any evidence either for higher than modern sea-level position or the Middle Holocene age of the overlying sand unit.

Diatom analysis of the barrier beach sequence from the Varandei Island (Fig. 2) revealed the gradual succession of fossil associations indicating changing sedimentation conditions.

Fine-grained grey sands with grass remains exposed at the base of coastal bluff (**sample B-5**) contain ecologically diverse diatom association including both marine and freshwater species. Taxonomically diverse marine benthic diatoms inhabiting littoral and sublittoral zones of the arctic seas (*Diploneis interrupta, D.bombus, D.smithii, D.litoralis, Paralia sulcata)* along with euryhaline species *(Achnanthes delicatula v.hauckiana, A.lemmermannii, Fragilaria pinnata)* typical of the arctic brackish waters (Polyakova 1997) predominate in this association (~ 80%). Freshwater diatoms are rare. They are represented by species dwelling in bottom sediments and on overgrowths in the Arctic inland basins (*Navicula bacillum, Pinnularia leptostauron, P.microstauron, P.viridis)*. The composition of diatom associations allows assuming that sedimentation went on either in the inner sublittoral or littoral zone under changing marine and subaerial conditions.

The overlying peat-grass layer (**sample B-4**) is distinguished by the highest species diversity and abundance of diatoms. Like in the underlying layer, the diatom association includes different species in terms of salinity preferences with predominance of typical freshwater lacustrine-bog forms primarily of *Eunotia, Pinnularia* and *Cymbella* genera. Halophobic species are also present. *Pinnularia microstauron, P.divergentissima, P.viridis, P.subcapitata, P.borealis, P.stomatophora, Eunotia fallax, E.praerupta, E.pectinalis, Cymbella hilliardii, Encyonema minutum, Neidium bisulcatum* dominate the association. However, species diversity of halophiles and brackishwater species is also high. These include *Nitzschia hybrida, Diploneis interrupta, D.bombus, D.litoralis, Amphora ovalis, Navicula cryptocephala, Cavinula pseudoscutiformis*. Their presence gives evidence for possible infiltration of seawaters or periodic flooding of the swamped coastal lowland during high tides or wind surges.

The abundance and diversity of diatoms sharply decrease in the overlying, mainly fine-grained, sands (**sample B-3**). The diatom association is represented by freshwater species typical of the bottom grounds of the northern shallow water basins *(Pinnularia viridis, P.molaris, P.streptoraphe, Neidium bisulcatum, Navicula importuna, N.semen)*. Rare freshwater planktic and rheophile species (*Stephanodiscus hantzschii, Luticola mutica)* are present, as well as fragments of marine Paleogene diatoms. The composition of diatom associations suggests the sediments were accumulated under relatively active hydrodynamic environment, probably, in temporary streams.

Upward the section (**sample B-2**), the composition of diatom associations changes. Planktic and rheophile species disappear, but aerophile diatoms (*Hantzschia amphioxys, Navicula contenta)* become abundant. These are typical for edaphic (soil) coenoses of diatoms. Subsurface deposits (**sample B-1**) represented by fine-grained well-sorted sands with grass roots contain diatom association entirely dominated by subaerial bog-soil species, mainly of *Eunotia* and *Pinnularia* genera *(P.brevicostata, P.microstauron, Eunotia parallela, E.lunaris, Hantzschia amphioxys* and others).

Thus, the composition of diatom associations indicates changes in sedimentation environment during accumulation of the barrier beach – from nearshore marine, littoral, probably marsches, to swampy laida and, finally, subaerial avandune. Temporary streams played an important role in the formation of the lower part of subaerial unit lying above 2.0 m asl. These streams redistributed abundant eolian material and supplied plant debris into shallow lakes and puddles during flood. The plant debris was accumulated in the form of thin interlayers. At present, similar conditions exist in the inner part of the dune belt between the avandune ridge and laida (Fig. 1). The uppermost part of the subaerial unit was accumulated due to active eolian-soil sedimentation typical for the topmost part of the dune belt on the barrier beach.

Conclusions

As a result of the complex investigations we came to the following conclusions. Barriers of the Pechora Sea were formed in the coastal zone by accumulation of coarse debris derived from the submarine coastal slope. In the course of coastal evolution, the barriers were moving onshore overlapping coastal laidas formed behind them. Eolian processes played an important role in shaping the shores. Eolian transportation of sand from beaches resulted in the accumulation of big dune ridges. The latter rework and overlap barriers. That is why the absolute height of the barriers in the Pechora Sea could not serve as an indicator of the sea-level position in the Holocene. Diatom associations evidence upward changes in sedimentation environments during the formation of coastal accumulative forms in the Pechora Sea, from nearshore marine, littoral, probably marsches, to swampy laida and, finally, subaerial avandune. According to radiocarbon datings, the modern avandune in the studied region began to form not earlier than 350-400 years ago.

This work was supported by INTAS grant no. 1489 and RFBR grant no. 02-05-65105.

References

Avenarius, I.G., 2001. Coastlines of the second half of the Holocene as a model for the coastal zone evolution under the global sea-level rise. In: Chelovechestvo i beregovaya zona Mirovogo okeana v XXI veke (The mankind and the coastal zone in the XXIst century). Moscow, GEOS, P. 266-274. (in Russian).

Avenarius, I.G., Repkina, T.Yu., 2001. Paleogeography of the Varandei area in the Late Valdai – Holocene (Barents Sea). In: Geologiya morei i okeanov (Geology of seas and oceans). Abstracts of the XIV International School in Marine Geology, Vol. 2, Moscow, P. 4-5. (in Russian).

Avenarius, I.G., Ermolov, A.A., Myslivets, V.I., Repkina, T.Yu., 2001. Relief and some aspects of the Late Valdai – Holocene paleogeography of the Varandei Island. In: Sedimentologicheskie protsessy i evolyutsiya morskikh ekosistem v usloviyakh morskogo periglyatsiala (Sedimentation processes and evolution of marine ecosystems under marine periglacial conditions). Vol. 1, Apatity, KNTs RAN, P. 135-147. (in Russian).

Badyukova, E.N., Kaplin, P.A., 1999. Coastal barriers. Geomorfologiya, 3, P. 3-13. (in Russian).

Ogorodov, S.A., 2001a. Morphology and dynamics of the Pechora Sea coasts. Proceedings of the Institute of Oceanology BAN, Varna, Vol. 3, P. 77-86. (in Russian).

Ogorodov, S.A., 2001b. About formation and evolution of coastal barriers in the Pechora Sea. In: Geologiya morei i okeanov (Geology of seas and oceans). Abstracts of the XIV International School in Marine Geology, Vol. 2, Moscow, P. 202-203. (in Russian).

Polyakova, Ye.I., 1997. Arkticheskie morya Evrazii v pozdnem kainozoe (Arctic Eurasian seas in the Late Cenozoic). Moscow, Nauchnyi Mir, 145 pp. (in Russian).

Popov, B.A., Sovershaev, V.A., Novikov, V.N., Biryukov, V.Yu., Kamalov, A.M., Fedorova, E.V., 1988. Coastal area of the Pechora-Kara Sea region. In: Issledovanie ustoichivosti geosystem Severa (Investigations of the geosystems stability in the North), Moscow, Izd. MGU, P. 176-201. (in Russian).

Zenkovich, V.P., 1957. About the origin of barrier beaches and lagoon coasts. Proceedings of the Institute of Oceanology AN SSSR, Vol. 21, P. 5-32. (in Russian).

COASTAL DYNAMICS DURING THE EROSION OF THE ICE COMPLEX AND TABER PERMAFROST DEPOSITS: A MODEL BASED ON THE FRAGMENTARY STATIONARY MATRIXES OF THE TRANSIENT PROBABILITIES

V. Ostroumov

Institute of Physicochemical and Biological Problems of Soil Science, Russian Academy of Sciences, Pushchino, Moscow region, 142290, Russia, Mail to: vostr@issp.psn.ru

The Markovian is one of the interesting properties of the time series of the **r**etreat **r**ate of the **c**oast **l**ine (RRCL) in the Arctic. The Markov chain based stochastical model can be used to simulate the dynamics of the shore line of the Arctic seas during thermal abrasion.

F. Are (1991) analyzed data on the RRCL monitored over a long term period. No considerable changes of the RRCL were found. It was shown that the averaged RRCL is practically constant within lithologically homogeneous sites during long term periods. This point is a base for using the Markov chain based stochastic model with a stationary matrix of transition probability to simulate the time series of the RRCL for homogeneous segments of the shore.

Within the ACD program coastal retreat rates are constantly monitored at the key site Malyi Chukochii Cape, East Siberian Sea. Currently, the coastal section consisting of ice rich permafrost deposit of Yedoma type (ice complex) is undergoing erosion. The observed retreat rate of the coastline was 14 m from 1984 to 1988, 11 m from 1988 to 1990, 3m from 1990 to 1991, 15m from 1991 to 1994, and 22 m from 1994 to 1999 (monitoring is carried out by S. Gubin, D. Fyedorov-Davydov, V. Sorokovikov, and V. Ostroumov). The average RRCL for the 15 years time series is 4.3 m/year.

The continuous year-by-year initial time series of the RRCL was calculated using the Markov chain based model with a stationary matrix of transient probabilities. Such model was used to calculate the simulated time series. In the case of homogeneous permafrost sediments along the profile, the modeling consists of the following steps: testing the initial time series for Marcovian; discretization of the initial time series; calculation of the transient probabilities; calculation of the transient probability matrix in cumulated form; calculation of the simulated Markov chain; calculation of the continuous RRCL time series.

a)

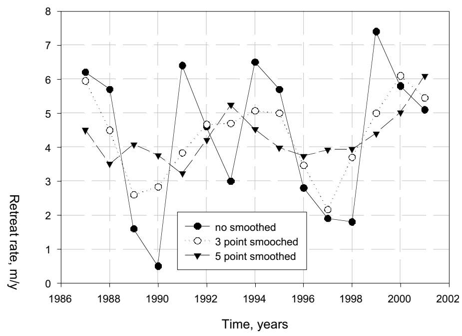

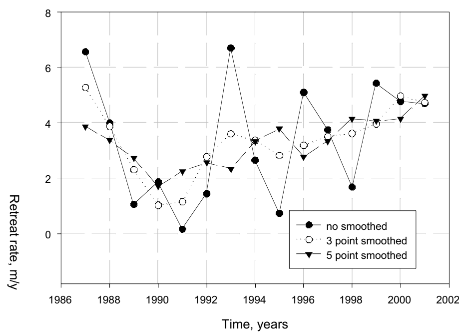

Figure 1. Initial (a) and simulated (b) time series of RRCL for a homogeneous site with Yedoma type ice complex deposits.

The simulated data can be compared with the initial time series (Fig. 1). The comparison shows that the simulated time series reflects the shape of the dynamic curves for the initial data set.

Along the mentioned profile, the following sequence can be observed: currently (1999) eroded suite of Yedoma deposit, 96 m width; taber deposit of ancient alas, 403 m width; another Yedoma type ice complex, 225 m width; once again taber deposits. Under the current average RRCL of 4.3 m/y, the 96 m suite of the currently eroding ice complex will be completely destroyed within 22 years. Then, the RRCL will decrease to 1.8 m/y. To describe such changes of the average RRCL at the lithological boundaries, a model with fragmentary stationary matrixes of transient probabilities is recommended. The algorithm for such a model has an additional step for changes of the stationary matrixes at the time of changes of the average RRCL.

a)

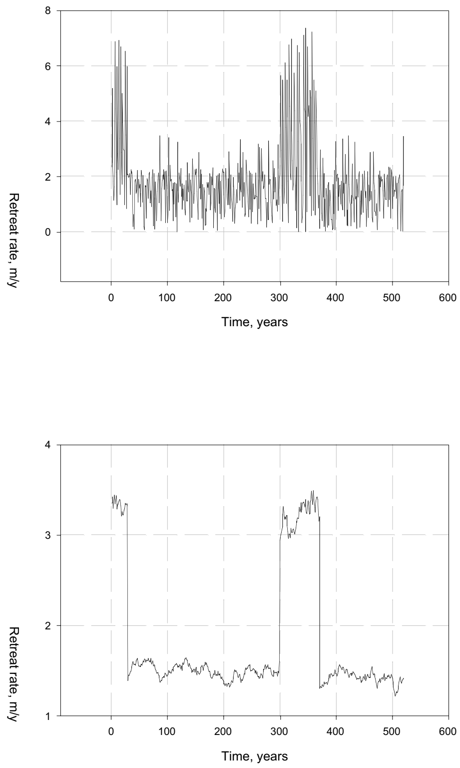

Figure 2. Time series of the RRCL simulated using the fragmentary stationary matrix of transient probabilities (a - not smoothed, b - 41-point smoothed data).

Fig.2 shows the results of simulations using the model based upon the fragmentary stationary matrix of transient probabilities. The contrast changes of the magnitude of the RRCL coincide with the geological boundaries (not smoothed curve, Fig. 2b). Some contrast change of the average RRCL is present in the smoothed curve as well.

The testing of the model and the obtained results confirms that the Markov chain based model can be a helpful instrument for simulations of the RRCL time series. Statistical models can be used in a complex with the deterministic empirical and analytical ones for simulations of the dynamics of Arctic coasts.

This work has been supported by INTAS (project 01-2329)

References

Are, F.E. 1998. The thermoabrasion of Laptev Sea shores and its input into sediment budget of the sea (in Russian). - *Earth Cryosphere* 1(II): 55-61.

MORPHOGENETIC CLASSIFICATION OF THE ARCTIC COASTAL SEABED

Yu. Pavlidis[1], S. Nikiforov[1] and V. Rachold[2]

[1] P.P. Shirshov Institute of Oceanology, Moscow, Russia, [2] Alfred Wegener Institute for Polar and Marine Research, Potsdam, Germany

Abstract

The Evolution of the arctic coastal zone is a result of the interaction of exogenic and endogenic processes. Previous classifications could not sufficiently characterize the variety of forms and regional features of the arctic seabed because the multitude of interactive processes have not been considered simultaneously. Based upon an a detailed analyses of morphology, origin, age, paleogeography, modern processes, geology and neotectonics, this paper presents a morphogenetic classification which divides the arctic relief into three large groups: structural, structural-sculptural and sculptural and their subtypes.

Introduction

A precise and standardized classification of the variety of relief forms of the Arctic shelf is essential for both scientific and applied purposes. The evolution of the arctic coastal zone, which is controlled by the interactions of modern wave and ice factors and the influence of numerous glaciations and large-scale sea level fluctuations, significantly differs from other coastal areas of the World Ocean. Glaciations have left coastal traces in the western part of the Russian Arctic whereas its eastern part was almost completely drained during glacial periods and the subaerial paleorelief is especially characterized by cryogenic forms: thermokarst, thermoabrasion, thermodenudation and cryodislocation.

Earlier classifications of the coastal seabed relief suggested by Ionin et al. (1990) for the World Ocean or by Shepard (1977) according to the peculiarity of geological structures or sedimentation processes could not characterize the variety of forms and regional features in the arctic zone. The classification presented in this paper is based upon scientifically evidenced information on morphology, origin and age as well as geological and neotectonic characteristics of the seabed relief. This kind of simultaneous analyses of a complex of interactive factors can be called “morphogenetic” approach.

The investigations are based on the results of long-term researches with the application of modern equipment including narrow-beam and multi-beam echo sounders, Parasound, side-looking radars, bathymetric maps and the analyses of numerous sediment samples. According to the Science and Implementation Plan of the Arctic Coastal Dynamics (ACD) project (IASC 2001) the classification will be designed for the integration into a circum-Arctic coastal Geo Information System (GIS).

Results and discussion

The seabed evolution is determined by both modern and paleogeographical processes such as vertical tectonic and glacio-isostatic movements. Among the exogenic and endogenic coastal processes it is possible to allocate active processes, which directly contribute to the formation of the shelf relief, and passive processes, which predetermine the display of the active processes and direct the course of their development. Active processes can be modern (hydrogenic, gravitational etc.), paleogeographical (glacial, erosional etc.), and in some cases anthropogenic processes. Structural forms, with few exceptions, are related to passive morphogenetic factors. By such an approach it is possible to allocate three major categories of the seabed relief: structural, structural-sculptural and sculptural. This kind of subdivision is relative in many respects because the majority of relief forms is caused by both endogenic and exogenic factors and processes. It is necessary to determine the prevailing value of various factors of concrete seabed forms. A certain subjectivity in allocating structural and sculptural forms of a relief and in their morphogenetic division into active and passive factors cannot be avoided. The necessity to characterize the relief "layer by layer" arises inevitably when specialized geomorphological maps have to be produced and a database to be used in a GIS environment within in international network are has to be designed. As an example the following layers could be used: first layer - endogenic background; second layer - relief forms connected with the action of paleogeographic factors; third layer - modern relief forms caused by the action of endogenic processes.

Typical structural forms are large seabed forms predetermined by geological structures and created by endogenic processes, i.e. folded and/or fault-fracture tectonics, volcanism, vertical movements of the Earth's crust etc. Geological structures underlie all forms of the shelf relief and determine the position of large relief forms, such as synclinal underwater depressions, anticlinal and brachyanticlinal underwater raisings, monoclinal plains, flexure ledges etc. This large group can be further divided into two genetic types and some subtypes. (1) The *tectogenic type* includes plicated forms (anticlinal, brachyanticlinal, synclinal, brachysynclinal, monoclinal, uniclinal), disjunctive (fault and grabens, horsts, fracture-blocks) and non broken structural dislocations (subhorizontal and inclined plains). (2) The *volcanogenic type* includes magmatic and mud volcanic subtypes. Usually relief forms created by volcanic processes like lava domes and mud volcanic cones (Norwegian Sea) are located in water depths of more than 200 m.

In our morphogenetic classification structural-sculptural forms are referred to a category of transitive, often relict formations. These forms can be divided into the following subtypes: (1) *erosion-tectonic* (structural-erosive with fluvial or glacial relief, structural-erosive-gravity created by turbidity currents), (2) *glacial-tectonic* (structural depressions in internal basins of fjords and covered by glacial-marine deposits, structural swells with accumulative superstructure, structural forms with a surface of glacial ablation corresponding to fjords and adjacent underwater trough valleys, structural forms with glacial ablation and accumulative marginal troughs and anticlinal swells blocked by moraines).

Exogenic subaerial and subaquatic processes are the most active ones. The sculptural relief of the seabed is created by destructive and accumulative processes such as ablative and accumulative activity of Late Quaternary glaciers on the shelves of the marginal and internal seas of polar and subpolar climatic zones. Glacial forms are most typical among the relict exogenic sculptural relief forms within the limits of the glacial shelf in the Arctic. The sculptural relief forms can be divided into seven types and several subtypes: (1) *glaciogenic* (glacial-ablative, glacial-accumulative and glacial-dynamic), (2) *cryogenic* (thermokarst relict forms such as extended underwater depressions and hollows documented by echosounding and acoustic profiling in the Laptev, East Siberian and Pechora Seas; the origin of these negative relief forms is connected with the thermal destruction of ice lenses and wedges during the late glacial transgression, the size ranges from 2 to 10 m depth, 10-100 m width and extension of 3-4 km depending on the thickness of the lenses of repeatedly-cavern-load ice; in the Chukchi Sea the relict thermokarst relief forms are large depressions which are covered by a 7-10 m thick Holocene sediment layer; cryodislocative relief forms represented by folds and frost mounds have a local distribution in the Arctic, for example Western Yamal Peninsula), (3) *hydrodynamic* (wave abrasion forming modern cliffs and benches and paleo underwater terraces, wave accumulation with ancient underwater accumulative forms and coastal barrier islands, spits, beaches, etc., abrasive-accumulative processes forming modern underwater coastal slopes, mainly subglacial accumulative and tidal forms such as sandy waves and ridges, tidal troughs, step tidal benches, etc.), (4) *torrentogenic* (accumulative and erosive as for example in the Bering Strait where due to strong quasistationary currents a subhorizontal plain lacking modern deposits is formed in the central zone while as a result of deposition underwater cones are generated in the adjoining southern Chuchi Sea), (5) *fluvial* (fluvio-glacial and potamogenic forms with ice-marginal valleys and channels of paleo-rivers, ancient and modern deltas, river mouth bars, etc.), (6) *gravitational* (rockfall-landslides, turbidity currents) and (7) modern *anthropogenic* (constructive forms connected with ground spoil, artificial islands, basements of port constructions, oil derricks etc., destructive forms with artificial cuts, port channels, waterways in gulfs and other near port constructions within shallow water).

Conclusions

The Arctic shelf can be described as a zone developed under long-term endogenic and exogenic interactions. The initial structure was created by the basement surface which was and is constantly reworked by a complex of paleogeographical and modern processes within various glacial and interglacial periods and sea level fluctuations. The classification suggested in the present article is based on scientifically evidenced data on morphology, origin and age and on the geological and neotectonic features of the seabed relief and considers the multitude of natural factors and their interactions and evolution in time. Three types of major relief forming processes were distinguished and further subdived: structural, structural-sculptural (transitive) and sculptural (formed by modern and paleogeographical exogenic processes).

This study is supported by INTAS (project number 2001-2332).

References

IASC Arctic Coastal Dynamics (ACD) 2001. Science and Implementation Plan, *International Arctic Science Committee*, Oslo, April 2001.

Ionin, A., Pavlidis Yu. and Yurkevich, M. 1990. Relief of arctic eastern shelf of Russia and its classification. In A. Aksenov (eds), *Geology and geomorphology of shelf and continental slope*: 24-50. Moscow: Nauka.

Shepard, F.P. 1977. Geological oceanography. N.Y.

COASTAL DYNAMICS AT THE WESTERN PART OF KOLGUEV ISLAND, BARENTS SEA

D.D. Perednya[1], M.O. Leibman[2], A.I. Kizyakov[2], B.G. Vanshtein[3] and G.A. Cherkashov[3]

[1]Moscow State University, Faculty of Geography, [2]Earth Cryosphere Institute SB RAS, [3]VNIIOceangeology

The coasts built of frozen deposits enclosing massive ground ice, are most dynamically developing in connection with tendencies of warming. In the European Arctic massive ground ice is found on Kolguev island. The western and northern coasts are actively affected by wave erosion and thermodenudation (complex of destructive processes on slopes).

The field study was undertaken 5 km south of the Sauchikha-river mouth at 69°12° N and 48°18°. Velikotsky (1998) has shown that thermodenudation plays a major role in coastal retreat in this region, and presented rough estimates of the retreat rate at the coasts complicated by thermocirques, as well as at the smooth-faced coasts, averaging at 1-2 m/yr and 0.1-0.2 m/yr, respectively.

Our field studies included: (1) measurements of retreat rates for various genetic types of the coasts; (2) establishing the dependence of coastal dynamics on geological structure and ice content of the coastal bluffs.

The studied coast has two genetically diverse levels (Velikotsky 1998): the lower level (wave-eroded bluffs with niches) and the upper level (gravitation or thermodenudation slopes). The lower level rises from the beach and is up to 10-15 m high. The upper level is above the lower one and is 20 to 40 m high. The break of the slope is related to a competent sandy layer in the middle of the geological profile, overlain and underlain by clayey deposits. A combination of smooth-faced wave-eroded bluffs and slopes or concave thermodenudation and nivation hollows are characteristic for the study area.

Erosion (bluffs) and combined accretion-erosion (river and creek mouths) coasts are found in the area. Three types of coasts are subdivided within the erosion group based on descriptions and airborne data: 1 high terraces with thermocirques and thawing massive ground ice, 2 high terraces with smooth-faced bluffs and gravitational slopes, and 3 low terraces (thermokarst depressions) with smooth-faced bluffs and gravitational slopes.

The river mouths of accretion-erosion coasts have no well defined estuaries and are separated from the sea by high beach-ridges (about 3 m).

The high terraces with thermocirques initially formed due to massive ice thaw, are now developing mainly due to thermoerosion of the thermocirque bottom and nivation of its scarp. Bluffs at the lower level are actively wave-eroded.

The high terraces with smooth-faced bluffs are built of relatively ice-poor sand and clay interbeddings. Wave-erosion activity forms niches and grottoes at the lower level, causing the failure of hung blocks.

The low terraces (thermokarst depressions) are characterized by a polygonal pattern which is possibly related to polygonal ice wedges at the surface. The terrace edges are dissected by narrow deep gullies, inheriting the polygonal pattern, and are complicated by nivation niches.

A narrow beach, wave-erosion niches, and steep to overhanging bluffs are typical for all forms of erosion coasts at western Kolguev island. Niches are open or protected by a debris cone at the sites with relatively ice-poor deposits. At the sites with thermocirques and, probably, at all sites with low cliff where the debris cone is not formed because of low debris yield, niches are filled by perennial snow patches which also fill the coastal gullies, providing the formation of the nivation hollows directly beneath the terrace edge.

Two of three thermocirques ("southern" and "central") described and mapped during the field study of 2002 are found on the aerial images of 1948 and 1969, while the third ("northern") one did not appear even on the map by Velikotsky (1998) based on survey of 1987.

During the last years thermodenudation is rather inactive and nivation, solifluction at the thermocirque scarps, and lateral thermoerosion in the bottoms of the thermocirques are developing.

Transects to measure scarp retreat at the most active and young "northern" thermocirque, formed after 1968 (according to aerial photography), were established (Fig.1). This scarp developed 150 m landward in less than 30 years, thus the retreat rate is not less than 5 m/yr. The stakes were set in staggered rows, allowing to map the terrace edge dynamics at an annual basis and to calculate the volume of erosion per meter of the coastline.

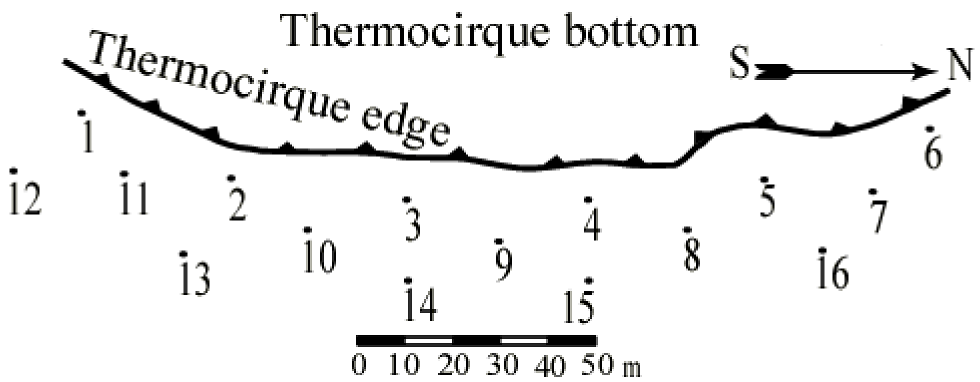

Figure 1. Monitoring network established at the edge of the "Northern" thermocirque.

As the smooth-faced bluffs represent the main portion of Kolguev coast, it is important to estimate their long-term dynamics. Our estimates are based on the comparison of aerial images of 1948 and 1968. In 20 years the backshore retreat approximates 60 m, while the terrace edge retreated 85 m (Fig. 2). Thus, the rate of retreat for this period averages 3 and 4 m/yr respectively.

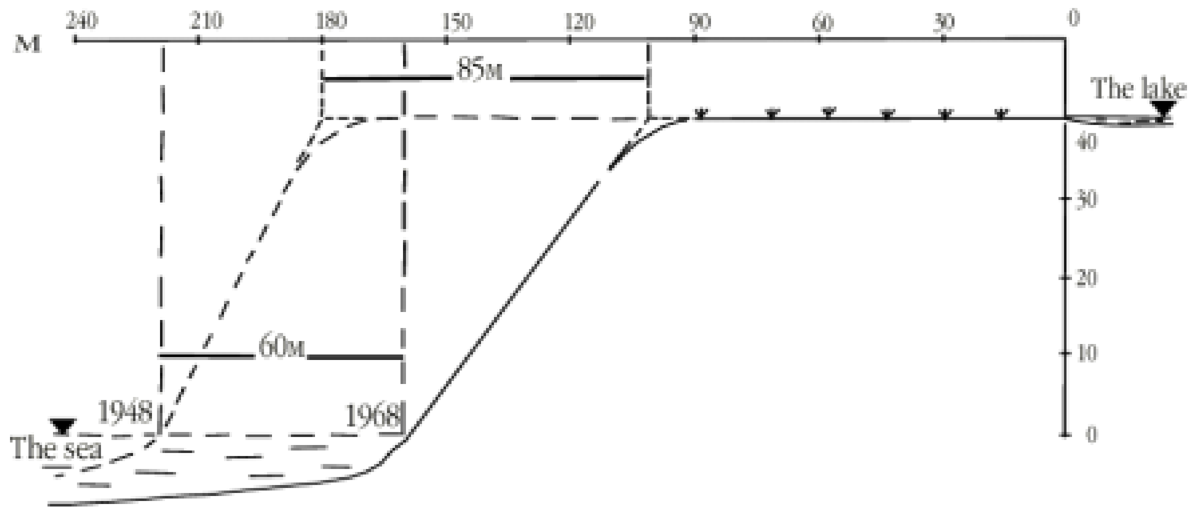

Figure 2. The scheme of coastal retreat at the low terrace (thermokarst depression).

Today the majority of the coastal bluffs are relatively stable. Actively retreating are the low terraces due to lateral thermoerosion and nivation, and the young “Northern” thermocirque due to slope processes and lateral thermoerosion. Thawing of perennial snow patches and new activation of coastal retreat processes is possible if air temperature increases or/and the circulation changes resulting in the melting of snow patches or the decrease of snow accumulation on the slopes of the western aspect in this region. The cyclicity in coastal retreat is controlled by the amount of ice thawing in combination with climate fluctuations.

The study is supported by INTAS, grant 01-2329.

Reference

Velikotsky, M.A. 1998. Modern shore dynamics of Kolguev island. In V.I.Solomatin, V.A.Sovershaev and I.I.Mazur (eds) Dynamics of the Arctic coasts of Russia: 93-101. Moscow: Faculty of Geography MSU.

MONITORING WEATHERING AND EROSION OF BEDROCK ON A COASTAL CLIFF, LONGYEARBYEN, SVALBARD

A. Prick

EU - Marie Curie Research Fellow, The University Courses on Svalbard (U.N.I.S.), Norway
angeliquep@unis.no

A rockwall constituted of sandstone and shale has been monitored on an all year-around basis since the summer 2001 in order to better understand the relationship between rock temperature, rock moisture content, weathering evolution and rock fall occurrence in a high latitude environment (Longyearbyen, 78°13'N). This rockwall is located along the Adventfjorden coastline; its base was sea-washed until the road leading to Longyearbyen Airport was built in 1984.

The rockwall temperature is monitored at depths of 40 cm, 10 cm, 1 cm and at the rock surface. The rockwall is experiencing numerous and sometimes considerable temperature fluctuations, even during the polar winter, and even under a thick snow layer. Nevertheless, surface temperature crosses the zero degree threshold only in the fall and in the spring; it gets very close to zero degree several times during the polar winter, due to milder weather conditions. The amplitude of temperature variations decreases from the surface downwards due to thermal flow dampening. Even daily temperature fluctuations reach 40 cm deep, but very attenuated, and with a delay of several hours. At 40 cm deep, the rock freezes once in the fall and remains frozen. No evidence of a widespread occurrence of thermal shocks is found; this denies their efficiency as active weathering agents at the study site.

Rock moisture content is monitored by daily weighing exposed rock tablets. All samples show simultaneous fluctuations of more or less same amplitude. Rock moisture content shows large and quick variations linked to weather conditions during the fall and spring. Winter is characterized by a progressive drying of the rock, probably because of sublimation in cold arid climate. Rocks rarely reach high saturation values, and when it is the case, this happens in the fall and in the spring.

Therefore, conditions favorable to cryogenic weathering (i.e. freezing of the rock when its moisture content is high) are met only rarely. But when these conditions are met, frost action can be very aggressive, because of the high rock moisture content, the quick cooling or the extended duration of freezing periods.

A regular evaluation of rock weathering (before cracking, weight loss or any other visible change) is assessed for rock pieces exposed to the natural environment using as a criteria their dynamic Young's modulus variations. These measurements are aimed at evaluating how long an exposure to the Svalbard environment has to be for the weathering process to be initiated and how fast this decay will progress. A non-destructive determination of Young's modulus is carried out using a Grindosonic apparatus.

The aggressivity of the environment on the weathering point of view is proven by the decrease in Young's modulus of 4 out of 5 porous limestones tablets after 5 months of exposure (Sept. 2001- January 2002) at the study site. A similar exposure did not cause any decrease in the Young's modulus of 5 samples of the local sandstone. Frost action does not act through the porous media of this poorly porous sandstone, but by wedging of its wide opened and well-developed crack system. Cryogenic weathering is thought to act on this rockwall by wedging; the dilation of rockwall cracks is automatically monitored every hour by crack extensometers.

Chemical processes are more and more considered as likely to play a role in cold environment weathering. There is locally some evidence of such weathering on the studied rockwall. This chemical weathering appears under two distinct forms, both occurring locally and with a variable intensity on the rock surface. First, iron oxidation can color the rock surface in a reddish, dark-brown color and disintegrate the iron carbonate nodules in fine materials, leaving small circular depressions on the clay-ironstone lenses. Secondly, salt outbursts can develop during dry summer periods and cover some rock beds. The salt source is the sedimentary rock itself, and not the seawater nearby. Although it is not clear whether these salts precipitation have rather a physical or a chemical weathering effect, as salt weathering can act both ways, it leads clearly to a local rock surface induration and / or desquamation. The described processes contribute to the so-called "granular weathering", i.e. they lead to the formation of very fine debris constituting the fine fraction of the talus slope.

Rock fall activity is evaluated using sediment traps and checking the decay evolution of painted squares on the rockwall. Five sediment traps are set at the base of the rockwall and collect the falling rock debris. These traps are 1.25 to 3.50 meters long and collected debris coming from rockwall portion estimated to be between 31 and 88 m^2 in surface. They are emptied about 4 times a week and the collected debris are sieved at 2 mm, dried and weight. Rock fall occurrence shows a very irregular distribution, with maximums in autumn and spring. The largest rock fall events happened on days when cryogenic weathering conditions were met.

MODERN COASTAL ORGANIC CARBON INPUT TO THE ARCTIC OCEAN

V. Rachold[1], M.N. Grigoriev[2], H.-W. Hubberten[1] and L. Schirrmeister[1]

[1] Alfred Wegener Institute for Polar and Marine Research, Research Unit Potsdam, Germany,[2] Permafrost Institute, Siberian Branch of the Russian Academy of Sciences, Yakutsk, Russia

In recent years several studies have underlined the importance of coastal erosion for the sediment budget of the Arctic Seas and shown that the contribution of coastal erosion to the material budget has often been underestimated.

In this paper we present a quantitative assessment of the organic carbon input to the Arctic Seas through coastal erosion. The evaluation is based upon a combination of data for coastal erosion sediment input and organic carbon concentrations of the coastal sections. Emphasis is laid on the Laptev Sea and East Siberian Seas, where our own field studies have been performed from 1998 to 2002. Based upon published information, the quantification can be extended to cover all Arctic Seas. It must be cautioned that these are the best available estimates of the contribution of coastal erosion to sediment and organic carbon input and may contain considerable error.

Our results are that in total ca. $430x10^6$ t yr^{-1} of sediment and $6.7x10^6$ t yr^{-1} of organic carbon enter the Arctic Ocean through coastal erosion (Table 1). Approximately 60% of the total TOC flux originates in the Laptev and East Siberian Seas. The predominant sources are Ice Complex deposits, which are widespread in Northeast Siberia. The highest coastal TOC flux is observed in the East Siberian Sea, even though the Laptev Sea coastline is considerably longer. This is due to the dominance of the Ice Complex along the coastline of the East Siberian Sea. Satellite images of the East Siberian and the Beaufort Sea clearly show the major sources of sediment: the strong river plume of the Mackenzie River is visible in the Beaufort Sea, whereas in the East Siberian Sea high turbidities, which are related to coastal sediment input, are observed along the coastline.

	Sediment flux	TOC flux
	(10^6 t yr^{-1})	(10^6 t yr^{-1})
White Sea[1]	60	0.3
Barents Sea[1]	59	0.5
Kara Sea[1]	109	1
Laptev Sea[2]	58.4	1.8
East Siberian Sea[2]	66.5	2.2
Chukchi Sea[3]	70	0.8
Beaufort Sea[4]	7.9	0.09
Total	430.8	6.69

Table 1. Sediment and TOC flux to the Arctic Ocean through coastal erosion (from: Rachold, V., Eicken, H., Gordeev, V.V., Grigoriev, M.N., Hubberten, H.-W., Lisitzin, A.P., Shevchenko, V.P., Schirrmeister, L. (in press). Modern terrigenous organic carbon input to the Arctic Ocean, In: Stein, R. and Macdonald, R.W. (Eds.) Organic Carbon Cycle in the Arctic Ocean: Present and Past. Springer Verlag, Berlin).

FROM THE "ARCTIC CLIMATE SYSTEM STUDY" TO A NEW GLOBAL PROJECT "CLIMATE AND CRYOSPHERE" OF THE WORLD CLIMATE RESEARCH PROGRAMME (WCRP)

V. Ryabinin

Joint Planning Staff for the World Climate Research Programme, WMO, 7 bis, Avenue de la Paix, Geneve, CH-1211, Switzerland, ryabinin_v@gateway.wmo.ch

During the last decade the polar climate studies of the WCRP have been regional. The Arctic Climate System Study (ACSYS) had three main objectives:

- To improve understanding of the interactions between the Arctic Ocean circulation, ice cover, the Arctic atmosphere and the hydrological cycle;
- To initiate long-term climate research and monitoring programs in the Arctic so as to determine key Arctic processes and Arctic climate variability and trends;
- To provide a scientific basis for a more accurate representation of Arctic processes in global climate models.

The decade of ACSYS is ending in 2003, and the WCRP is planning a major international conference to summarize the project achievements. More information on the project is available at the ACSYS home page address: http://acsys.npolar.no.

The Joint Scientific Committee for WCRP endorsed CliC as a new project in 2000. The project aims are to:

- Assess and quantify the impacts of climatic variability and change on components of the cryosphere and their consequences for the climate system, and determine the stability of the global cryosphere;
- Improve understanding of the physical processes and feedbacks through which the cryosphere interacts within the climate system;
- Improve the representation of cryospheric processes in models to reduce uncertainties in simulations of climate and predictions of climate change;
- Enhance the observation and monitoring of the cryosphere in support of process studies, model evaluation, and change detection.

The CliC home page address is located at: http://clic.npolar.no. CliC is a global project. Its science plan of CliC refers to the following main questions:

(1) How stable is the global cryosphere?

- How well do we understand and model the key processes involved in each cryospheric component of the climate system?
- How do we best determine the rates of change in the cryospheric components?

(2) What is the contribution of glaciers, ice caps and ice sheets to changes in global sea level on decadal-to-century time scales?

- How can we reduce the current uncertainties in these estimates?

(3) What changes in frozen ground regimes can be anticipated on decadal-to-century time scales that would have major socio-economic consequences, either directly or through feedback on the climate system?

(4) What will be the annual magnitudes, rates of change, and patterns of seasonal redistribution in water supplies from snow- and ice-fed rivers under climate changes?

(5) What will be the nature of changes in sea-ice mass balance in both polar regions in response to climate change?

(6) What is the likelihood of abrupt climate changes resulting from regime changes in ice shelf - ocean and sea ice - ocean interactions that impact the ocean thermohaline circulation?

(7) How do we monitor cryospheric components as indicators of change in the climate system?

Several of these questions are of importance for ACD.

ACSYS has developed an ACSYS Data and Information Service (ADIS). The aim of ADIS is to provide a meta-data directory to help other researchers locate historical or newly available Arctic data sets, which are stored at different institutions and data centres. Arctic data sets in the disciplines of meteorology, oceanography, sea-ice and hydrology may be of interest for the ACD. Main data providers associated with ACSYS and CliC are listed below:

- Global Run-off Data Centre,
- Global Precipitation Climatology Centre,
- National Snow and Ice Data Center,
- Polar Science Center,
- Alfred Wegener Institute,
- Norwegian Polar Institute,
- Scott Polar Research Institute,
- UCAR Joint Office for Science Support (e.g. for SHEBA),
- NOAA National Oceanographic Data Center,
- Canadian Ice Service,
- Russian Research Institute for Hydrometeorological Information.

The development of data provision services will continue under CliC. The ACD participants are invited to benefit from using the ACSYS/CliC data and to voluntarily contribute data to ADIS and Data and Information Service of CliC (DISC).

EFFECTS OF COASTAL PROCESSES ON THE BIOGEOCHEMISTRY OF THE MARINE NEAR-SHORE ZONE: THE AMERASIAN ARCTIC

I.P. Semiletov

International Arctic Research Center and Pacific Oceanological Institute, Fairbanks, AK/Vladivostok, Russia, ***igorsm@iarc.uaf.edu***

Controversy surrounds the role of the river output and coastal erosion in land-shelf transport of terrestrial carbon in the Arctic. The East-Siberian and Laptev Seas (the most shallow and wide arctic shelf seas) are the most compelling to study the biogeochemical consequences of coastal processes in the changing Arctic. Between 1994 and 2000 the Laboratory of Geochemistry in the Polar Regions, Pacific Oceanological Institute (POI), performed eight near-shore expeditions in the eastern Siberian seas, three surveys along the Lena River stream, and the Trans-Arctic expedition-2000 along the Northern Sea Route (from Archangel'sk to Vladivostok, Fig. 1). A Set of the surface sediment and particulate matter samples has been studied in Fairbanks at the Institute of Marine Sciences and the International Arctic Research Center, University Alaska Fairbanks (UAF) and in Vladivostok at the POI. Hydro-chemical anomalies obtained over the shallow Siberian shelves demonstrate the significant role of coastal erosion and consecutive destruction of the land-derived organic matter in formation of the biogeochemical regime in the Arctic seas (Fig. 2 and Refs below). Transport of particulate organic carbon forced by the coastal erosion might be similar in value to the dissolved organic carbon transport by the rivers, whereas the total transport of terrestrial particulate eroded material is more significant than solid transports by rivers. The near-shore zone of the Siberian seas is mainly a source of atmospheric CO_2 emission, though the Arctic continental margin in whole may serve as a net CO_2 sink. Major results were presented at many international conferences and workshops.

References

Dudarev O.V., Semiletov I.P, Botsul A.I. et. al. (2001): The coastal erosion as significant source of the particulate matter into the Arctic Shelf. In.: Proc. 2nd Wadati Conf. on Global Change and Polar Climate, Tsukuba, Japan, 176-178

Semiletov I.P. (1999a): On aquatic sources and sinks of CO2 and CH4 in the Polar Regions, Journal of Atmospheric Sciences 56/2, 286-306.

Semiletov, I.P. (1999b): Destruction of the coastal permafrost ground as an important factor in biogeochemistry of the Arctic Shelf waters, Transactions [Doklady] of Russian Academy of Sciences, 368/6, 679-682.

Semiletov I.P. (2000): On biogeochemical consequences of coastal processes in the Eurasian Arctic Seas. In: Shelf-Basin Interactions Pan Arctic Meeting (agenda and abstracts), 7-9 November 2000, Callaway Gardens, Georgia, USA, 96-98.

Semiletov I.P.(ed.) (2001): Changes in the atmosphere-land-sea system in the Amerasian Arctic, Proc. Arctic Regional Center, vol.3, Vladivostok, Dalnauka Press, 273 pp.

Semiletov I.P. (2003): On Marine Environment Consequences of the Terrestrial Carbon Transport to the Siberian Arctic Shelf: the Laptev and East-Siberian Seas, resubmitted to GRL.

Semiletov I.P., McRoy, C.P, Pipko I.I.,.Savelieva N.I, Gukov A.Yu, and I.V. Semiletova (2003): On the Chemical Signature of the Lena River from Yakutsk to the Laptev Sea, submitted to JGR.

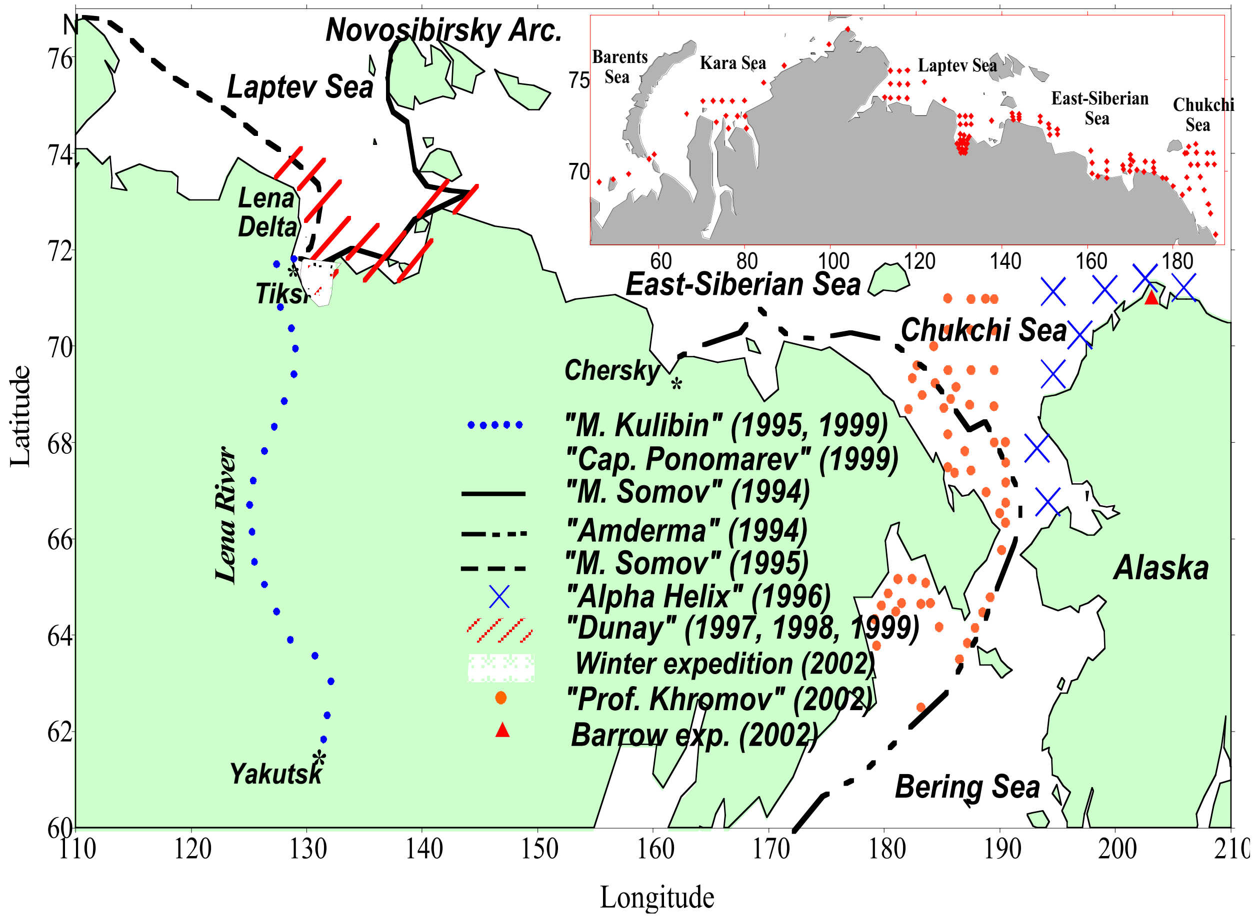

Figure1. The study area.

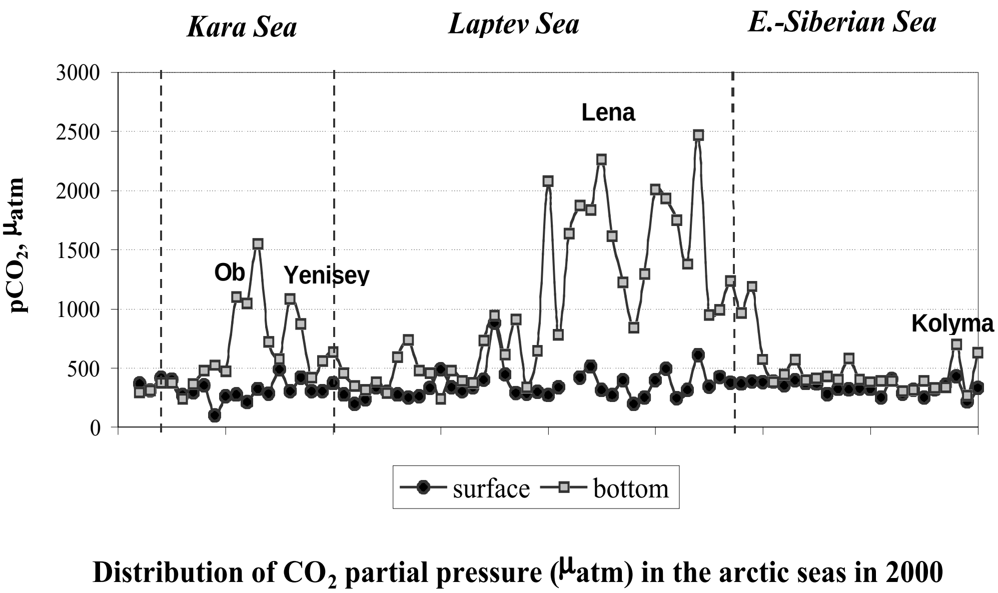

Figure 2. CO_2 partial pressure in the Arctic Seas (Semiletov 2001).

NEW INVENTORY OF ICE SHORES IN THE WESTERN RUSSIAN ARCTIC

A.I. Sharov[1] and A.F. Glazovskiy[2]

[1]Institute of Digital Image Processing, Joanneum Research, Graz, Austria, [2]Institute of Geography, Russian Academy of Sciences, Moscow, Russia

Hydrographic studies aimed at the detection of changes of ice shores in the western Russian Arctic and a preliminary analysis of their character, possible reasons and typical indicators were performed by interpreting spaceborne multitemporal (IN)SAR data obtained over the Russian Arctic in 1993 – 1998 and comparing them with available topographic maps. Studies revealed drastic changes in glacier extent that occurred in the Russian High Arctic in the second part of the XX-th century. Frontier parts of nearly all tidewater glaciers have retreated several hundreds to thousands of meters and shorelines have changed significantly. The maximum retreat of ice shores was recorded at Vera Glacier on North Novaya Zemlya that has receded 4,7 km between 1952 and 1998. Very interesting exceptions to the common glacial retreat in the Arctic were recognized in SAR interferograms: fronts of several large tidewater glaciers, e.g. Brounova, Eastern, Impetuous glaciers have advanced by several kilometres comparing to their positions in 1950-s. High planimetric accuracy of our hydrographic determinations was verified by comparing with the results of field surveys using a ship radar in September-October 2001. General lowering of the glacier surface has been revealed by measuring the height of ice walls. All change values (linear, areal and volumetric) are documented in the form of a new inventory of ice shores in the western Russian Arctic, which represents one of basic components of a regional coastal reference database RECORD.

Frontal velocities of nearly 100 glacier snouts were precisely measured from the ERS-1/2-SAR interferograms for the first time in the history of their explorations. The velocities of several glaciers were measured several times using different interferograms and the results were very consistent. The frontal velocities of 10 test glaciers were surveyed during the field campaign 2001 using precise geodetic equipment and compared with the INSAR velocities measured in the lab. In spite of harsh environment, the spatial correlation between the INSAR velocities and those surveyed in the field was quite high, though the INSAR velocities were somewhat lower than those from geodetic surveys. The revealed tachometric differences of up to 40% are explained. Corrected values of frontal glacier velocities were included in the inventory of ice shores. Several important conclusions on the amount, character and origin of current changes of ice shores in the Russian Arctic have been derived. A wide range of useful features as well as the attractive appearance and up-to-daintiness of our inventory makes it an ideal basis for scientific and administrative activities in the study region.

COASTAL FORMATION IN THE WESTERN SECTOR OF THE RUSSIAN ARCTIC REGION DURING THE PLEISTOCENE-HOLOCENE

N.A. Shpolyanskaya, Yu.B. Badu and I.D. Streletskaya

Geographic Faculty, Moscow State University, Vorob'evy gory, Moscow, 119992 Russia

The recent position of the Arctic shelf and the Arctic Ocean coastline is the result of their evolution in the Late Cenozoic under the action of two groups of natural processes. The first group includes global processes caused by tectonic and climatic factors, which resulted in considerable changes in sea level and in the appearance of wide glacier covers (Velishko 1998; Kaplin and Selivanov 1999). The second group combines permanent exogenous processes, complicated by permafrost mostly including large underground ice fields (Rozenbaum and Shpolyanskaya 1998, 2000; Trofimov 1986).

We have traced the dynamics of the coastal zone of the western sector of the Russian Arctic region (northern Europe and Western Siberia) during approximately the last 250 kyr.

At the end of the Pliocene-beginning of Pleistocene**,** climate became more severe and the sea transgression began along the entire Arctic coast of Eurasia. The vast cold-water sea basin gradually occupied the northern regions of the Russian Plain and Western Siberia, and glaciers covered the land. Both glaciation and sea transgression were maximal in the Middle Pleistocene (II_{2-4}) approximately 250 to 150 ka ago. The sea depth at the Barents and Kara shelves was not more than 100 m. The western part of the northern Russian Plain, including the Kola and Kanin peninsulas, mountain system of Novaya Zemlya and the Urals, and mountains of Central Siberia were covered by glaciers.

Air temperature decreased by 6-7^0 as compared to the present-day temperature. Nevertheless, the conditions were not favorable for development of permafrost, since the entire land was covered by either sea or glaciers. This created specific conditions for coastal processes. Coasts were formed under the action of glaciers (Fig. 1a).

The Late Pleistocene, Mikulino (Kazantsevo) Interglacial (III_1) - warm interglacial period replaced the period of glaciation. The sea transgression was considerably less intense. The sea occupied only northern lowlands (Fig. 1b). During the peak warming (125 ka ago), the air and ground temperatures exceeded the present-day temperature by 2.5-3.5^0_ and were positive over the major part of the land. The cryolithozone with a temperature of -2 to -6^0_ and a thickness of up to 400 m existed only in the Polar Urals and Pai-Khoi and at latitudes higher than 65^0 N in Western Siberia. The cryolithozone with thick tabular ice could form at depths of more than 40 m on the Kara shelf; and with tabular ice and fossil ice vein in the shallower shelf regions.

In this epoch, the coastal processes were more diverse than in the previous period. The coasts of Scandinavia and the Kola Peninsula were highly dissected (the fiord type) and showed the features of not only glacial erosion but also fracture tectonics. Offshore slopes of a fault origin were steep. Protrusions of land in place of the recent Kanin Peninsula, Timan Range, Pai Khoi, Polar Urals, and ancient Taimyr Island were similar to the Kola Peninsula coasts. The remaining land was the sea plain composed of very dense Middle Pleistocene glacial-marine silty clays (perennially frozen on Kara Sea islands). Abrasion and accumulation (thermal abrasion and accumulation on Kara Sea islands) proceeded here, and flattened coasts with high cliffs and deepened submerged slope were formed in this region. The zone of active coastal accumulation with bars, spits, etc. was formed in shallow straits.

Late Pleistocene, Valdai (Zyryan-Sartan) epoch (III_{2-4}) - prolonged cold stage replaced the epoch of warming. The regression of the Arctic Basin continued and terminated as a deep regression in the Late Valdai (Sartan) period (III_4). This epoch, which began 18-20 ka ago, is considered as the most cold period in the Pleistocene. The sea regression resulted in the Arctic ocean receding to a bottom contour of 110-140 m (Fig. 1c). The climate was pronouncedly continental, and the air temperature was lower than the present-day temperature by 7 - 10^0_; the epoch was characterized by a very dry climate. Ice caps generated again, although they were considerably smaller than in the Middle Pleistocene. Glaciers did not approach the coasts.

The low-temperature cryolithozone existed on land; its thickness was up to 700 - 800 m within plains and 1000 m and more in mountain regions. Within shelves, the cryolithozone also existed, especially at water depths of 0-2.5 m (below fast ice), with a temperature of -11 to -14^0_ and thickness of 30 to 400 m.

Under such conditions, the coastal processes could not be active. The high ice coverage of the sea (which restricted wave activity), very short warm period (when coasts were almost not clear of fast ice), and frozen coasts hardly promoted the development of abrasion and thermal abrasion. The material of eroded coasts settled not far from the coast because of rather stagnant water. During this period, the main type of the coasts was insignificantly thermoabrasional and accumulative. The processes of thermal erosion developed in the large valleys of ancient rivers, which were similar to narrow extended bays, and formed thermoerosional accumulative coasts.

The Holocene (IV) - the warm interglacial period, which began 10.5 ka ago and still continues. The post-glacial (Flandrian) sea transgression proceeded at that time and formed the present-day coastline configuration 6 ka ago. From that time, sea level fluctuated only insignificantly. The period of climatic optimum - the epoch of warming when the normal annual air temperature exceeded the present-day temperature by 2^0 - began precisely in that period. Frozen rocks thawed in this region. The cryolithozone remained only in the northeastern European region and northward of the Arctic Circle in Western Siberia (Fig. 1d). At the shelf of the southeastern Barents Sea and of the Kara Sea, the relic cryolithozone existed in the area flooded by the sea.

Among the coastal processes of that time that are still significant, abrasional -abrasional-accumulative and thermoabrasional - thermoabrasional-accumulative processes were most frequent (affected 80% of the coastline length) in the regions without permafrost and in the cryolithozone, respectively. The thermal abrasion of the Kara and Barents sea coasts is very rapid. A constantly heavy sea of 1-3 points over one summer season results in an average erosion rate of 1 – 2 m/yr in the Yamal, Gydan, Yugor, and Taz coasts, that are composed of icy silty-clayey sediments (Vasiliev et al. 2001). At the eastern Yamal and northern Gydan coasts, the silty-sandy sediments with very high ice content (up to 70-80%) are eroded at a higher rate (2-5 and up to 10–15 m/yr in individual years). Frozen rocks with a low ice content, which compose, for example, the western coast of the Taz Peninsula and the Kolguev Island coasts, are eroded slowly (0.1 – 0.3 m/yr).

In conclusion, we should note that the Pleistocene-Holocene dynamics of the Arctic coastal zone formed the clearly defined steps of marine interfluvial plains separated by ancient cliffs, which once were the boundary of the maximal transgression of the sea basin, near which took place thermoabrasion and accumulation of coastal sediments. Virtually a constant position of the present-day coastal zone during the last 6 kyr indicates that, during this period (in the climatic optimum and later), the coasts have changed mainly due to the processes of thermal abrasion (with thermal denudation and thermokarst), and thermal abrasion-accumulation at the coasts composed of rocks with high ice content and underground tabular ice. The same process will proceed everywhere at the Arctic coasts under consideration.

The present study was supported by INTAS, grant 01- 2329, and the Russian Foundation for Basic Research, project no. 02-05-64263.

Reference

Kaplin, P.F. and A.O., Selivanov (1999) Sea-level changes and coasts of Russia: past, present, future. GEOS, Moscow. (in Russian).

Rozenbaum, G.E. and Shpolyanskaya, N.A. (1998) Late Cenozoic permafrost history of Russian Arctic. In Permafrost Periglacial. Processes, 9, 247-273.

Rozenbaum, G.E. and Shpolyanskaya, N.A. (2000). Late Cenozoic permafrost history of Russian Arctic and the tendency for the future evolution. Nauchnii Mir, Moscow. (in Russian).

Trofimov, V.T. (ed) (1986) Exodynamic of West Siberia platform. Izdatelstvo Moskovskogo Universiteta. (in Russian).

Vasiliev, A.A., Pokrovsky, S.I. and Yu.L. Shur (2001) Dynamics of the coastal thermoerosion of West Yamal. Kriosfera Zemli, 5 (1), 44-52. (in Russian).

Velishko, A.A. (ed) (1998) Climate and environment changes during the last 65 million years (Cenozoic: from Paleocene to Holocene). GEOS, Moscow. (in Russian).

Legend for Figure 1 (next page)

a. The West Arctic Ocean coastline position in the Middle Pleistocene. Maximal glaciation and sea transgression (II_{2-4}).
b. The West Arctic Ocean coastline position in the Late Pleistocene. Mikulino (Kazantsevo) Interglacial (III_1).
c. The West Arctic Ocean coastline position in the Late Pleistocene. Late Valdai (Sartan) epoch (III_4).
d. The West Arctic Ocean coastline position in the Holocene (IV). The warm interglacial period (6 ka ago).
1 - The sheet glaciation and caps.
2 - The subaeral cryolithozone in the mountains.
3 - The subaeral cryolithozone in the plains and valleys.
4 - The frost penetration shelf deposits.
5 - The relict subaerial cryolithozone.
6 - The relict submarine cryolithozone.
7-14 - The types of coasts:
7 -the thermo-abrasional glacial shores, 8 - glacial trough coasts, 9 - abrasion shores, 10 - abrasion-accumulative shores, 11 - thermo-abrasional shores, 12 - thermo-abrasional and accumulative shores, 13 - thermo-erosional and accumulative shores, 14- accumulative shores.
15 - 16 - The types of deposits:
15- loam and clay, 16 - sand, sandy loam and loam.
17-18 - The boundaries:
17- land , 18 - shelf.

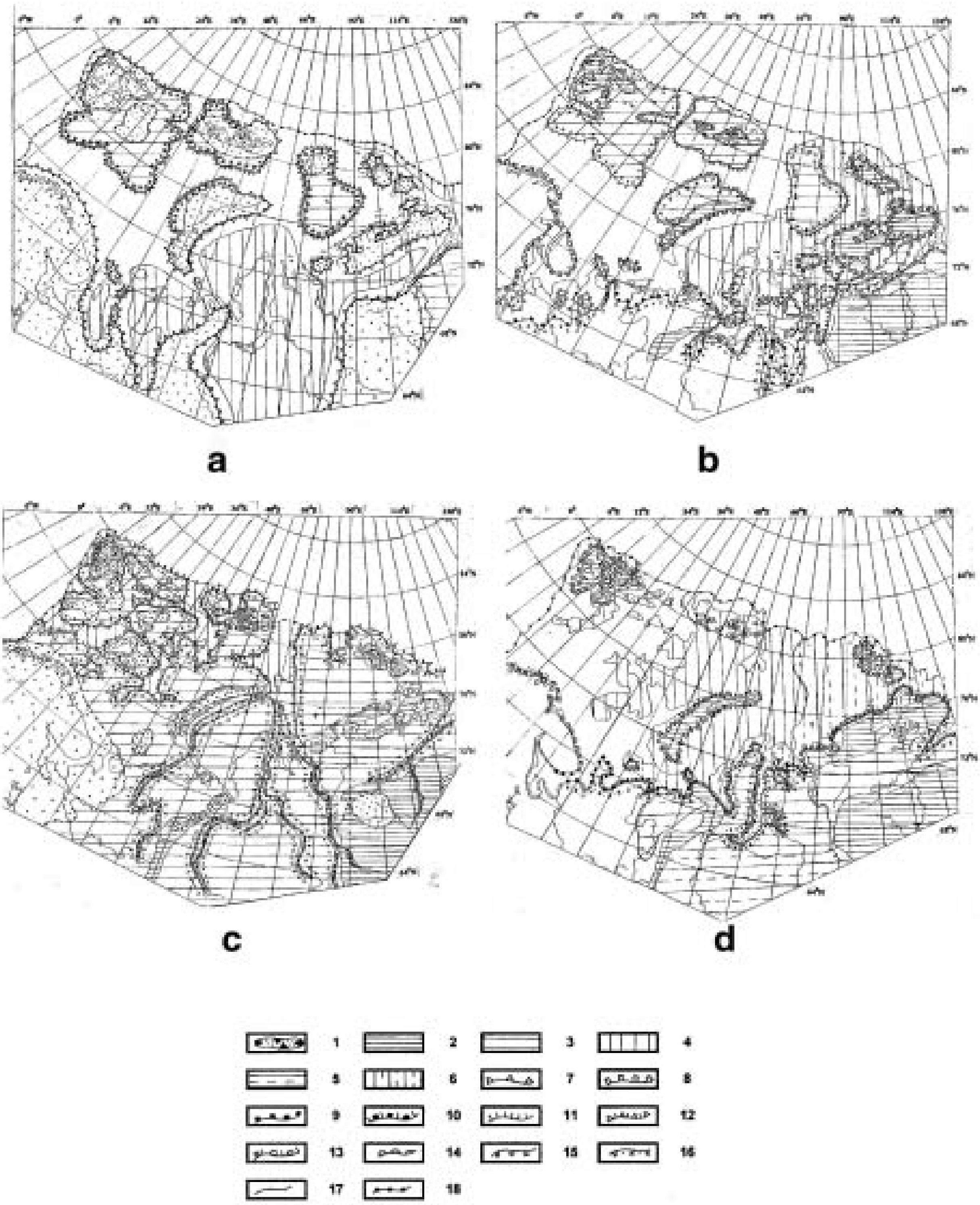
a
b
c
d
1
2
3
4
5
6
7
8
9
10
11
12
13
14
15
16
17
18

THE ASSESSMENT OF STRESS-STRAIN CONDITIONS OF COASTAL SLOPE BY USE OF SEISMIC RECONNAISSANCE

A.G. Skvortsov and D.S. Drozdov

Earth Cryosphere Institute, SB RAS, Russia, e-mail: ds_drozdov@mail.ru

Seismic research held within the present project are carried out according to the basic principles of seismic techniques of slope stability analysis. This technique was developed by the participants of the project during the long-term research on various types of slopes, mainly on sliding slopes. The technique is based on the theoretically and experimentally correlation of seismic properties of ground on stress-strain condition of the soil mass. Very important feature of this technique is the opportunity to control preliminary changes in slopes stability some months or even years prior to the beginning of the discontinuity. Thus, the results of seismic research provide an opportunity of spatial-time forecasting of slope destruction.

The tasks and the stages of seismic research in 2002 according to the present project were the following:

- To carry out in the Temperate zone the in-situ modeling of natural conditions of seismic research to chose the technique of similar seismic research for the Arctic coastal zone.
- To execute the in-situ experiment in order to assess the features of stress-strain conditions of the coastal slope at the key site “Bolvanskiy” at the Barents sea coast at the mouth of the river Pechora.

The results of the first stage have shown that reliable information on the stress-strain conditions of slope can be received based on the rate of compressional waves and their anisotropy in the uppermost part of a geological section of 1 m thickness. Particularly, this conclusion is completely coordinated with the laws of the seismic variability characteristics of slopes which were studied in previous years. From the methodical point of view this conclusion is extremely important for conditions of the Arctic coastal slopes in permafrost zone, since it shows, that the stress-strain conditions of the coastal mass can be assessed using the distribution of seismic characteristics in the active layer (seasonally-thawed layer).

The research of the second stage were carried out taking into account this conclusion. It was conducted in September 2002 at Cape Bolvanskiy at the northern slope of about 25 m in height. The seismic operations were executed on four profiles 50-60 m in length located perpendicularly to the coastal line. The technology of operations provided information on rate distribution of compressional and shear waves both in the active layer and in the top part of perennially frozen ground.

The preliminarily processing of these results allows us to trace the weakened zone in the active layer, along which the development of discontinuity and fissures in the frozen soil mass.

This study is supported by INTAS (N 2332)

A NEW SHORELINE CHANGE DATABASE FOR THE MACKENZIE-BEAUFORT REGION, NWT, CANADA

S.M. Solomon

Geological Survey of Canada (Atlantic), Bedford Institute of Oceanography, P.O. Box 1006, Dartmouth, NS, Canada B2Y 4A2

Recent oil industry activity in the Mackenzie Delta region of the Canadian Beaufort Sea has resulted in new demands on the Government of the Northwest Territories to develop a framework for managing the coast. This requirement demands updated data on coastal dynamics in the region. The Beaufort Sea coast is transgressive with typical average shoreline recession rates in the range of 1-2 m per year, however rates are known to be very variable both in space and in time. Past efforts used analog methods to analyze coastal change on a regional basis by comparing features on air photos taken in the late 1940s and early 1950s with an air photo survey from 1972. Since then regional air photo surveys were flown in 1985 and 2000. The 2000 survey used differential GPS for positioning and is therefore the most accurate base map available for updating measurements of coastal change. Digital orthoimages of the 2000 photos at a resolution 1.25 m were used to georeference 1985 photography and the shoreline and cliff edges were digitized for both years. Root mean square errors and comparison of features which were known to remain constant indicate that georeferencing was accurate to within 10 m. Measurements of coastal change were made every 100 m along the year 2000 (Y2K) shoreline. Shoreline change along the exposed coastal areas varied from –338 m to +68 m (negative change refers to retreat or erosion) over the 15 year period. Much of the exposed coastal regions are experiencing average erosion rates of –1 to –5 m a^{-1}. A large zone of stable coast line is associated with an intertidal sand flat deposited in the lee of several islands at the mouth of one of the major Mackenzie distributaries. The nearshore in this region is shallow (< 2 m) and a series of 5 or more shoreface bars create an extremely dissipative environment despite exposure toward the NW storm direction. The highest rates of retreat (> 10 m a^{-1}) are associated with spits or low tundra bluffs which are directly exposed to waves and storm surges caused by the northwesterly wind storms. Shoreline retreat rates are also quite high (5-10 m a^{-1}) in areas where coastal mapping has identified high ground ice content.

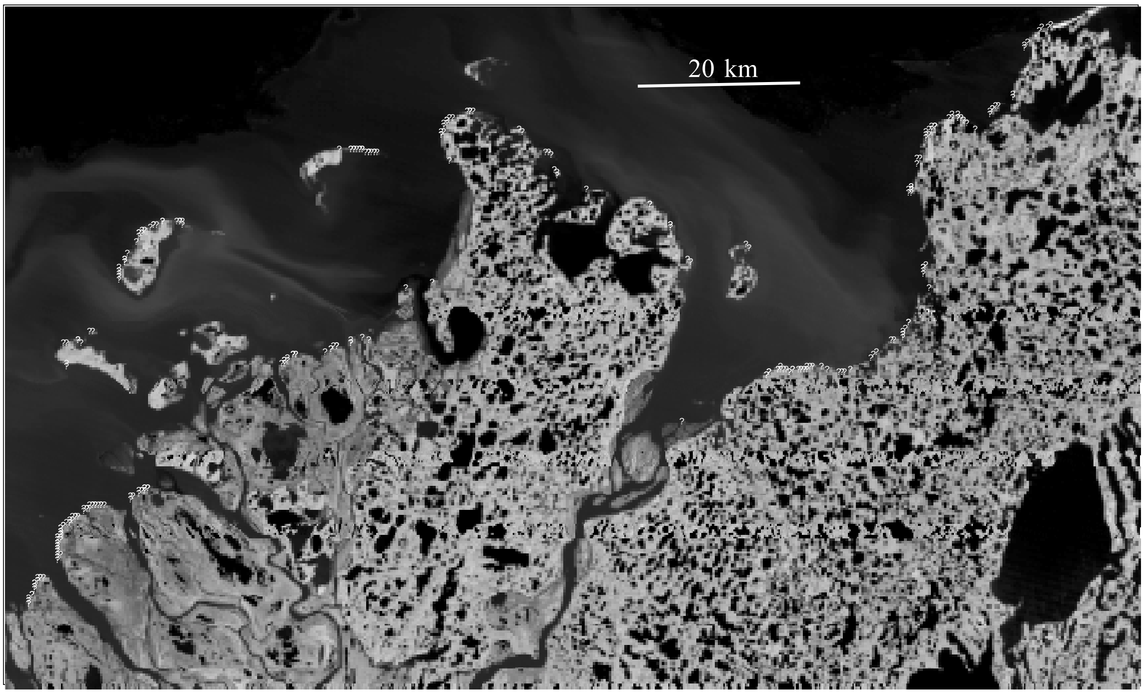

Figure 1. White dots are measured shoreline retreat locations where rates have exceeded 2 m a^{-1} between 1985 and 2000.

THE MECHANISM OF THE SEA COAST DESTRUCTION IN __RR_-SALE, WESTERN YAMAL

Vasiliev A.[1], Kanevskiy M.[1] and Firsov Yu.[2]

[1] Earth Cryosphere Institute, Moscow, Russia, [2] VNIIOkeangeologia, St.-Petersburg, Russia

The key site Marre-Sale is located in Western Yamal on the coast of the Kara Sea. The observations of coastal dynamics have been carried out since 1978. The 4.2 km study site is related to the second and the third marine terraces. The geological section is composed of marine clay with layers of sands, quite often folded (probably by glaciers). The top part of the section is represented mainly by continental deposits (alluvial, lacustrine, eolian etc) of sands, peat near the surface, and rarely sandy-loams and loams. At the study site we can allocate three basic lithological types of coastal sediments: 1) mainly sandy; 2) mainly clay; and 3) sandy-clay (marine clay with layers of sands and loams usually underlying the strata of continental sands). The last type is widespread in the study area.

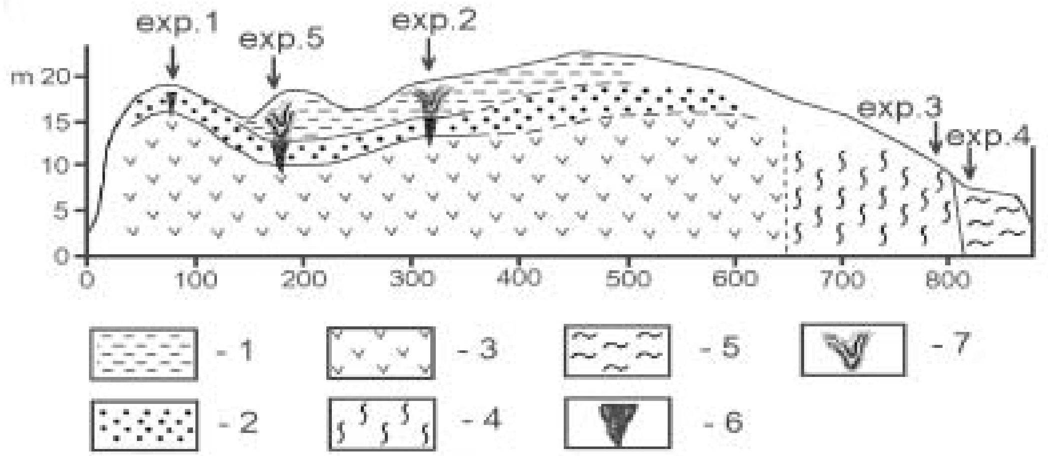

Figure 1. The section of the Quaternary sediments, Marre-Sale key site, northern part. 1 – syncryogenic continental sediments, which had thawed and then froze again epigenically (sand, sandy-loam with ice-wedge casts); 2 – syncryogenic ice-rich continental sediments (sand, sandy-loam with ice wedges); 3 – epicryogenic marine sediments (homogeneous clay with rare sand layers); 4 – folded epicryogenic marine and littoral sediments, frozen before the beginning of fold formation (interstratification of clay and sand); 5 – folded epicryogenic marine and littoral sediments, which had thawed after the fold formation had completed and then froze again epigenically (interstratification of clay and sand); 6 – ice wedges; 7 – ice-wedge casts, filled with sandy-loam and peat.

The cryogenic structure of coastal sediments is complicated. Depending on the cryogenic origin we can recognise four types of permafrost stratigraphic sections: 1) syngenetically frozen ice-rich continental sediments (thickness up to 5-7 m), and bedded by marine and littoral epigenically frozen sediments; 2) syngenetic continental sediments (thickness up to 7-10 m) withthe upper part (thickness up to 4-6 m) that had thawed and then frozed again epigenically; 3) marine and littoral epicryogenic sediments froze before the beginning of fold formation; and 4) marine and littoral epicryogenic sediments that thawed after the fold formation had completed and then frozed epigenically. Usually the sediments of the first and second type are bedded by the sediments of the third or the fourth type. In a number of sections the thickness of syngenetically frozen sediments is reduced, and epicryogenic marine sediments lie practically below the active layer. Figure. 1 shows the section of the Quaternary sediments with various types of cryogenic structure.

The gravimetric moisture content of the sediments (without taking into account polygonal-wedge and massive ground ice) consists of 20-30% for sand (maximum up to 45% in syncryogenic sediments), 30-50% for clays and loams (maximum up to 100-120% in the layers of epigenetic clays). The ice wedges (width up to 3 m) were found at different depths. In syncryogenic sediments of the first type the ice wedges lie close to surface (at 10-20 cm under the active layer), the size of polygons changes between 15 and 30 m. In the sediments of the second type, ice wedges lie below 4-6 m, quite often penetrating into the underlying marine sediments. In the marine sediments (both in sands and clays) small massive ground ice bodies are found.

In September 2002, observation of the coast was carried out following the long heavy storm. The observations allowed us to recognise different segments of the coast, distinguished by the different mechanism of destruction. The mechanism can vary during the further degradation of the cliff, but the observation executed immediately after the heavy storm allows us to reveal "starting mechanism" of destruction.

During the observations, the coordinates of borders between the segments with various mechanism of destruction and various complexes of destructive processes were determined. These coordinates, like were coordinates for the top and base of the cliffs at the key site, were determined with the help of electronic tachymeter (DTM-350) and differential satellite method (DGPS) with the use of the equipment GeoExplorer3. The precision of fixing the top edge of the cliff reaches 0.1-0.2 m, and with the help of DGPS - 0.5-1 m.

More than 20 segments with the various mechanism of destruction were recognized during the observation of the coast. It was found that the major factors influencing the destruction mechanism are the composition, cryogenic structure and ice content of the sediments, as well as the wave activity. Thus, the presence of the ice-rich clays determines the high activity of thermodenudation, thermoersion, slumping processes, mudflows etc. These processes can be considered as a consequence of coastal erosion, because the basic reason of their activation is the breach of the equilibrium profile of the slope owing to erosion at the cliff base.

In total during the observation four major types of destruction were recognized:

1. Coastal erosion and thermoerosion processes. These processes accompanied by formation of wave niches and breakage of the basal part of the cliff (Fig.2). Such mechanism develops mainly at the sites where the ice-rich clay sediments lie at the basis of cross-section and at the sites with high wave activity.

2. Talus mechanism of destruction. This mechanism develops mainly at the sites of the coast composed by ice-poor sands. Quite often it is accompanied by deflation of sands and slope erosion.

3. Slumping mechanism of destruction. This mechanism is developing within the total height of the coastal slope. It is characteristic for the sites with ice-rich clay. Frequently at these sites thermoersion, thermodenudation and mud flows develop as well.

4. Thermodenudation processes. These processes are characteristic for sites where polygonal-wedge ice and massive ground ice occur. As a result of thermodenudation and slope erosion thermocirques and thermoerosion ravines are formed within the limits of the coastal slope. At some sites, the slopes are complicated with ground mounds ("baidjarakhs").

Frequently the combined type of destruction (1+2, 2+3 etc.) is recognized. The talus processes at the top part of the section and landslides at the base of the slope form in widespread combination. At the same time, erosive cliffs and wave niches were found quite often in the base of such slopes. This combined mechanism is characteristic of sites where ice-rich clay sediments lie in the base of the cliff and ice-poor sandy sediments lie in the upper part of the section.

Figure 2. The wave niche at the base part of the cliff, formed by the ice-rich folded marine and littoral sediments, Marre-Sale key site**.**

Table 1 shows a portion of the table reflecting the results of coastal observation at Marre-Sale area in September 2002, (numbers of sites increase from south to north). The received data indicates that morphology and gradients of the cliff are determined by various mechanisms of destruction connected to features of geological and cryogenic structure of sediments. The digital database concerning the dynamics of sea coast in Marre-Sale area was enlarged on the basis of these coastal observations.

Table 1. Results of the observation over the sea coastal dynamics at the key site Marre-Sale, total extent 4.2 km fragment (September 2002).

Seg-ment	Extent of the segment	Major type of destruc-tion	Structure of the section	Description of the cliff and its morphometric parameters	Major factors of coastal destruction
1	200	2	Mainly ice-poor sands, in the upper part with peat	Relatively stable slope with the gradient 30-35^0, almost plain, with height 10 m, locally - erosive cliff with the height up to 0.7 m.	Talus processes, locally coastal and slope erosion
2	160	2	Mainly ice-poor sands, in the base of the section with clay layers	Relatively stable slope with the gradient 30-35^0, almost plain, with height 14 m, with erosive cliff (height up to 2.5-3 m)	Talus processes, locally coastal and slope erosion, slumping processes
3	220	1+2	Mainly ice-poor sands; earlier at this site ground massive ice bodies had been found	The slope with the gradient 40-45^0, almost plain, with height 24 m, erosive niche with the height up to 0.5m and depth up to 1 m.	Coastal erosion, talus processes
4	180	2+3	Ice-poor sands, bedded by clays	The slope with the gradient 40-45^0, almost plain, with height 22 m, the beach locally is blocked by landslides	Talus at the top part of the slope, slumping processes at the base part
…	…	…	…	…	…
23	300	1+2	Ice-rich sands and sandy-loams with ice wedges (thickness of sands 4-5 m), bedded by ice-poor clays	The slope with the gradient 50-60^0, with height 22 m, erosive niche with the height up to 2 m and depth up to 3.5 m.	Coastal erosion, talus processes at the top part of the slope, crumbling of huge ground blocks at the base part locally - slumping processes

This work was supported by INTAS Grant 2329.

ESTABLISHING OF FOUR SITES FOR MEASURING COASTAL CLIFF EROSION BY MEANS OF TERRESTRIAL PHOTOGRAMMETRY IN THE KONGSFJORDEN AREA, SVALBARD

B. Wangensteen_, T. Eiken_, R.S. Ødegård_ and J.L. Sollid_

_ Department of Physical Geography, University of Oslo, Norway, P.O. Box 1042 Blindern, N-0316 OSLO, Norway. _ Gjøvik University College, Norway. P.O.Box 191, N-2802 Gjøvik, Norway.

Abstract

Four sites for measuring coastal cliff erosion in the Kongsfjorden area on Svalbard (79˚ N, 13˚ E) were established in the period August 2nd to 8th 2002. The sites were chosen to compromise different kinds of material and exposure. Both cliffs in unconsolidated material and cliffs in bedrock where chosen. Photos were taken at distances ranging from 7 to 15 metres from the cliff walls with a Hasselblad camera. Both the camera positions and some established fixed points were surveyed. At site 1 and 4 a number of bolts were also drilled in to the cliff and surveyed. These are used as control points for the photogrammetric orientation of the photos. At the other two sites only the camera position and direction were measured. At each site photographs were taken from two to three different camera positions to get three-dimensional coverage of the cliffs.

The photos were scanned and digital terrestrial photogrammetry was applied to construct digital terrain models of the cliffs. The plan is to photograph the sites again in two years time and to construct a new set of digital terrain models. The erosion rate can be found by simply taking the difference between these two sets of terrain models. Due to the short distance between camera and cliff, the accuracy is in the millimetre range.

The study area

The Kongsfjorden area is situated at the western coast of Spitsbergen, the largest island of the Svalbard archipelago (see Fig. 1). The area has continuous permafrost with measured depths ranging from 130 to 150 near the shores of Ny-Ålesund (Orvin 1944; Liestøl 1976). The mean annual air temperature in Ny-Ålesund is –5.8˚C (1975-2000 data obtained from Ketil Isaksen at the Norwegian Meteorological Institute). The tidal range is about 2m. The shores of the area are made up of a mixture of cliffs in unconsolidated material, cliffs in bedrock and glacier fronts terminating in the sea. The selected sites consist of low cliffs in bedrock and unconsolidated material, both with stony beaches in front (Ødegård et al. 1987). The geology of site 1, 3 and 4 is lime- and dolostone (Carbon and Perm) while site 2 is in an area of gneiss (upper Proterozoic). The unconsolidated beach material is of Quaternary origin (Hjelle 1993). The area has earlier been subjected to some related research activities concerning coastal processes e.g. cryogenic weathering of cliffs (Ødegård and Sollid 1993).

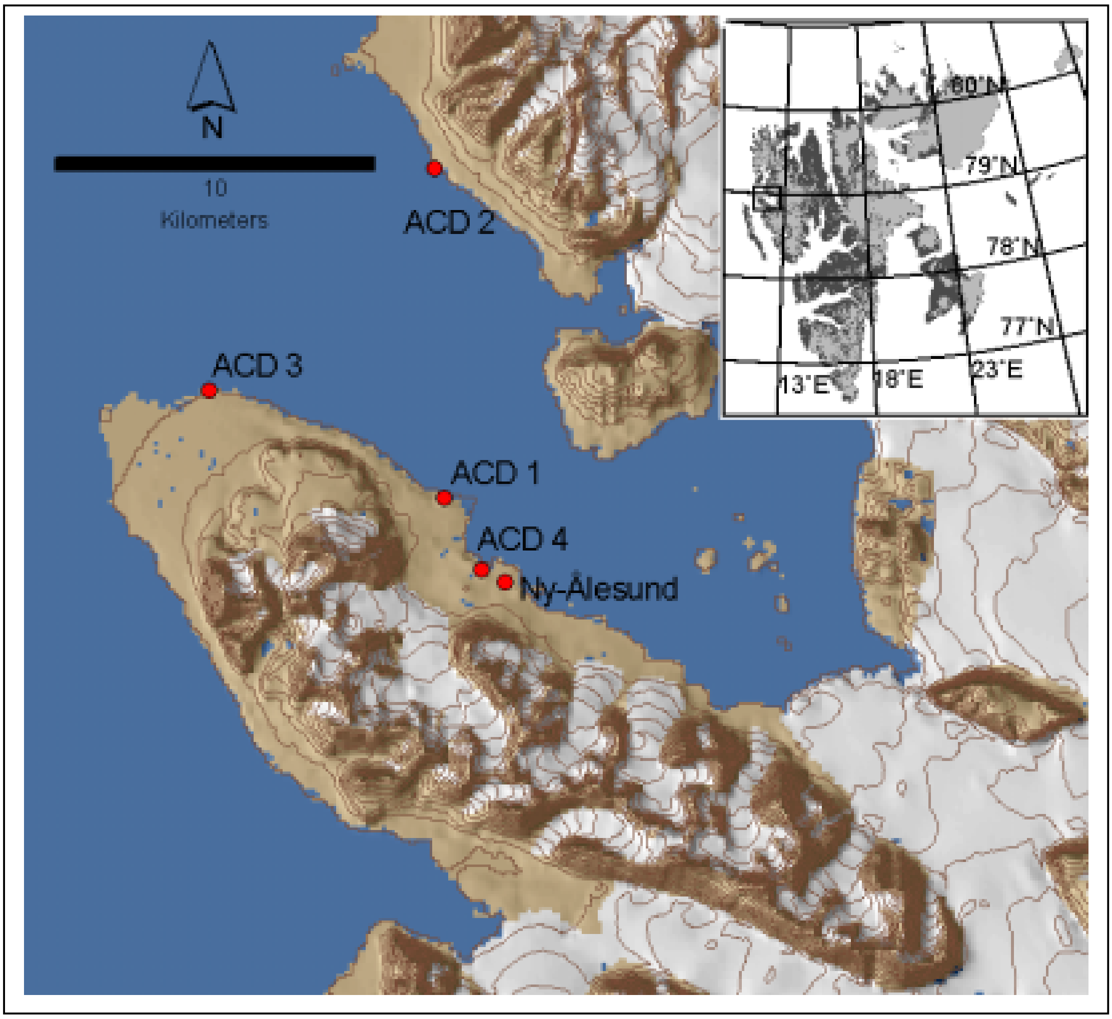

Figure 1. Map of the site locations in the Kongsfjorden area.

Technique and precision

The camera set up used at the sites is shown in Fig. 2. At all sites a fixed point for global reference was established. A bolt was drilled into the bedrock and its position measured by GPS. The positions of the camera stations were measured by GPS and surveyed from the fixed point to create both a global and a local reference. The photos were acquired with a stereo overlap as seen in Fig. 2 by using a Hasselblad camera with a 60 mm lens. At two of the sites bolts to be used as photogrammetric control points were drilled into the cliff wall as well. At the sites consisting of unconsolidated material no control points were established. The distances between the camera stations and the cliff wall varied between 7 and 15 metres for the four sites. The distance between the camera stations was approximately half of the photo distance. The coordinate system is transformed in a manner to simulate the geometry of aerial photogrammetry. The z-axis is pointing out of the cliff and the xy-plane is parallel to the cliff wall and also the line between the photo stations (Fig. 2). The camera was mounted on top of the theodolite with a special device (Fig. 3). This makes it possible to measure the exact position of the camera and to ensure that the photo stations are on line parallel to the cliff wall. The camera positions are also used in the photogrammetric orientation of the scenes. For the scenes from the sites of unconsolidated material this set up also gives the opportunity to measure the photo angle used for exterior orientation of the scenes. This is important since no control points are available.

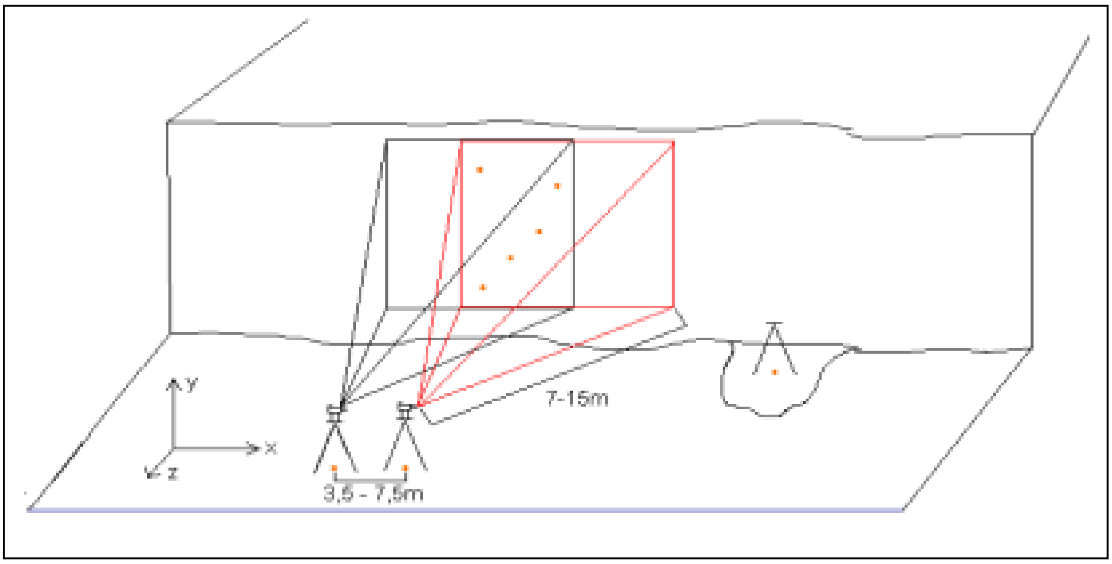

Figure 2. The set up of camera and fix points at the sites.

The photos where scanned at a resolution of 11 µm (2,300 dpi) and imported into the Z/I Imaging digital photogrammetric workstation software. After the photo pair or triples have been used to create a photogrammetric stereo model it is possible to automatically generate a high precision digital terrain model (DTM). The Match-T algorithm (Krzystek 1991) in Z/I Imaging utilizes cross-correlation to detect the same points in the different photos of the stereo model and then measures the elevation by measuring the y-parallax. Photo distances in the range of 7-15 m gives a scale of 1:117 to 1:250. With the above mentioned scanning resolution the XY-resolution is in the order of 1.2 – 2.5 mm. The accuracy of elevation measurements done by photogrammetry is about 0.20-0.40‰ of the photo distance. This gives an elevation accuracy (Z-direction) of 1.4 – 2.8 mm for the 7 m photo distance and 3.0 – 6.0 mm for the 15 m photo distance. To be able to use the Z/I software the coordinate system had to be rotated and all coordinates up scaled by a magnitude of 100, both to simulated aerial photography wich is the normal input to the software.

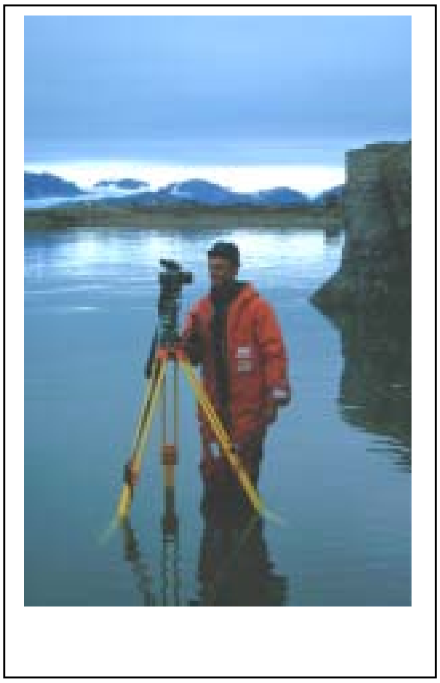

Figure 3. Camera on theodolite.

Results

The automatically generated DTM for site 4 is shown in Fig. 4, both as a shadowed relief of the digital terrain model and as contour lines on top of the orthophoto of the cliff wall. The height and width of the area covered by the model is 3.3 m and 2.8 m respectively. When investigated the three-dimensional model follows the terrain quite nicely. But all the points in the generated digital terrain model are laying some centimetres above the surface. This error is probably due to the theodolite-camera centre offset. The position of the theodolite is taken to be the projection centre of the photos and used in the photogrammetric calculations. Hence the theodolite-camera centre offset has to be determined to determine the exact position of the projection centre. Some photos of an indoor house wall with known and marked points have been taken at the Agricultural University of Norway. By the use of bundle adjustment of these photos in the Z/I-Imaging software it should be possible to calculate the offset between the camera centre and the theodolite.

Preliminary conclusion and future work

The method of close up digital terrestrial photogrammetry seems suitable for creating accurate digital terrain models of coastal cliffs and hence promising for calculating erosion rates in the order of millimetres to centimetres. The plan is to acquire a new set of photos of the same sites in 2004 to generate new terrain models that will enable the erosion rate calculations. André (1997) reports a rock wall retreat in the range 0 to 1.58 mm/year in the same area. The coastal cliff erosion rate is unknown but believed to be higher than the rock wall retreat rate and hopefully greater than the accuracy of the technique used.

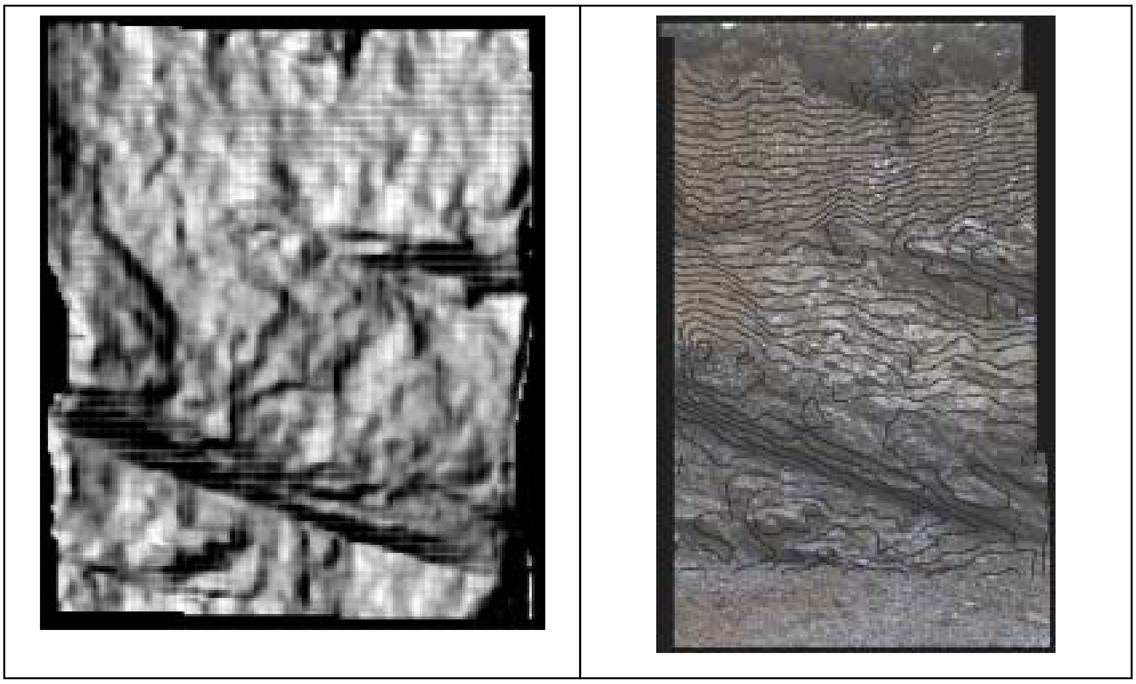

Figure 4. Two representations of the digital terrain model; a shaded relief to the left and contours with 5 cm equidistance on an orthophoto to the right. The size of the model area is 3.3 m by 2.8 m (height and width respectively).

Acknowledgements

The fieldwork was financially supported by the INTAS-project *Arctic coasts of Eurasia: dynamics, sediment budget and carbon flux in connection with permafrost degradation* (INTAS-2001-2329) and the Norwegian Research Council on behalf of the Norwegian Polar Committee .

References

André, M.-F. (1997) Holocene Rockwall Retreat in Svalbard: A triple-rate evolution. Earth Surface and Processes and Landforms 22, pp. 423-440.

Hjelle, A. (1993). Geology of Svalbard. Polarhåndbok No. 7, Norsk Polarinstitutt, Oslo.

Krzystek, P. (1991) Fully Automatic Measurement of Digital Elevation Models with Match-T. In Proceedings of the 43rd Photogrammetric Week, Vol. 15 of Schriftenreihe der Universität Stuttgart, pp. 203-213, Stuttgart.

Liestøl, O. (1976). Pingos, springs and permafrost in Spitsbergen. In Norsk Polarinstitutts Årbok 1975, pp. 7-29.

Orvin, A.K. (1944). Litt om kilder på Svalbard (in Norwegian). Norsk Geografisk Tidsskrift 10.

Ødegård, R., Sollid, J.L. and Trollvik, J.A. (1987) Coastal Map Svalbard A 3 Forlandssundet 1:200.000. Department of Physical Geography, University of Oslo.

Ødegård, R. and Sollid, J.L. (1993) Coastal cliff temperatures related to the potential for cryogenic weathering processes, western Spitsbergen, Svalbard. Polar Research 12(1), pp.95-106.

WATERBIRDS ON THE EDGE: IMPACT ASSESSMENT OF CLIMATE CHANGE ON ARCTIC-BREEDING WATER BIRDS

C. Zöckler and I. Lysenko

UNEP-WCMC Cambridge, U.K.

Executive Summary

The purpose of this study is to investigate the potential impacts of climate change on a number of Arctic breeding of water birds species. The study applies the HadCM2 general circulation model (GCM) of the Hadley Centre to assess the direct impacts of a changing climate on the breeding conditions of five selected Arctic waterbird populations. Additionally, the current distribution of 20 species is being compared with changes in vegetation predicted by two climate scenarios, a moderate one based on rise in temperature of only 1.7^{0}C (HadCM2SUL) and an extreme scenario with a rise of 5^{0}C (UKMO) at the time of CO_2 doubling (2070-2099).

Analysis of spring and summerdata of temperature and precipitation of the last 50 years, interpolated over the area of the species‘ currently known distribution, demonstrate a significant correlation between the mean June temperature and the juvenile percentage as a measure of breeding success in the Arctic inboth tested populations of the Greater White-fronted Goose (*Anser albifrons*) and in the Taimyr population of the Knot (*Calidris c. canutus*). The Nearctic population of the Knot (*C. c. islandica*), as well as the Curlew Sandpiper (Calidris ferruginea) breeding on the Taimyr Peninsula, did not show a correlation with the mean June temperature.

Under the HadCM2 model, an increase of 1% CO_2/yr results in a moderate increase of the mean June temperature in the Arctic breeding area of Taimyr breeding White-fronted Goose. The conditions for the Taimyr population is particular favourable for the period around 2020. In 2050, the temperature, according to the scenario, seems to fall again, but never below the average of the last 30 years. However, a considerable cooling on the breeding grounds of the goose population in West Greenland could lead to a drop in size of the fragile population, which winters only in the western part of the British Isles. According to the climate model, the temparture around 2080 would not be above the mean values of today.

For three tested wader populations, the pattern of response towards certain climate variables is not consistent and for these species we did not project the mean June temperature or other climate variables into a future scenario. More species need to be tested to ensure the inclusion of the right variables into future sceanrios. Despite these uncertainties, the study maintains that all Arctic water bird population breeding in the predicted area of cooler spring and summer temperatures between Northeastern Canada and West Greenland remain of special concern. Most of them, including the Nearctic Knot and the Sanderling (*Calidris alba*) winter regularly in British coastal waters.

The results of the vegetation models show a large variation in the impact of predicted changes in vegetation on the 20 species. According to the moderate HadCM2Sul, 76% of Tundra Bean Geese (*Anser fabalis rossicus/serrirotris*) will be affected by the alteration of tundra habitats, whilst only 5% of the Sanderling will be affected. For two of the three globally threatened water birds occurring in the Arctic, namely the Red-breasted Goose (*Branta ruficollis*) and the Spoon-billed Sandpiper (*Eurynorhynchos pygmeus*), 67% and 56% respectively of their

current breeding range will change from tundra to forest. The values for the extreme UKMO scenario are even higher, reaching 99% for the Red-breasted Goose. This additional loss of habitat will place these two species at a higher risk of extinction. The Emperor Goose (*Anser canagicus*), already in decline and with 55% of its small range affected, is highlighted as needing further conservation attention.

The results from this study require careful interpretation. Although in Alaska there is already evidence of an increase in forest area, and pollen analyses from the Holocene indicate that vast shifts in forest areas occurred duringinterglacial periods, scientists still argue about the likelihood of such scenarios and about the rate, speed and scale of forest growth into the tundra. However, the results of this study reflect an important component in a matrix of factors affecting the continued existence of Arctic-breeding water birds. They have to be interpreted in relation to other factors affecting the populations of these birds, such as natural predation, hunting (mainly outside the Arctic) and effects of climate change (in particular sea-level rise) outside the Arctic. Further research will be carried out to refine the existing results, based on better distribution data and refined GCMs. Other important components such as sea level rise and change in river runoff in the Arctic and on the major staging areas during migration will be taken into account.

The study was generously supported by WWF under Project No. 98046.

4 Appendix

Appendix 1. Metadata of the existing ACD key sites.

DATE PREP.	COASTAL SECTION NAME	TYPE SITE	COUNTRY	REGION	LAT	LONG	CONTACT:
02 Nov 00	North Head	Key	Canada	Mackenzie Delta	69.72	-134.49	S.Solomon (solomon@nrcan.gc.ca)
14 Feb 01	Elson Lagoon, Barrow, Alaska	Key	United States	Alaska	70.32	-156.58	Jerry Brown (jerrybrown@igc.org)
25 Jan 01	Cape Krusenstern	Key	USA	NW Alaska	67.67	-163.35	J.W.Jordan (jwjordan@sover.net)
22 Jan 01	Marre-Sale	Key	Russia	West Siberia	69.70	66.50	Alexandr Vasiliev (emelnikov@mtu-net.ru)
25 Jan 01	Bolvansky cape	Key	Russia	European North	68.30	54.50	Alexandr Vasiliev (emelnikov@mtu-net.ru)
13 Mar 01	Muostakh Island, Buor-Khaya Bay	Key	Russia	Laptev Sea Coast	71.61	129.94	Mikhail N. Grigoriev (grigoriev@mpi.ysn.ru)
13 Mar 01	Bykovsky Peninsula	Key	Russia	Laptev Sea Coast	71.79	129.42	Mikhail N. Grigoriev (grigoriev@mpi.ysn.ru)
13 Mar 01	Bolshoy Lyakhovsky Island, Novosibirsky Archipelago	Key	Russia	Laptev Sea Coast, Dmitri Laptev Strait	73.33	141.35	Mikhail N. Grigoriev (grigoriev@mpi.ysn.ru)
13 Mar 01	Terpyai-Tumsa Cape	Key	Russia	Laptev Sea Coast, Olenek Bay	73.57	118.40	Mikhail N. Grigoriev (grigoriev@mpi.ysn.ru)
01 Sep 01	Pesyakov Island	Key	Russia	Pechora (Barents) Sea Coast	68.75	57.60	Stanislav Ogorodov (ogorodov@aha.ru)
01 Sep 01	Varandei Island - Peschanka River	Key	Russia	Pechora (Barents) Sea Coast	68.82	58.10	Stanislav Ogorodov (ogorodov@aha.ru)
01 Sep 01	Peschanka River - Cape Polyarnyi	Key	Russia	Pechora (Barents) Sea Coast	68.91	58.60	Stanislav Ogorodov (ogorodov@aha.ru)
01 Sep 01	Cape Konstantinovskii - Cape Gorelka	Key	Russia	Pechora Bay Coast of Pechora (Barents) Sea	68.56	55.50	Stanislav Ogorodov (ogorodov@aha.ru)
15 Sep 01	Kharasavei settlement area	Key	Russia	Kara Sea Coast, Yamal Peninsula	71.10	66.70	Stanislav Ogorodov (ogorodov@aha.ru)
15 Sepr 01	Cape Mutnyi - Ly-Yakha River	Key	Russia	Baidaratskaya Bay Coast of Kara Sea, Yamal Peninsula	69.30	68.10	Stanislav Ogorodov (ogorodov@aha.ru)
15 Sep 01	Yary village - Levdiev Island	Key	Russia	Baidaratskaya Bay Coast of Kara Sea, Ural region	68.80	66.90	Stanislav Ogorodov (ogorodov@aha.ru)
15 Sep 01	Yamburg Harbour area	Key	Russia	Ob' Bay Coast of Kara Sea	67.90	74.80	Stanislav Ogorodov (ogorodov@aha.ru)
10 Oct 01	Beaufort Lagoon, Arctic National Wildlife Refuge, Alaska	Key	United States	Alaska	69.88	-142.30	Janet Jorgenson (janet_jorgenson@fws.go) Torre Jorgenson (tjorgenson@abrinc.com)
22 Oct 01	Cape Maly Chukochiy	Key	Russia	East Siberia Sea, Kolyma Lowland Coast	70.08	159.92	Vladimir Ostroumov (Vostr@issp.serpukhov.su)
20 Nov 01	Onemen gulf	Key	Russia	Chukotka	64.81	176.92	A.N. Kotov (nauka@anadyr.ru)
11 Jan 02	Chukchi Sea, Barrow, Alaska	Key	United States	Alaska	71.30	-156.75	Bill Manley (William.Manley@ colorado.edu)
22 Jan 03	Kongsfjorden Area, Spitsbergen, Svalbard	Key	Norway	Barents Sea	78.93	11.83	Johan Ludvig Sollid (j.l.sollid@geografi.uio.no)
01 Feb 03	Nahodka Bay	Key	Russia	Kara Sea, Ob Estuary	67.23	72.21	Olga Medkova (Olga_Medkova@mail.ru)

Appendix 2. Agenda of the 3rd ACD Workshop.

Sunday, December 1

10.00 - 17.00 INTAS meetings (for INTAS teams only)

1. Arctic coasts of Eurasia: dynamics, sediment budget and carbon flux in connection with permafrost degradation. INTAS Open Call 2001-2329

2. Arctic coastal dynamics of Eurasia: classification, modern state and prediction of its development based on GIS technology. INTAS Open Call 2001-2332

18.00 Ice-breaker

Monday, December 2

09.00 - 09.30 Welcome and opening of the workshop – J.L. Sollid, V. Rachold and O. Rogne

09.30 - 10.00 Arctic Coastal Dynamics: status report and objectives of this workshop - V. Rachold and S. Solomon

10.00 - 11.00 Reports: Beaufort and Chukchi Sea

CARBON ESTIMATES FROM TWO BEAUFORT SEA KEY SITES, ALASKA - J. Brown and M.T. Jorgenson

A NEW SHORELINE CHANGE DATABASE FOR THE MACKENZIE-BEAUFORT REGION, NWT, CANADA - S.M. Solomon

CURRENT COASTAL RESEARCH IN CANADA’S WESTERN ARCTIC -G. Manson, D. Forbes, J.C. Lavergne, M. Craymer, J. Hines, H. Swystun and T. Milne

ALASKAN LANDFAST SEA ICE VARIABILITY AND EPISODIC EVENTS - A. Mahoney, H. Eicken and L. Shapiro

11.00 - 11.30 Coffee

11.30 - 12.00 Reports: Beaufort and Chukchi Sea (continued)

MONITORING OF THE ONEMEN BAY COAST (CHUKOTKA) - A.N. Kotov and O.D. Tregubov

FIFTY YEARS OF COASTAL EROSION ON HERSCHEL ISLAND, YUKON TERRITORY. A REMOTE SENSING INVESTIGATION - H. Lantuit and W.H. Pollard

12.00 - 13.15 Reports: East Siberian and Laptev Sea

THE SENSITIVITY OF ARCTIC SHELF SEAS TO VARIATIONS IN ENVIRONMENTAL FORCING: 10 YEARS OF PROGRESS IN UNDERSTANDING THE “LAPTEV SEA SYSTEM” - J.A. Hölemann, H. Bauch, S. Berezovskaya, I. Dmitrenko, H. Kassens, S. Kirillov, T. Müller-Lupp, S. Priamikov, J. Thiede, L. Timokhov and C. Wegner

A DIVERSITY OF PERMAFROST SEDIMENTS OF THE THERMAL ABRASION COASTS OF EAST SIBERIA SEA AND IT’S DESCRIPTION IN THE STOCHASTIC MODEL OF THERMAL ABRASION - V. Ostroumov

THE EXPEDITION LENA 2002 - H.-W. Hubberten, M.N. Grigoriev, F. Are and V. Rachold

THE GIS-BASED QUANTIFICATION OF THE SEDIMENT AND ORGANIC CARBON FLUX TO THE LAPTEV AND EAST SIBERIAN SEAS THROUGH COASTAL EROSION - M. N. Grigoriev, M. Lack and V. Rachold

MODERN COASTAL ORGANIC CARBON INPUT TO THE ARCTIC OCEAN - V. Rachold, M.N. Grigoriev, H.-W. Hubberten and L. Schirrmeister

13.15 - 14.15 Lunch

14.15 - 15.30 Reports: Kara and Barents Sea

THE ASSESSMENT OF STRESS-STRAIN CONDITIONS OF COASTAL SLOPE BY USE OF SEISMORECONNAISSANCE (SEISMIC-SERVICE) - A.G. Skvortsov and D.S. Drozdov

COAST FORMATION IN THE WESTERN SECTOR OF THE RUSSIAN ARCTIC REGION IN THE PLEISTOCENE-HOLOCENE - N.A. Shpolyanskaya, Yu.B. Badu and I.D. Streletskaya

THE COASTAL RESEARCHS IN THE AREA OF GEOCRYOLOGICAL STATION "CAPE BOLVANSKIY", THE ESTUARY OF PECHORA RIVER - G.V. Malkova (Ananjeva), D.S.Drozdov, M.Z. Kanevskiy and Yu.V. Korostelev

DYNAMICS AND EVOLUTION OF BARRIER BEACHES IN THE PECHORA SEA - S.A. Ogorodov and Ye.I. Polyakova

THE MECHANISM OF THE SEA COAST DESTRUCTION IN MARRE-SALE, WESTERN YAMAL - A. Vasiliev, M. Kanevskiy and Yu. Firsov

15.30 - 16.00 Coffee

16.00 - 17.30 Reports: Kara and Barents Sea (continued)

COASTAL DYNAMICS IN THE PECHORA SEA UNDER TECHNOGENIC IMPACT - S.A. Ogorodov

CHARACTER OF THE COASTAL DESTRUCTION AND DYNAMICS OF THE YUGORSKY PENINSULA COAST - A.I. Kizyakov, D.D. Perednya, Yu.G. Firsov, M.O. Leibman and G.A. Cherkashov

COASTAL DYNAMICS AT THE WESTERN PART OF KOLGUEV ISLAND, BARENTS SEA D.D.Perednya, M.O.Leibman, A.I.Kizyakov, B.G.Vanshtein and G.A.Cherkashov

INVESTIGATIONS OF COASTAL DYNAMICS AT THE KEY SITES IN WESTERN RUSSIAN ARCTIC (2001-2002 FIELD WORKS) - G.A. Cherkashev, B.G. Vanshtein, Yu.G. Firsov and M.V. Ivanov

Tuesday, December 3

09.00 - 10.00 Reports: Reports: Norwegian and Greenland Seas

ESTABLISHMENT OF FOUR SITES FOR MEASURING COASTAL CLIFF EROSION BY MEANS OF TERRESTRIAL PHOTOGRAMMETRY IN THE KONGSFJORDEN AREA, SVALBARD - B. Wangensteen, T. Eiken, R. Ødegård and J.L. Sollid

THE SPATIAL DISTRIBUTION OF COAST TYPES ON SVALBARD - B. Etzelmüller, R.S. Ødegård and J.L. Sollid

THE FIT-FOR-USE OF THE GEBCO COASTLINE TO ESTIMATE COASTAL LENGTH - A CASE STUDY FROM SPITSBERGEN - R. Ødegård, B. Wangensteen and J.L. Sollid

10.00 - 11.00 Reports: Methods, Techniques - Circum-Arctic

THE LANDSCAPE MAP OF THE RUSSIAN ARCTIC COSTAL ZONE -D.S. Drozdov, G.V. Malkova (Ananjeva) and Y.V. Korostelev

THE ARCTIC COASTAL CLASSIFICATION FOR ESTIMATION OF INDUSTRIAL EFFECT - M.M. Koreisha, F.M. Rivkin and N.V.Ivanova

A CIRCUM-ARCTIC ENVIRONMENTAL FORCING DATABASE FOR COASTAL MORPHOLOGICAL PREDICTION: DEVELOPMENT AND PRELIMINARY ANALYSES - D.E. Atkinson and S.M. Solomon

11.00 - 11.30 Coffee

11.30 - 12.30 Reports: Methods, Techniques - Circum-Arctic (continued)

	FROM THE "ARCTIC CLIMATE SYSTEM STUDY" TO A NEW GLOBAL PROJECT "CLIMATE AND CRYOSPHERE" OF THE WORLD CLIMATE RESEARCH PROGRAMME (WCRP) - V. Ryabinin
	CHARACTERIZATION OF COASTAL POLYNYAS IN THE ARCTIC WITH REMOTE SENSING TECHNIQUES AND COMPARISON WITH NUMERICAL MODEL INVESTIGATIONS - S.T. Dokken
	WATER BIRDS ON THE EDGE FIRST CIRCUMPOLAR ASSESSMENT OF CLIMATE CHANGE IMPACT ON ARCTIC BREEDING WATER BIRDS - C. Zöckler, I. May and I. Lysenko
12.30 - 13.00	General discussion, identification of working groups
13.00 - 14.00	Lunch
14.00 - 15.30	Working group meetings
15.30 - 16.00	Coffee
16.00 - 18.00	Working group meetings

Wednesday, December 4

09.00 - 10.30	Report of the working groups / general discussion
10.30 - 11.00	Coffee
11.00 - 13.00	Working group meetings
13.00 - 14.00	Lunch
14.00 - 15.30	Working group meetings /Steering Committee Meeting
15.30 - 16.00	Coffee
16.00 - 18.00	Working group meetings / Steering Committee Meeting

Thursday, December 5

09.00 - 10.30	Report of the working groups / general discussion
10.30 - 11.00	Coffee
11.00 - 13.00	Working group meetings
13.00 - 14.00	Lunch
14.00 - 16.00	Working group meetings
15.30 - 16.00	Coffee
16.00 - 18.00	Final discussions

Appendix 3. Participants of the 3rd ACD Workshop.

1. Feliks Are*, St. Petersburg University, Russia (but@peterlink.ru)
2. David Atkinson**, Canadian Geological Survey, Dartmouth, Canada (datkinso@nrcan.gc.ca)
3. Jerry Brown*, International Permafrost Association, Woods Hole, USA (jerrybrown@igc.org)
4. George Cherkashov*/***, VNIIO, St. Petersburg, Russia (cherkashov@mail.ru)
5. Sverre Dokken, Norwegian Computing Center, Oslo, Norway (Sverre.Dokken@nr.no)
6. Dmitry Drozdov***, Earth Cryosphere Institute, Moscow, Russia (ds_drozdov@mail.ru)
7. Bernd Etzelmüller***, Oslo University, Norway (bernd.etzelmuller@geografi.uio.no)
8. Mikhail Grigoriev*/***, Permafrost Institute, Yakutsk, Russia (grigoriev@mpi.ysn.ru)
9. Jens Hölemann, Alfred Wegener Institute, Bremerhaven, Germany (jhoelemann@awi-bremerhaven.de)
10. Hans-Wolfgang Hubberten*, Alfred Wegener Institute, Potsdam, Germany (hubbert@awi-potsdam.de)
11. Alexandr Kizyakov**, Earth Cryosphere Institute, Moscow, Russia (kizyakov@mtu-net.ru)
12. Hugues Lantuit, Dpt. of Geography, McGill University, Montreal, Canada (superlantuit@vif.com)
13. Andy Mahoney**, Geophysical Institute, University of Fairbanks, USA (mahoney@gi.alaska.edu)
14. Rune Ødegård, Gjøvik University College, Norway (rune.oedegaard@hig.no)
15. Stanislav Ogorodov**, Moscow University, Russia (ogorodov@aha.ru)
16. Volodya Ostroumov***, Institute of Physicochemical and Biological Problems of Soil Science, Pushchino, Russia (vostr@ibbp.psu.ru)
17. Dmitry Perednya**, Moscow State University, Russia (kizyakov@mtu-net.ru)
18. Volker Rachold*/***, Alfred Wegener Institute, Potsdam and Bremerhaven, Germany (vrachold@awi-bremerhaven.de)
19. Feliks Rivkin***, Production and Research Institute for Construction Engineering Survey, Moscow, Russia (f-rivkin@narod.ru)
20. Odd Rogne, International Arctic Sciences Committee, Oslo, Norway (iasc@iasc.no)
21. Vladimir Ryabinin, Joint Planning Staff for World Climate Research Programme, WMO Secretariat, Geneva, Switzerland (Ryabinin_V@gateway.wmo.ch)
22. Johan Ludvig Sollid*/***, Oslo University, Norway (j.l.sollid@geografi.uio.no)
23. Steve Solomon*, Canadian Geological Survey, Dartmouth, Canada (solomon@agc.bio.ns.ca)
24. Frits Steenhuisen, Arctic Center, University of Groningen, Netherlands (f.steenhuisen@let.rug.nl)
25. Irina Streletskaya***, Moscow State University, Russia (strelets@gol.ru)
26. Alexander Vasiliev***, Earth Cryosphere Institute, Moscow, Russia (z_v_a_a@dio.ru)
27. Bjørn Wangensteen, Oslo University, Norway (bjorn.wangensteen@geografi.uio.no)
28. Ian May, UNEP- World Conservation Monitoring Centre (UNEP-WCMC), Cambridge, U.K. (Ian.May@unep-wcmc.org)

* Steering Committee Member, ** Young Investigator, *** INTAS Team Leader